CHITOSAN MEMBRANES FOR THE REMOVAL OF ZINC FROM SIMULATED WASTEWATER

HENDRIK CHRISTOFFEL VAN DER MERWE

Thesis submitted for the degree Philosophiae Doctor
in Chemical Engineering at the North-West University, Potchefstroom Campus

Promoter:	Prof. H.W.J.P. Neomagus
Co-promoter:	Dr. M.A. van der Gun

May 2006
Potchefstroom

DECLARATION

The material incorporated in this thesis is my own work, except where indicated to the contrary.

This material has not been submitted to another university for any other degree.

Signed: 

.....

H.C. van der Merwe

Student number: 105858692

Date: 10/04/2006

Place: Potchefstroom

ACKNOWLEDGEMENTS

The author hereby wishes to express his sincere gratitude towards the following people for their continuous support throughout the project.

Promoter: Prof. H. Neomagus
(School of Chemical and Minerals Engineering: NWU)

Co-promoter: Dr. M.A. van der Gun
(School of Chemical and Minerals Engineering: NWU)

Co-analysts: Prof. L.R. Tiedt
(Head: Lab. for Electron Microscopy: NWU)
Mr. J. Kotze
(School of Chemical and Minerals Engineering: NWU)
Mr. H. Grant
(School of Chemical and Minerals Engineering: NWU)
Mr. B. Rebolo
(School of Chemical and Minerals Engineering: NWU)
Mr. C. Nkalanga
(Department of Chemical Engineering: VUT)
Mr. O. Mahle
(Department of Analytical Chemistry: VUT)

Financial support and equipment supplied are credited to Vaal University of Technology (VUT) without which this project would not have been possible.

ABSTRACT

The utilisation of South African produced chitosan membranes for the removal of heavy metal ions from contaminated water was explored.

South African produced chitosan was used to manufacture membranes for the adsorption of heavy metals by phase inversion. The optimum process parameters were determined as 7 mass% chitosan in 5 mass% acetic acid solution in the dissolution stage, a 4 mass% sodium hydroxide solution in the precipitation stage, and a crosslinking time of 6 hours in the stabilisation stage. The adsorption properties of the membranes were studied for the transition metal ion Zn(II), and followed a Langmuir isotherm. The maximum adsorption capacity determined, was 135 $mg.g^{-1}$ dry chitosan, at a temperature of 303-313 K, the affinity parameter increased according to temperature from 0.016-0.020 $L.mg^{-1}$. The adsorption characteristics were influenced by temperature, co-ions, membrane thickness, and pH.

Chitosan membranes contain only 4-6% chitosan and can be visualised as hydrated polymeric network, in which the chitosan forms a rigid honeycomb structure. The water in the membrane is present as fixed water, that is integrated with the chitosan, and free water, that can be removed from the membrane by applying a pressure difference. The free water content equals the porosity of the membrane. The physical properties of the chitosan membranes are: a wet density of 1100 $kg.m^{-3}$; a chitosan content of 5.2 mass%; a free water volume of 65 mass%; a fixed water of 30 mass%; a maximum pore radius of 40 nm; and a total surface area of $1.15 \cdot 10^{5}$ $m^{2}.kg^{-1}$.

The transport through chitosan membranes can be described analogous to ultrafiltration membranes. The clean water flux of the membranes is in the order of 12 $L.m^{-2}.hr^{-1}.bar^{-1}$, and the transport of solute and solvent could well be modelled, at low solute concentrations, with a generic membrane model derived from irreversible thermodynamics. Concentration polarisation occured at high zinc concentrations and here the transport model deviates from experiments.

Recoveries obtained with zinc were up to 90% from the loaded membrane. The membranes were stable for 2 regeneration cycles.

In comparison with other adsorbents chitosan formulations, the SA produced chitosan membranes have good adsorption characteristics and a good possibility of

recovery of the zinc from the loaded membrane. However, it was also found that the long term stability of the membranes still has to be improved.

OPSOMMING

Die studie verleen homself tot die gebruikmaking van chitosan membrane om die verwydering van oorgangsmetale vanuit oplossings te bestudeer.

Chitosan afkomstig van Suid Afrika is gebruik om die membrane te ontwerp deur gebruikmaking van die fase omsettings metode. Die optimum vervaardigingskonsentrasies is bepaal as 7% chitosan in 'n oplossing van 4% asynsuur. Die membraan is dan gepresipiteer in 'n presipitasie bad met 'n konsentrasie van 5% natrium hidroksied en daarna gekruisbind vir 6 ure gedurende die stabilisasie stadium. Die adsorpsie eienskappe van die membraan vir die metaal Zn(II) is bestudeer en daar is gevind dat die Langmuir isotherm gevolg word. Die maximum adsorpsie kapasiteit is 135 $mg.g^{-1}$ droë chitosan by 303-313 K. By die adsorpsie kapasiteit is gevind dat die affiniteits konstante toeneem met temperatuur van 0.016-0.020 $L.mg^{-1}$. Daar is gevind dat temperatuur, ione, membraan dikte en pH die adsorpsie karakteristieke beinvloed.

Chitosan membrane bevat ongeveer 4-6 mass% chitosan. Die membraan kan dus gesien word as 'n gehidreerde network, waar die chitosan 'n vaste heuningkoek struktuur vorm. Die water in die membraan is teenwoordig as vaste water, wat geintegreer is met die chitosan, en vrye water, water wat verwyder kan word deur 'n drukverskil toe te pas. Die vrye water is gelykstaande aan die porositeit van die membraan. Die fisiese eienskappe van die chitosan membraan is: 'n nat digtheid van 1100 $kg.m^{-3}$, chitosan samestelling van 5.2 mass%, vrye water volume van 65 mass%, vaste water van 30 mass%, 'n maksimum porie grootte van 40 nm en 'n totale oppervlak area van $1.5 \cdot 10^{5}$ $m^2.kg^{-1}$.

Die oordrag deur die membraan kan beskryf word op die selfde wyse as ultrafiltrasie membrane. Die vloei van skoon water deur die membrane is in die orde van 12 $L.m^{-2}.hr^{-1}.bar^{-1}$, en die vloei van oplossing en oplosmiddel kan gemodeleer word met 'n algemene model wat afgelei is van onomkeerbare termodinamoka by lae konsentrasies. By hoë sink konsentrasies vind konsentrasie polarisasie plaas wat die vloei model laat afwyk van die eksperimentele resultate.

Herwinning van sink tot so hoog as 90% van die membraan kapasiteit is verkry en die membrane was stabiel tot en met 2 herwinnings siklusse.

Die adsorpsie karakteristieke van chitosan membrane ten opsigte van ander adsorpsie materiale en ander chitosan vorme is goed. Dus is die herwinning van

sink deur gebruik making van chitosan membrane moontlik, alhoewel die stabilitiet vir herhaaldelike herwinning en gebruik verhoog moet word.

TABLE OF CONTENTS

Glossary

Adsorption capacity: The amount of adsorbed metal defined as the mg of metal per gram of dry chitosan.

Bedvolume: Ratio of the volume permeated trough the membrane to the volume of the membrane.

Crosslinking: The chemical binding of two chitosan polymer chains using glutaraldehyde.

Deacetylation: The removal of the acetyl groups from chitin to produce chitosan.

Demineralisation: The process of removing minerals, in the form of mineral ions, to purify the chitin.

Deproteinisation: The removal of protein from the raw material to recover and purify the shells for conversion to chitin.

Fixed water: Water that is fixed to the chitosan matrix and as such forms part of the membrane structure.

Free water volume: The volume in the membrane that is unoccupied by the macromolecules and the fixed water.

Free water: The water that can be removed from the chitosan matrix using mechanical force. The free water equals the free water volume.

Maximum adsorption capacity: The maximum amount of adsorbed metal defined as the mg of metal per gram of dry chitosan.

Phase inversion: The process whereby chitosan is transformed from a liquid to a gel state.

Wet membrane density: The density of the wet chitosan membrane after cohesive water has been removed from its edges.

List of symbols

A	Membrane surface area (m^2)
A_{1655}	Fractional infra-red adsorption at wave number 1655
A_{3450}	Fractional infra-red adsorption at wave number 3450
b	Adsorption affinity parameter ($L.mg^{-1}$)
C	Final concentration ($mg.L^{-1}$)
c_b	Concentration in the bulk solution ($mg.L^{-1}$)
C_e	Equilibrium concentration after recirculation ($mg.L^{-1}$)
C_{in}	Initial concentration ($mg.L^{-1}$)
c_{in}	Solute concentration in the bulk liquid ($mg.L^{-1}$)
c_m	Membrane interface concentration ($mg.L^{-1}$)
c_s	Solute concentration ($mg.L^{-1}$)
c_t	Permeate concentration after a single pass ($mg.L^{-1}$)
Δc	Change in concentration ($mg.L^{-1}$)
ΔH_{ads}	Adsorption enthalpy ($J.mol^{-1}$)
J_P	Pure water flux ($L.m^{-2}.hr^{-1}$)
J_S	Solute flux ($mg.m^{-2}.hr^{-1}$)
J_V	Volume of solvent flux ($L.m^{-2}.hr^{-1}$)
J_{Vlim}	Limiting volume flux ($L.m^{-2}.hr^{-1}$)
K	Mass transfer coefficient ($L.m^{-2}.hr^{-1}$)
k	External mass transfer coefficient ($L.m^{-2}.hr^{-1}$)
K_F	A measure of sorption capacity for Freundlich isotherm ($L.g^{-1}$)
K_L	A measure of the sorption capacity for Langmuir isotherm ($L.g^{-1}$)
L_P	Transport coefficient ($L.m^{-2}.hr^{-1}.bar^{-1}$)
m	Mass of dry chitosan (g)
m_{dm}	Mass of dry membrane (kg)
m_{wm}	Mass of wet membrane (kg)
M_w	Molecular weight ($kg.kmole^{-1}$)
n	Freundlich sorption intensity (-)
ΔP	Pressure difference (bar or Pa)
Q_e	Equilibrium adsorption ($mg.g^{-1}$ of wet chitosan membrane)
q	Adsorption ($mg.g^{-1}$ of dry chitosan)

q_e	Equilibrium adsorption ($mg.g^{-1}$ of dry chitosan)
$q_{theoretical}$	Calculated theoretical adsorption ($mg.g^{-1}$ of dry chitosan)
q_m	Maximum adsorption capacity ($mg.g^{-1}$)
r_P	Maximum pore radius (m)
R	Gas constant (8.314 $J.mol^{-1}.K^{-1}$)
S_{KC}	Surface area ($m^2.m^{-3}$)
T	Temperature (K)
t	Time (hr)
t_0	Efflux time for pure solvent (hr)
V	Volume of liquid through the membrane (L)
V_{fmp}	Volume of the free water in the membrane pores (m^3)
V_{wm}	Volume of the wet membrane (m^3)
x	Membrane thickness (m)
x_c	Mass fraction chitosan in the membrane ($kg.kg^{-1}$)
x_w	Mass fraction water ($kg.kg^{-1}$)

Greek symbols:

ε	Fraction free water volume ($m^3.m^{-3}$)
η	Viscosity (Pa.s)
η_r	Relative viscosity (Pa.s)
ρ_{wm}	Density of the wet membrane ($kg.m^{-3}$)
τ	Tortuosity (-)
γ	Surface tension ($N.m^{-1}$)
$\Delta\pi$	Osmotic pressure difference (bar)
σ	Reflection coefficient (-)
θ	Contact angle
ω	Solute permeability ($mg.m^{-2}.hr^{-1}.bar^{-1}$)

Abbreviations

DDA	Degree of deacetylation
DOC	Degree of crosslinking
MF	Microfiltration
NF	Nanofiltration
PCI	Pressure Control Indicator

RO	Reverse osmosis
UF	Ultrafiltration
SEM	Scanning Electron Microscopy

List of tables

List of figures

CHAPTER 4

CHAPTER 5

CHAPTER 6

APPENDICES

Chapter 1: Introduction

1.1. Background

A clean supply of water is an essential requirement for a sustainable healthy community. It acts as a source of potable water, and supports the growth of aquatic life, thereby providing valuable food supplements. Despite its importance, water throughout South Africa is frequently used to remove domestic and industrial waste products from the community (Horan, 1991), and is as a result widely polluted. This introductory chapter provides the contextual information behind the motivation of the project.

Two acts, the Water Services Act (1998) and the National Water Act (1998), as published in the Government Gazette 18 May 1999 No. 9225 (SA, 1998a), describe water legislation in South Africa (Appendix A-1). The aim of both acts is to improve water supply, water quality and water resource management. This is clearly an important issue in an arid country such as South Africa where most of the economically exploitable water resources are already fully developed (Van Veelen, 1999).

These laws and statutory orders for the prevention of water pollution and waste disposal impose stricter limits and make more demands on the treatment and discharge of especially toxic waste. As a result, industrial enterprises have to be prepared to treat wastewater containing toxic contents according to the most progressive and efficient methods so as to limit pollution and prevent the contamination of natural waters in the future (Volesky, 1989).

A particular area of concern is the release of heavy metals into sewage streams and natural waters by the industrial sector. Impure water containing excessive levels of metals such as copper, zinc, nickel and mercury, is hazardous to human, animal, aquatic and plant life. Due to their toxic and often carcinogenic nature, and the careless, large scale disposal of these metals into the environment, heavy metals have been prioritised as leading contaminants in South Africa (Bux *et al.*, 1994).

Wastewater containing heavy metals originates from many different sources. Industries, such as mining operations (typical coal mine effluent composition, see Table A-2.1, Appendix A-2), metal-plating operations, fertiliser manufacturers, paint manufacturers, electronic device manufacturers and many other industrial operations

often dispose wastewater containing dilute concentrations of heavy metals. The major sources of waste that result from normal plating and metal finishing operations are alkaline cleanings, acid cleanings, spent plating-bath solutions and rinse waters (see Tables A-2.2 – A-2.6, Appendix A-2 for typical rinse water compositions). In the metal plating industry, large amounts of water are used for rinsing, in order to remove the process solution film from the surface of the work pieces. Since heavy metal ions are often toxic at low concentrations and are not biodegradable, they must be removed from the contaminated water (Pulles *et al.*, 1995). The economical value of some heavy metals is another incentive to recover these metals from wastewater.

The conventional way of treating solutions containing very high concentrations of heavy metals is precipitation, where the heavy metal ions are removed from the water by formation of an insoluble salt of the ion (normally hydroxides or sulphides). If required the resulting supernatant liquid has to be treated further to meet the required standards for disposal (Volesky, 1989). Different methods that are currently in use for heavy metal recovery in the electroplating industries are listed in Table A-2.7 (Appendix A-2). Typical efficiencies for the membrane processes reverse osmosis (RO) and electrodialysis (ED) carried out for South African metal plating rinse waters are given in Table A-2.8 (Appendix A-2).

Figure 1.1 gives a summary of the application of the different methods to remove heavy metals from industrial wastewater.

In this study, the removal and recovery of zinc is investigated, since this is the only metal, which consistently appears in industrial effluent samples in high concentrations (Schoeman & Steyn, 1995, Appendix A-2).

A number of studies (Schoeman & Steyn, 1995, Kemmer, 1989, Lewis, 1999) on the zinc removal from wastewater streams with the aim of zinc recovery have already been published. The predominant current recovery process is the precipitation of zinc as zinc hydroxide through the addition of lime. This process alone (which can only reduce the metal concentration to about 100 $mg.L^{-1}$) cannot reduce the zinc concentrations (ranging from up to 2000 $mg.L^{-1}$ zinc) to the disposal levels dictated in the legislation (<5 $mg.L^{-1}$). Zinc can also be removed by cation exchange (either on a sodium or a hydrogen cycle), reverse osmosis, filtration, electrochemical treatment and evaporation techniques each with its own characteristic advantages and disadvantages (Kemmer, 1989 and Table A-2.7-8, Appendix A-2).

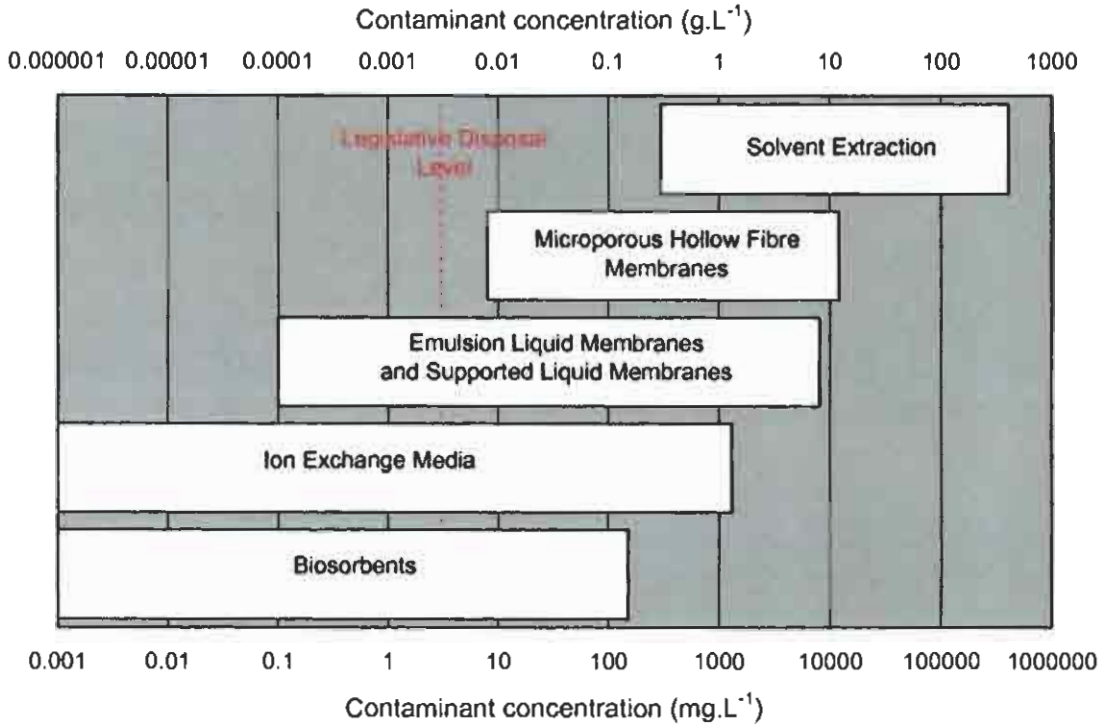

Figure 1.1: Niche areas for treatment methods.

To date, none of these processes has been widely adopted in the reduction of zinc waste as they either: generate waste streams (*e.g.* reverse osmosis); have high capital costs (*e.g.* cation exchange); or are energy intensive (*e.g.* evaporation, filtration and electrochemical treatment) (Lewis, 1999). These problems are especially significant when the zinc is in solutions containing less than 100 $mg.L^{-1}$ dissolved metals (Volesky, 1989).

In the search for possible replacements for these conventional processes, intensive studies have been conducted on biological water treatment, but inferior water quality is still obtained, mainly due to the high concentrations of heavy metals often proving toxic to activated sludge biomass (Bux *et al.*, 1994).

Adsorption processes are another alternative method to separate heavy metals from wastewater. Commercial adsorption processes exist, generally using activated carbon as the adsorbent (Lewis, 1999). Recently, several other (biological) adsorbents, like peat moss (Huang *et al.*, 1996), rice husk (Khalid & Ahmad, 1998), marine algae (Matheickal & Yu, 1999), sheep manure waste (Kandah, 2001) chitosan flakes (Bassi *et al.*, 2000) and chitosan beads (Guibal *et al.*, 1998 and Kawamura *et al.*, 1997) have been studied as alternative adsorbents for the removal

of heavy metals from contaminated water. These materials can be obtained from plant, microbial or animal origin, are abundantly available in the biosphere and have a great commercial potential.

In a review of low-cost adsorbents, Babel and Kurniawan (2003) reported that chitosan, a deacylated (poly)-glucose amine, is one such adsorbent with notable high adsorption capacities. Chitosan is a derivative of chitin, a biopolymer that is synthesised at an approximate rate of 10 Gton/year and is mainly found in the exoskeleton of arthropods like crabs, shrimps and lobsters. Chui *et al.* (1996), Jha *et al.* (1988) and Rorrer *et al.* (1993) reported that chitosan shows an exceptionally high affinity to cadmium, copper, zinc, chromium, mercury, manganese and nickel. The complexing properties of chitosan are caused by an advantageous location of both hydroxide and amine groups. It is proven that chitosan forms chelate compounds with metal ions with the release of hydrogen ions. Therefore, chitosan regeneration and metal recovery are obtained through pH manipulation. Since ligands are frequently only active when ionised, a pH shift can be used to deactivate the ligand and remove the metal ligand complex (Volesky, 1989).

These studies have motivated this intensive study on the potential application of chitosan (synthesised from South African derived chitin) in the removal of heavy metals from industrial wastewater. Currently, there is no effort to recover chitin from the waste material resulting from the fishing industry in South Africa, which may be a valuable source of chitosan.

Chitosan is an adsorption material that is used in the form of flakes, beads and membranes. It is known from literature that, when using chitosan flakes (the form in which chitosan is obtained from chitin), metal ions do not completely penetrate the particle and the metal preferentially adsorbs near the outer surface of the particle (Guibal *et al.*, 1998). As metal ions penetrate the porous particle and are adsorbed onto the exposed amine sites from the outer surface inwards, the formation of adsorbed metal clusters may constrict or completely block pores, rendering amine sites deep in the interior of the particle inaccessible for heavy metal ion adsorption (Rorrer *et al.*, 1993), resulting in relatively poor adsorption capacities. Therefore, most research is not focussed on chitosan flakes but on other formulations of chitosan, like chitosan beads (Grant, 2000, Jansen, 2002, Osifo, 2005), immobilised chitosan (Nkalanga, 2003) and chitosan membranes (this thesis).

An advantage of using chitosan membranes can be the improved contact between wastewater and chitosan material, since the contaminated water is pressed through the membrane (convective transport), in contrast to chitosan beads, where diffusion is the main transport mechanism in the chitosan material (Kaminski & Modrzejewska, 1997). If additionally contaminants are present which could be separated by ultrafiltration, the use of an adsorptive membrane may reduce the number of separation units in practice.

1.2. Motivation for, and objectives of the investigation

The motivation for this research project stems mainly from the legislatively and economically driven need for a new water treatment process in the removal of heavy metals. The overall objective of the study is to investigate the suitability of chitosan membranes for the treatment of industrial wastewater on a laboratory scale. This study was carried out at the North-West University in Potchefstroom and the Vaal University of Technology in Vanderbijlpark, both situated in South Africa. The specific objectives of this study are the following:

- To prepare chitosan membranes from South African waste.
- To characterise the membrane structure.
- To model the transport through the membrane.
- To evaluate the membranes, with respect to the adsorption and desorption of zinc from simulated industrial wastewater.
- To compare adsorption and desorption to other adsorbents.

1.3. Scope of the investigation

This thesis reports on the removal of zinc ions from simulated wastewater using chitosan membranes as described in Chapter 1. Chapter 2 deals with the raw material production and characterisation. The characterisics of the selected biopolymer, chitosan, is correlated with the respective manufacturing and/or processing parameters.

Chapter 3 deals with membrane preparation and the importance of solution viscosity during the preparation stage. The membrane production procedure is optimised to obtain maximum flux and adsorption capacity. The experiments, carried out for this purpose, were designed according to a statistical design procedure. The effect of

membrane crosslinking, to prevent the membrane dissolving in acidic media, was also investigated.

In Chapter 4, a thorough membrane characterisation is presented, in order to identify the structure of the produced chitosan membranes. This characterisation provides additional information for describing the transport through the chitosan membranes.

A model, to describe the transport through chitosan membranes, is presented in Chapter 5, and the investigation into the influence of relevant process parameters on the membrane performance is reported.

In Chapter 6, the adsorption characteristics of zinc-ions on chitosan membranes are reported. Adsorption isotherms are presented and the relevant adsorption parameters are outlined. The adsorption capacity of chitosan membranes is also compared with that of chitosan powder, chitosan flakes, chitosan beads, chitin and other adsorption materials. Results from dynamic studies are used to determine the breakthrough curve of chitosan membranes, are reported, as are the effects of contaminants and of pH on adsorption capacity. Finally, the regeneration of chitosan membranes is studied. In Chapter 7, general conclusions are presented and recommendations are made. A critical evaluation and interpretation of the accumulated experimental results is executed, and the advantages and disadvantages of the implementation of chitosan membranes for the recovery of heavy metals on an industrial scale are presented.

Chapter 2: Chitosan production and characterisation

2.1. Introduction

Chitosan materials, isolated from aquatic organisms, are a new class of potentially inexpensive and environmentally benign solid adsorbents that exhibit a high selectivity towards heavy metal ions. Several studies (Bassi *et al.*, 2000, Eiden *et al.*, 1980, Guan *et al.*, 1996, Guibal *et al.*, 1999a, Guibal *et al.*, 1999b, Huang *et al.*, 1996, Jha *et al.*, 1988, Kawamura *et al.*, 1997, McKay *et al.*, 1989, Rorrer *et al.*, 1993) have produced results where chitosan (produced from chitin) is used for the removal of metal ions from contaminated water.

Chitin is the second most abundant naturally occurring polysaccharide in the world after cellulose. It consists of amino sugars with a regular distribution of amino groups and is present in the exoskeletons of arthropods, crustaceans and insects (Peter, 1995). Although chitin can also be extracted from the cell walls of diatoms, algae, fungi, microfauna, plankton and yeasts, the shells of molluscs, and the bones of cuttlefish, it is only manufactured on a commercial basis from crab, lobster, prawns and shrimp shell wastes. In December 2001, Biopolymer Engineering Inc. (Eagan, USA), announced that it had completed the first phase of a chitin extraction plant, using the langostino lobster as the raw material. Here chitin is converted to chitosan in the world's largest chitosan manufacturing facility with a capacity of 2000 tons per year (www.biopolymers.com).

The various chitin sources differ in their chitin content, with crab and prawn shells containing up to 40% chitin (Kyoon No & Meyers, 1997). Element analyses carried out for chitin isolated from various sources give a value of approximately 9% nitrogen, nitrogen being active in adsorption. Chitin is a biodegradable and non-toxic organic compound. It is insoluble in water, dilute mineral acids, and alkalis (Ghandi, 1997). Chitin (Figure 2.2) consists of (1-4)-2-acetamido-2-deoxy-β-D-glucan units, some of which are deacetylated (Volesky, 1989, Roberts, 1992). Its structure resembles that of cellulose (Figure 2.1), except that acetylamino groups (Chui *et al.*, 1996) have replaced the hydroxyl groups in the position as indicated in Figure 2.1.

In general, chitin is found in association with proteins and minerals such as calcium carbonate (Chui *et al.*, 1996), and a demineralisation- and deprotonation step is

therefore normally required before obtaining chitin in a pure form either as flakes or fine powder (Gandhi, 1997).

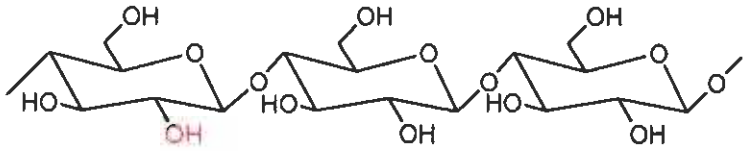

Figure 2.1: The chemical structure of cellulose.

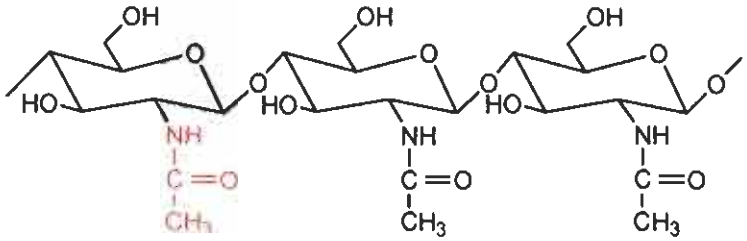

Figure 2.2: The chemical structure of chitin.

Chitosan is a biopolymer that is obtained by deacetylation. It is a chemical derivative where at least 50% of the acetyl groups have been removed from the chitin (DDA>50%). Another criterion for distinguishing between chitin and chitosan is the solubility of the polymers in dilute aqueous acid: chitin is insoluble while chitosan forms viscous solutions (Peter, 1995). Chitosan is a polysaccharide formed primarily of repeating units of (1-4)-2-amino-2-deoxy-β–D-glucan (or D-glucosamine), the presence of amino groups in chitosan makes it superior to chitin as metal adsorbent. The structure of chitosan is shown in Figure 2.3.

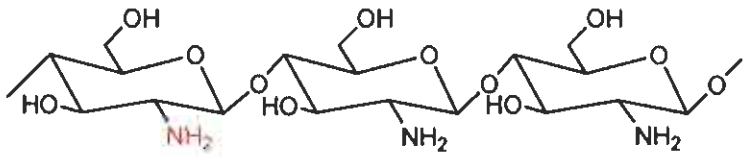

Figure 2.3: The chemical structure of chitosan.

Section 2.2 describes on the production of chitin and chitosan from different sources, and the characterisation of the produced chitosan in terms of molecular weight and degree of deacetylation (DDA).

The results of preparation and characterisation are given in Section 2.3. Finally, the conclusions are presented in Section 2.4.

2.2. Experimental procedure

Chitin and chitosan were prepared from different sources and were compared to commercially available chitosan. Section 2.2.1 reports on the production of chitin from different sources and Section 2.2.2 reports on the production of chitosan. In Section 2.2.3, the different techniques relevant to chitosan characterisation are discussed.

2.2.1. Chitin production

Three different sources of chitin were used in this study:

Chitin A: Rock lobster was used as raw material to produce chitin flakes which was carried out by BioSpec (Cape Town, South Africa).

Chitin B: Industrial grade chitin powder (obtained from crab shells) was purchased from SIGMA (Cat. No. 41795-5).

Chitin C: Chitin flakes were produced from a mixture of lobster (10%), crab (2%) and prawn shells (88%) obtained as waste from a South African restaurant (Rio del Sol, Vanderbijlpark).

The chitin was produced using the equipment shown in Figure 2.4 and according to the procedure given in Figure 2.5.

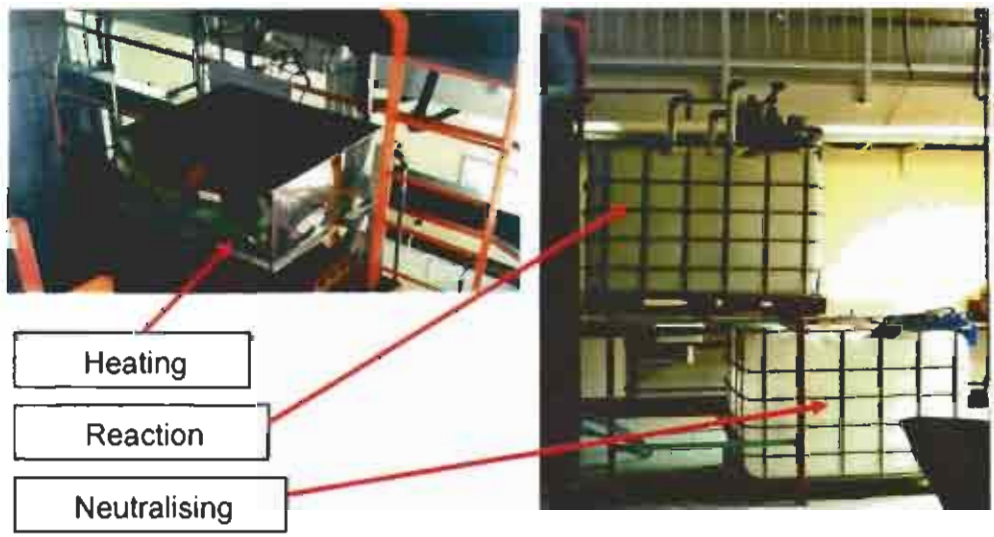

Figure 2.4: Equipment for the production of chitin and chitosan.

The production of chitin flakes (Chitin A and Chitin C) from crustacean shells using the method of Chui *et al.* (1996) requires the following:

1. Shell crushing: The crustacean shells were crushed in a crusher (Dickie and Stockler Pty. Ltd.) five times, to a diameter of 1 - 5 mm.
2. Deproteinisation: The crushed shells were added to the reaction tank for deproteinisation under well-mixed conditions for 6 hours. The reaction was carried out at 100°C. A ratio of 0.5 kg of 8 mass% sodium hydroxide solution for every 1 kg flakes was used. The sodium hydroxide solution was prepared by adding sodium hydroxide (97% pure supplied by Saarchem Ltd.) to de-ionised water that was preheated in the heating tank to a temperature of 80°C.
3. Primary washing: The deproteinised shells were then transferred back to the reaction tank and washed with de-ionised water in three cycles (five times the volume of water per volume of flakes was used for a period of 10 minutes per cycle).
4. Demineralisation: After primary washing, demineralisation was carried out in the reaction tank in a 10% hydrochloric acid (33% pure supplied by Saarchem Ltd.) solution, under well-mixed conditions for 6 hours.
5. Secondary washing: After demineralisation, the flakes were washed again in the reaction tank with five times the volume of water per volume of flakes under well-mixed conditions for 10 minutes.
6. Drying: After secondary washing, the chitin was finally dried in an oven at 50°C for 6 hours.

Steps 2 through 5 are followed by filtration through a nylon mesh to recover the shells. The spent hydrochloric acid from the demineralisation cycle was stored in the neutralisation tank.

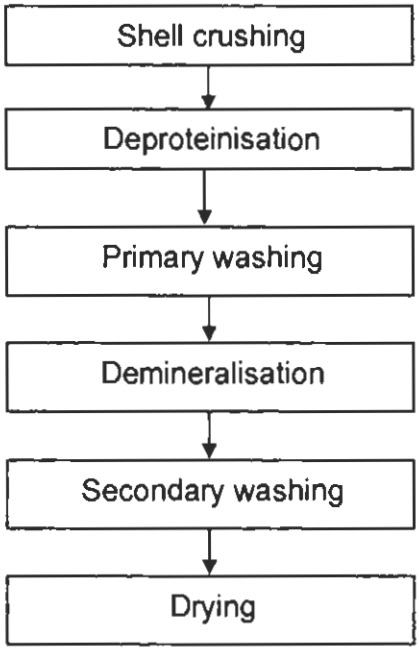

Figure 2.5: Procedure for the production of chitin flakes.

2.2.2. Chitosan production

Three different types of chitosan flakes were produced for this study:

Chitosan A: Produced from Chitin A

Chitosan B: Produced from Chitin B

Chitosan C: Produced from Chitin C

Chitosan A, Chitosan B and Chitosan C flakes are produced by the method of Huang *et al.* (1996) also in the equipment shown in Figure 2.4 and according to the procedure given in Figure 2.6:

1. Deacetylation: The chitin was transferred into the reaction tank for deacetylation (45 kg of sodium hydroxide solution per kg of chitin) for 6 hours at a reaction temperature of 120°C. The 50 mass% sodium hydroxide solution was prepared by adding sodium hydroxide (97% pure supplied by Saarchem Ltd.) to de-ionised water that was preheated in the heating tank to a temperature of 80°C.
2. Washing: After deacetylation, the chitosan was washed in the reaction tank with five times the volume of water per volume of flakes under well-mixed conditions for 10 minutes.
3. Drying: The chitosan was then dried in an oven at 50°C for 3 hours.

The deacetylation step is followed by filtration through a nylon mesh to recover the chitosan. The spent sodium hydroxide from the deacetylation cycle was used to neutralise the spent hydrochloric acid (stored in the neutralisation tank) from the chitin production under well-mixed conditions before disposal.

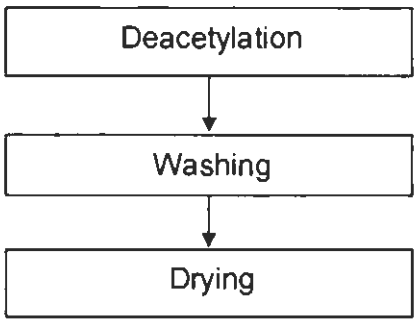

Figure 2.6: Procedure for the production of chitosan.

2.2.3. Characterisation of chitosan

After the production of chitosan, the molecular weight and the degree of deacetylation were determined using the methods as described by Kotze (2001).

A Size Exclusion Chromatography/Multiple Angle Laser Light Scattering (SEC/MALLS) technique was used to characterise the molecular weight of the chitosan using TSK GW columns with an on-line double detection system including a Waters R410 differential refractometer and a Dawn Wyatt multiangle laser light scattering photometer (for more detail, see Appendix B-1.1).

To determine the degree of deacetylation (DDA) of the chitosan samples, infrared spectroscopy (IR-spectroscopy) was chosen, specifically the pellet method. A Fourier transform infrared analyser with a Nicolet MAGNA-IR 550 Spectrometer Series II was also used for this purpose (for more detail, see Appendix B-1.2).

2.3. Results and discussion

Chitin was produced according to the procedure given in Section 2.2.1. The production of chitin has a yield of 26% and a total mass of 12 kg was produced. The chitosan was produced according to the process outlined in Section 2.2.2 and was

obtained as flakes (Shown in Figure 2.7) with an average diameter of 1.5 mm. The yield of chitosan was 18%.

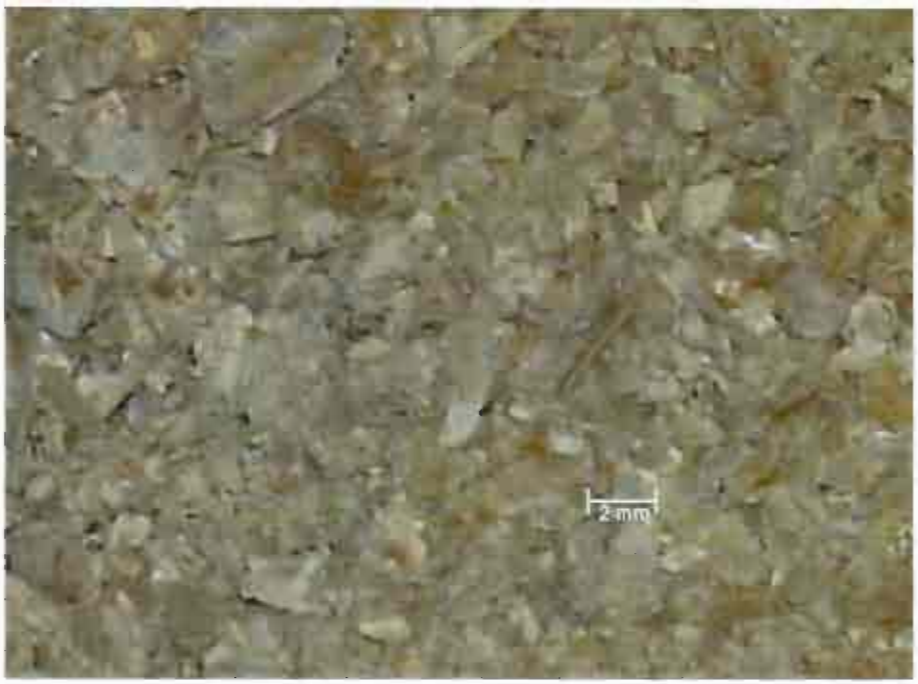

Figure 2.7: Chitosan flakes.

The physicochemical parameters for the different types of chitosan used in the studies are given in Table 2.1 and Table 2.2. The three different types (A, B and C) as mentioned in Section 2.2.2 were compared to the DDA and molecular weight of commercially available chitosan (D: Low molecular weight chitosan (Cat. No. 41796-1), E: High molecular weight chitosan (Cat. No. 41796-5), and F: Industrial grade chitosan (Cat. No. 41796-3), all purchased from SIGMA).

Table 2.1 shows that the molecular weight of the chitosan depends on the source of the raw material (Chitin) and that the DDA is equal for the different sources. The chitosan A, B and C have a DDA of 77%, 78% and 79% respectively, after a deacetylation period of six hours (Kotze, 2001). Comparing the results with the commercially available chitosan, it can be concluded that chitosan A is most similar to the industrial grade chitosan.

Table 2.1: Parameters of produced chitosan.

	Produced chitosan		
Characteristics	Chitosan A	Chitosan B	Chitosan C
Molecular weight ($kg.kmol^{-1}$)	144 200	298 900	201 300
Degree of deacetylation (DDA)	77%	78%	79%

Table 2.2: Parameters of commercial chitosan.

	International chitosan		
Characteristics	Chitosan D	Chitosan E	Chitosan F
Molecular weight ($kg.kmol^{-1}$)	60 000*	400 000*	150 000*
Degree of deacetylation	>98%*	>98%*	>98%*

**values taken from suppliers*

2.4. Conclusions

Chitosan was produced from both cape rock lobster and from a mixture of crushed lobster, crab and prawn shells with an average diameter of 1.5 mm. The yield in the production of chitin was 26%, and the successive conversion to chitosan resulted in a yield of 18%. The molecular weight of the chitosan was found to depend on the source of the raw material, while the DDA of the chitosan produced from both sources did not differ significantly. The structure and molecular weight of the chitosan, produced from the cape rock lobster (M_w = 144 200 $kg.kmole^{-1}$) compared very well with the industrial grade chitosan (M_w = 150 000 $kg.kmole^{-1}$), however the DDA of the produced chitosan (DDA=77%) is lower than that of the industrial grade chitosan (DDA>98%).

Chapter 3: Membrane preparation

3.1. Introduction

South Africa contains numerous, under-utilised materials of biological origin with great commercial potential. Specifically chitosan has been shown to demonstrate an exceptionally high potential as an alternative adsorbent for heavy metals (Volesky, 1989). From a review study by Guibal (2004), it is known that chitosan-gels have better adsorption properties than chitosan flakes. One, not frequently studied, formulation of chitosan gels is in the form of membranes, the efficiency of which (flux and adsorption) depends on the manufacturing process. This chapter reports on the optimum manufacturing conditions for chitosan membranes.

The literature survey (Section 3.2), reports on chitosan membrane preparation and the importance of solution viscosity during the preparation stage. In Section 3.3, the experimental design, experimental procedures and membrane optimisation are discussed. The results and discussion are presented in Section 3.4; and the final conclusions in Section 3.5.

3.2. Literature survey

Only two studies, Kaminski and Modrzejewska (1997) and Krajewska (2001) address the adsorption of heavy metals on gel type chitosan membranes. Both studies describe the preparation of chitosan membranes as a phase inversion method that is divided into three steps (see Figure 3.1).

The processing steps are: solution preparation; phase inversion; and crosslinking. Important parameters that influence the solution preparation are the chitosan characteristics (*e.g.* molecular weight and degree of deacetylation), chitosan concentration and the organic acid concentration. These parameters are important in describing the dissolution time and viscosity of the chitosan solution (Kawamura *et al.*, 1997).

The second step (phase inversion) is influenced by the alkalinity of the solution. Less important parameters when casting a membrane using the phase inversion technique are the reaction time, if sufficient, and the temperature; normally the phase inversion is carried out at room temperature. In the third step the membranes need

to be crosslinked to make them insoluble in acidic media. Important factors during crosslinking are the type of reactant used for crosslinking, the method of crosslinking and the duration.

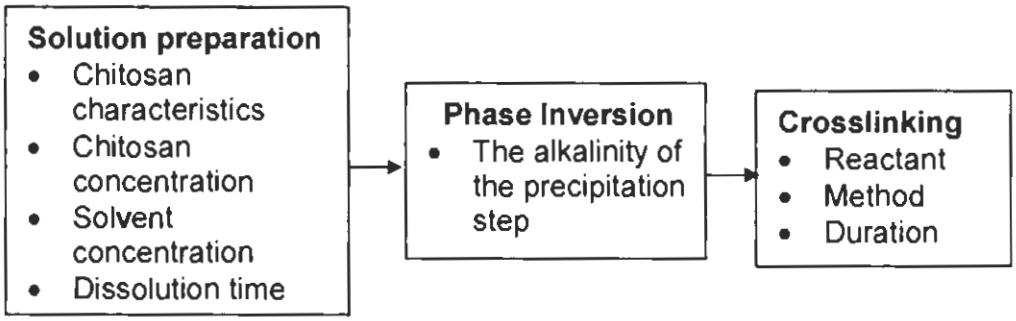

Figure 3.1: The process of membrane preparation and the factors influencing the processing steps.

- Solution preparation

Chitosan is soluble in solutions of most acids, especially organic acids (*e.g.* formic-, acetic-, malic-, tartaric-, adipic- and citric acid), in which it forms clear viscous solutions (Hudson & Smith, 1998). The viscosity of the solution allows the formulation of different chitosan-gels (*e.g.* beads or membranes).

In general, the dissolution time (Collins, 1973) and viscosity of the chitosan solution influence the membrane strength. It is essential that the chitosan is completely dissolved during solution preparation so as to avoid an inhomogeneous solution resulting in membranes that contain cracks. The viscosity influences the density of the available adsorption sites and their accessibility and is therefore the most important factor in membrane preparation (Conway *et al.*, 1999). The viscosity depends on a number of variables, which are (Young, 1980):

1. The concentration of the chitosan
2. The concentration of the solvent
3. The molecular weight of the chitosan
4. The degree of deacetylation of the chitosan
5. The temperature

By varying the viscosity, chitosan membranes with the desired apparent density and amino group concentration can be manufactured (Kawamura *et al.*, 1997). The

primary factor affecting the viscosity is the chitosan concentration in the organic acid solution.

- Phase inversion

After its formation the viscous chitosan solution is cast on a support and immersed in an alkaline solution for phase inversion, during which the chitosan is converted from the dissolved state to a gel state. By varying the concentration of the alkaline solution, the membrane morphology (pore radius, porosity, and specific surface area) can be controlled (Kawamura *et al.*, 1997).

- Crosslinking

The produced chitosan membrane is soluble at low and high pH owing to protonation of the amine or glycosamine nitrogen functionality and deprotonation of a hydroxyl group of quinolinol, respectively. Since the recovery of adsorbed metals from the chitosan is performed at low pH, the membranes should be crosslinked (Inoue *et al.*, 1996) in order to counteract the dissolution of chitosan (Yang & Zail, 1984) and enhance the performance in acidic and alkaline environment. Crosslinking can be carried out by the chemical binding of two chitosan polymer chains with a covalent bond (Le Dung *et al.*, 1994), which affects the physical, mechanical and thermal properties of chitosan (Guan *et al.*, 1996).

The crosslinking reaction results in the blocking of some adsorption sites, as they are involved in the crosslinking reaction (Huang *et al.*, 1996). Chemical crosslinking can be carried out with dialdehydes, esters or ethers, or epichlorhydrin (Milot *et al.*, 1997). The use of a bifunctional reagent, glutaraldehyde, was first reported by Koyama and Taniguchi (1986), and is the most frequently used reagent in chitosan modification. In this study chitosan was crosslinked with glutaraldehyde according to the procedure described by Guibal *et al.* (1999b) and schematically shown in Figure 3.2.

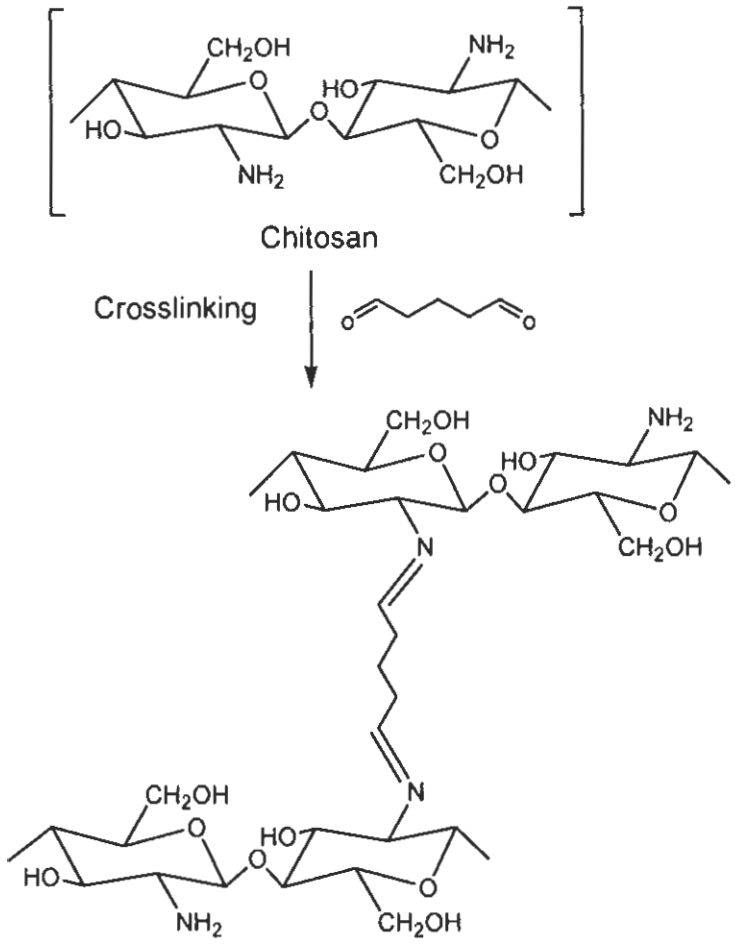

Figure 3.2: Crosslinking of chitosan using glutaraldehyde (Guibal *et al.*, 1999b).

3.3. Experimental

This section focuses on the procedures for the optimisation of membrane production with respect to membrane flux and zinc adsorption as these are influenced by the chitosan-, acetic acid-, and sodium hydroxide concentrations and the degree of crosslinking.

3.3.1. Experimental design

The starting point of the experimental design was to list the most important parameters that influence the membrane manufacturing process. The effects of these parameters on both transport and adsorption characteristics of the membrane were measured, and a statistical design procedure was used to determine the optimum membrane manufacturing conditions.

Statistica for Windows (Cerisier, 1994) was used to do a central composite design while response surface methods were used to achieve a second order composite design. In this procedure, the influence of a number of factors on the response were simultaneously obtained, and empirical equations set up so as to draw three-dimensional plots of the responses obtained. The purpose of the design was to fit a n-dimensional surface to the points with the method of least squares. The surface could then be analysed mathematically and the relationship between the different factors could be determined. Several variables were simultaneously changed to identify the interactions between variables and determine the optimum conditions.
This procedure reduced the number of experiments required to optimise conditions. The experimental profile of the experiments is given in Appendix C-1. The range values for the factors were determined for the experimental design (minimum and maximum values were assigned for the different parameters), and a set of experiments were designed.
The correlation coefficient for the statistical fit (R^2), is a measure of the quality of fit (if the R^2 is 0.9, it implies that 90% of the responses is explained by the fit, and the other 10% are suspected to be uncontrollable factors). The correlation coefficient for the experiments in this chapter is at least 0.9. For all experiments, chitosan membranes were manufactured in triplicate and the data present the average of the three values. The error was determined statistically and the coefficient of variation (which gives the standard deviation as a percentage of the arithmetic mean) was 2%.
To describe and evaluate the manufactured membranes, it is important to know the properties and characteristics of the chitosan membranes. For the adsorption of heavy metals from wastewater, the adsorption capacity and the flux through the membrane are the two most significant characteristics of the membrane.

3.3.2. Experimental membrane preparation

In this section, the preparation of chitosan membranes is reported. As mentioned in Section 3.2, the viscosity of the chitosan solution is of high importance in membrane production. For viscosity studies, different types of chitosan (Chitosan A-F) that vary in molecular weight and DDA were used. In addition, the process variables for manufacturing the membrane (chitosan-, acetic acid- and sodium hydroxide concentration) were also varied. The membranes were produced using a phase

inversion method as described by Kaminski and Modrzejewska (1997), which has been used by several other researchers (*e.g.* Guibal *et al.*, 1999a and Kawamura *et al.*, 1997) to produce chitosan beads.

The method consists of the solution preparation, phase inversion and crosslinking steps (see Figure 3.1).

- Solution preparation

The effects of the type of chitosan (molecular weight and degree of deacetylation) and process variables (chitosan concentration and acidic acid concentration) were evaluated using the viscosity as the most important parameter affecting the membrane properties (Kaminski & Modrzejewska, 1997).

The viscosity of the chitosan solution was determined after the complete dissolution of chitosan into the acetic acid solution. The apparatus used for the viscosity measurement was the Ostwald Viscometer (see Appendix C-2.1). The temperature was kept constant at 25°C during viscosity measurements.

The solution was prepared by dissolving chitosan (1 to 9 mass%) in a 1 to 7 mass% acetic acid solution (96% pure supplied by Merck) using a magnetic stirrer at 100 rpm for 24 hours (Figure C-3.1, Appendix C-3). These conditions were sufficient to obtain a homogeneous chitosan solution.

- Phase inversion

The viscous chitosan solution was poured into a mould on a flat surface (glass plate). The mould and chitosan solution were carefully placed into a 1 to 9 mass% aqueous solution of sodium hydroxide (97% pure supplied by Saarchem Ltd) for 15 minutes at a constant temperature of 25 °C. After the membranes were formed, they were washed using flowing de-ionised (<0.5 µS/cm) water for 2 minutes, and the membrane and the mould were removed from the glass plate. The membrane was then removed from the mould and conditioned in de-ionised water for 1 hour, after which it was again washed in de-ionised water until a neutral pH was obtained. Throughout the process of manufacturing, the temperature was kept constant at 25 (± 1) °C. The average dimensions of the disk shaped membranes are 0.8 mm thickness with a 47 mm diameter.

- Chemical crosslinking

To prevent chitosan dissolving in acidic media, the membranes were crosslinked according to the procedure described by Guibal *et al.* (1999b). In this method, the membranes were crosslinked in a 2.5 mass% solution of glutaraldehyde (25% pure supplied by Merck) at 25 °C. A volume of 1.5 cm^3 glutaraldehyde solution per gram of wet membrane was used, which corresponds to an equimolar ratio. After crosslinking the membranes were washed thoroughly to remove all glutaraldehyde.

3.3.3. Membrane optimisation

The membranes were tested using a 500 $mg.L^{-1}$ zinc solution (99% pure $ZnSO_4 \cdot 7H_2O$ supplied by Merck) at 25°C in de-ionised water. This concentration is the average reported amount in the industrial wastewater to be treated (Schoeman & Steyn, 1995). This relatively high concentration has also been used to ensure full occupancy of the adsorption sites. The solution was continuously stirred above the membrane to prevent concentration polarisation. Figure 3.3 shows the equipment used for flux and adsorption determination.

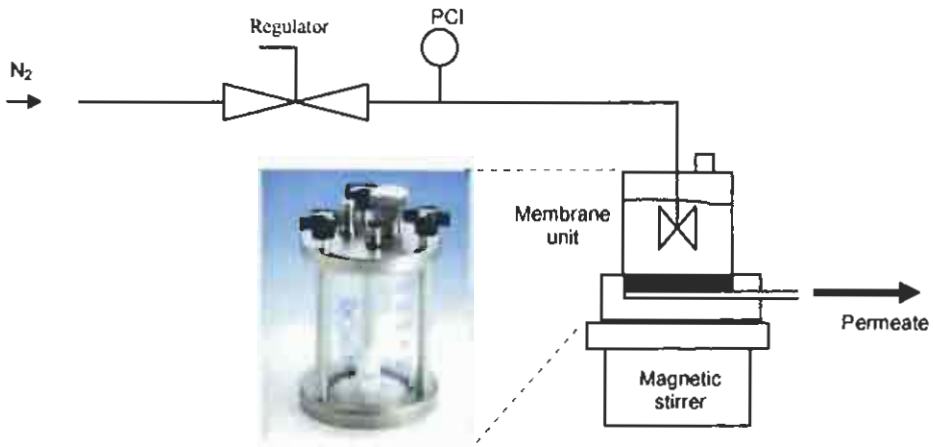

Figure 3.3: Liquid flux set-up for flux and adsorption studies.

The pH of the zinc solution was controlled at a pH of 5 using dilute sulphuric acid (from 98% pure supplied by Saarchem Ltd); dilute sodium hydroxide (from 97% pure supplied by Saarchem Ltd) and measured with a Jenway 3310 pH meter. The membrane was clamped in the membrane holder and the zinc solution was pressed through the membrane at 25°C. The flux and adsorption were tested under a 50 kPa

pressure difference, applied to the cell using pressurised nitrogen from a gas bottle. For the optimisation procedure, one litre of solution was transported three times through the membrane, until equilibrium (the zinc concentration in the filtrate did not change) was reached. The time required for one litre of solution to permeate through the membrane was in the order of tens of hours. The adsorption capacity of the membranes was tested by quantitative analysis of the zinc ion concentration present in the filtrate using Atomic Absorption Spectrophotometer analysis (Perkin Elmer, Aanalyst200 Model B3150070).

The flux is expressed as the volume flow through the membrane per unit area and time

$$J_V = \frac{V}{A \cdot t} \qquad \text{.....3.1}$$

while the adsorption capacity is described by the amount of heavy metal adsorbed per unit of dry adsorbent

$$q_e = \frac{(C_{in} - C_e) \cdot V}{m} \qquad \text{.....3.2}$$

3.4. Results and discussion

In this section, the effect of preparation on the performance of chitosan membranes is reported. The effect of the molecular weight, and DDA on the viscosity is discussed in Section 3.4.1, and the effect of crosslinking on the flux and adsorption In Section 3.4.2. Section 3.4.3 evaluates the flux, and Section 3.4.4 the adsorption as functions of the process variables. Finally, Section 3.4.5 presents the optimised conditions for the manufacture of the membrane.

3.4.1. Viscosity of chitosan solution

Figure 3.4 shows the effect of the chitosan molecular weight and DDA on the viscosity of a 7% chitosan in a 4% acetic acid solution (Table C-3.1, Appendix C-3). It is clear that the viscosity increases with an increase of the molecular weight of the chitosan in the chitosan/acetic acid solution. Chitosan A and Chitosan F, having

approximately the same molecular weight, but having a difference in DDA of 77% to 98% have the same viscosity in solution (Figure 3.4). The effect of the degree of deacetylation on the viscosity is not significant, as was reported by Muzzarelli (1977). It was also observed visually that the dissolution time of chitosan increases as the molecular weight of chitosan increases, as was noted by Collins (1973).

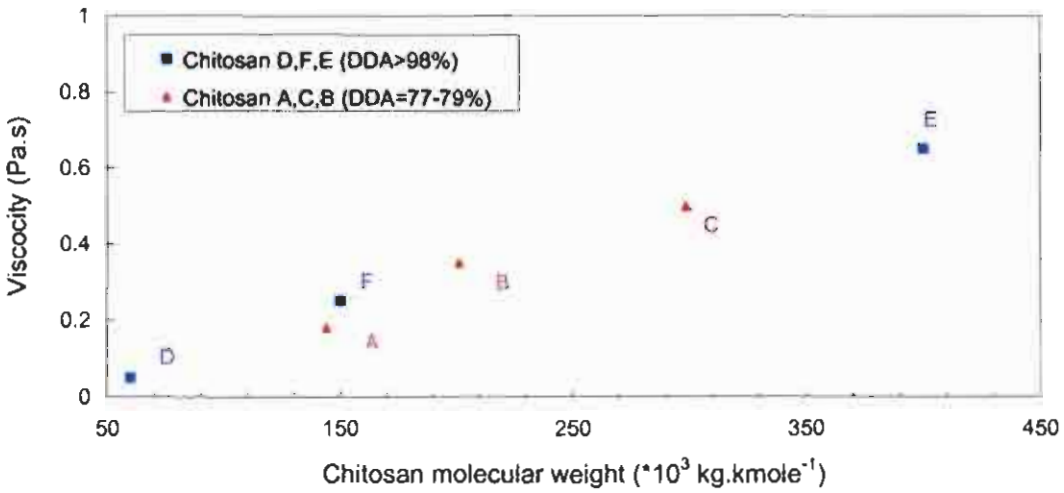

Figure 3.4: Effect of chitosan molecular weight and DDA on the viscosity of a solution of 7% chitosan in 4% acetic acid.

From this figure it can also be seen that Chitosan A has a relatively low molecular weight and therefore results in less viscous solutions. For this reason a higher chitosan concentration can be used and thus a higher adsorption capacity is obtained in the preparation of stable chitosan membranes. Therefore, Chitosan A was selected for further studies.

Figure 3.5 shows the effect of the chitosan- and acetic acid concentration on the viscosity of the Chitosan A solution (Appendix C-1). From this figure, it can be seen that the chitosan concentration has the largest effect on the viscosity of the polymer-solution as viscosity increases significantly with the chitosan concentration, but only marginally with an increase in acetic acid concentration, as was also reported by Muzzarelli (1977). The effect of chitosan concentration is attributed to the difference in molecular dimensions between the chitosan and the acetic acid (Young, 1980). Similar trends were obtained for the other chitosans used (chitosan B-F).

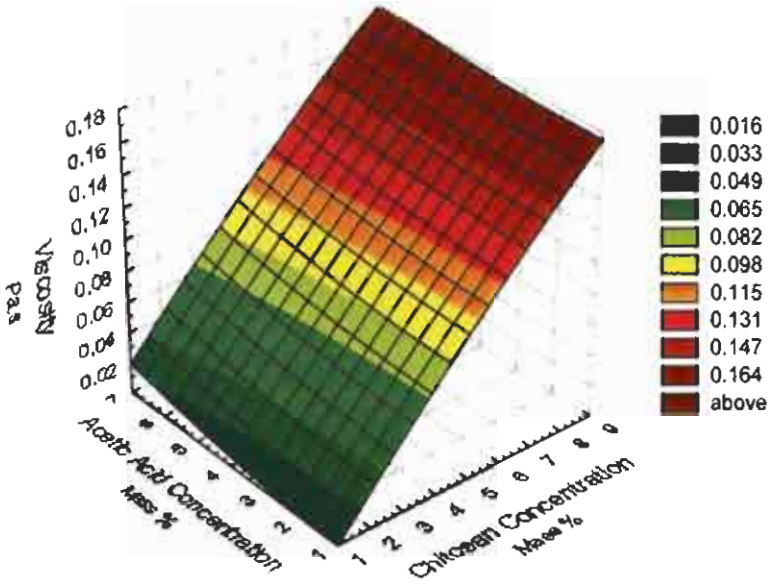

Figure 3.5: Influence of the chitosan concentration and acetic acid concentration on the viscosity of the chitosan solution (Chitosan A at 298K).

3.4.2. The effect of crosslinking on the flux and adsorption

The effects of crosslinking time were determined by crosslinking chitosan membranes for periods of 0, 3, 6, 9, 12, 15, 18, 21 and 24 hours. The effect of crosslinking time on the flux of a 500 mg.L^{-1} Zn^{2+} solution is given in Figure 3.6 (Table C-3.2, Appendix C-3).

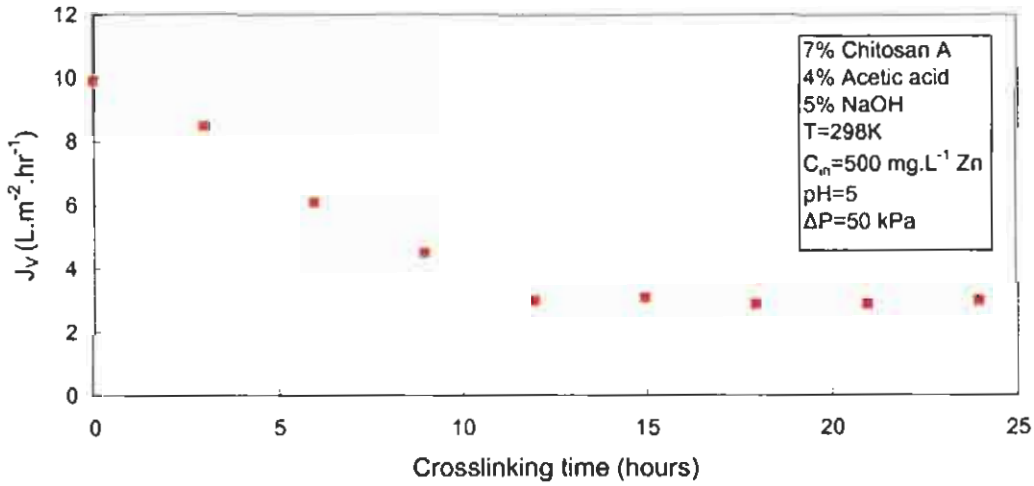

Figure 3.6: Effect of crosslinking time on the flux through the membrane.

From this figure, it can be concluded that the flux decreases relative to the increase in crosslinking time and reaches a constant minimum at 3 $L.m^{-2}.hr^{-1}$ after 12 hours. This trend can be explained by:

- Crosslinking resulting in less free water volume and thus lower flux (Collins, 1973).
- The degree of crosslinking increasing with time initially, until no further crosslinking occurs and the degree of crosslinking remains constant. This has also been reported by Collins (1973), and explains the period after 12 hours, where the flux remains constant.

The effect of crosslinking time on adsorption capacity is shown in Figure 3.7. (Table C-3.2, Appendix C-3). With increasing crosslinking time the adsorption of the zinc decreases in the time range of 0 to 12 hours crosslinking time. After a crosslinking time of 12 hours, the adsorption capacity remains constant. This trend is comparable to the effect of crosslinking time on flux through the membrane. Because amino groups are used in the crosslinking reaction (see Figure 3.2) less amino groups are available as adsorption sites as crosslinking progresses (*e.g.* Guibal *et al.*, 1999b).

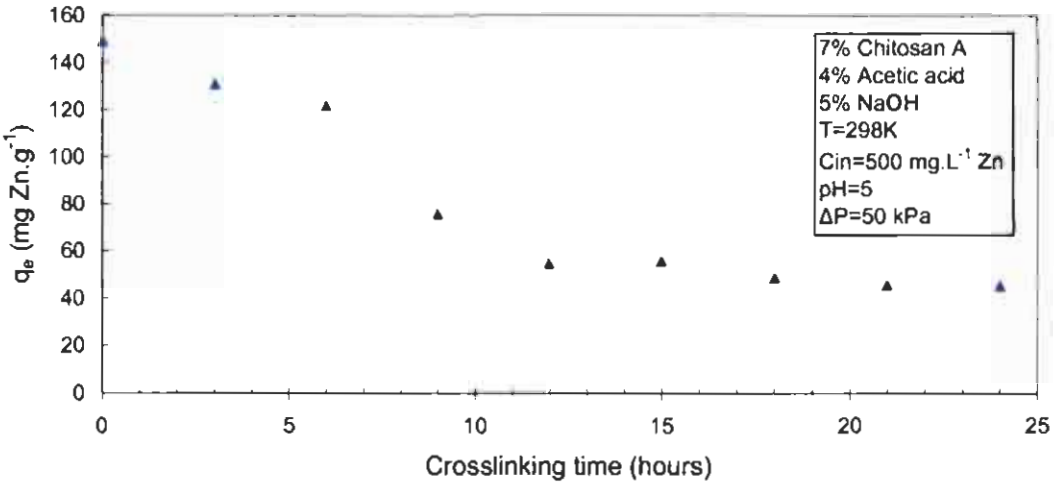

Figure 3.7: Effect of crosslinking time on the adsorption capacity.

The minimum crosslinking time required to render the chitosan stable in an acidic solution was determined by crosslinking chitosan membranes for periods of 0, 3, 6, 9, 12, 15, 18, 21 and 24 hours and visual inspection of the membranes after being in

contact with the acidic medium at a pH of 2. It is also important to note that, visually, membranes produced at longer cross-linking times showed more brittleness than those produced at shorter times.

From this, it was concluded that the membranes crosslinked for at least 6 hours are insoluble in the pH range of 2 and higher. Minimum crosslinking time resulted in higher flux and adsorption capacity. The percentage of crosslinking was determined to be 19% after 6 hours of crosslinking using the method as described by Osifo (2005).

3.4.3. The effect of chitosan-, sodium hydroxide-, and acetic acid concentration on the flux through the membrane

Figure 3.8 gives the effect of the relationship between the precipitation bath (NaOH) concentration and the acetic acid concentration on the flux through the membrane.

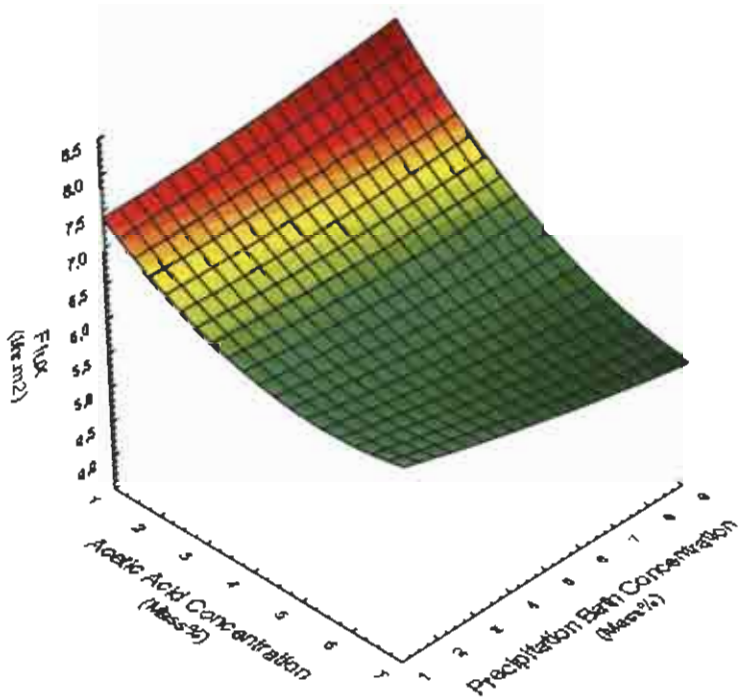

Figure 3.8: Effect of precipitation bath (NaOH) concentration and acetic acid concentration on the flux through the membrane.

This figure shows that the sodium hydroxide concentration has a negative influence on the flux through the membrane when the acetic acid concentration is high. A possible explanation for this phenomenon is that low sodium hydroxide concentrations result in a more open structured membrane. At lower acetic acid concentrations, the flux through the membrane tends to increase with sodium hydroxide concentration.

The effect of the sodium hydroxide concentration on the flux seems to be less pronounced than the effect of the acetic acid concentration. For acetic acid, the flux also decreases with an increase in concentration, especially at a sodium hydroxide concentration of 5 mass% and higher. For sodium hydroxide concentrations of 5 mass% and lower it reaches a minimum flux at an acetic acid concentration of 4 mass%.

A mono-variant technique was used to investigate the effect of the chitosan concentration in the membrane on the flux and the results are given in Figure 3.9 (Table C-3.3, Appendix C-3). This figure shows that, for a chitosan concentration of 2.5 – 7.5 mass% the chitosan concentration has only a marginal effect on the membrane flux. Below a concentration of 2 mass%, the flux increases significantly, because at this low concentration of chitosan, a loose, mechanically unstable membrane is produced (Section 4.3.6). At a concentration above 7.5 mass%, the flux increases due to the formation of cracks in the membrane (Section 4.3.6). These cracks can act as shortcuts for the water to be treated and are therefore undesirable. The recommended chitosan concentration used for the production of chitosan membranes is therefore between 2.5 and 7.5 mass%.

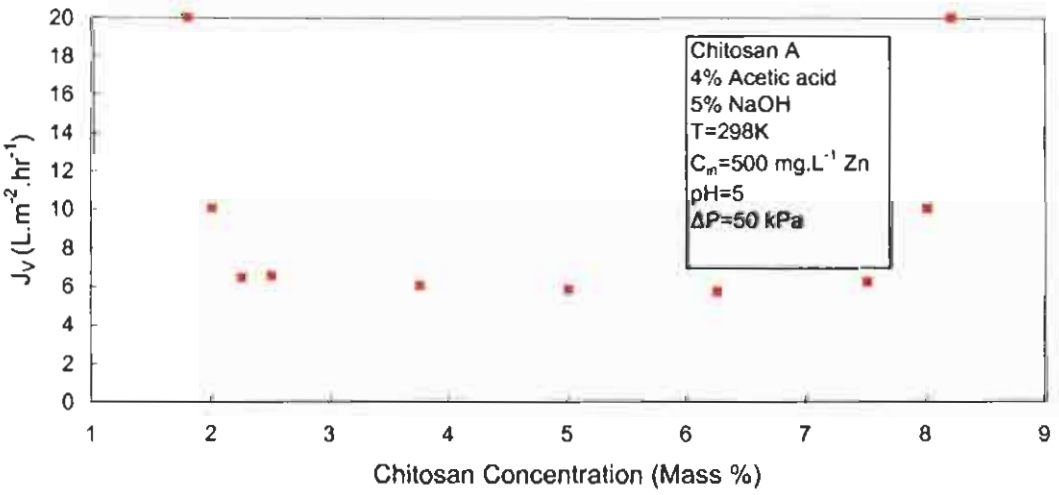

Figure 3.9: Effect of chitosan concentration on the flux through the membrane.

3.4.4. The effect of the production parameters on adsorption

Figure 3.10 gives the effect of the acetic acid- and precipitation bath concentration on the adsorption characteristics of the membrane. This figure shows that the adsorption increases as the acetic acid concentration increases. This can be due to the improved dissolution of the chitosan polymer in higher acetic acid concentrations, which makes the functional groups better accessible (slight change in porosity). The sodium hydroxide concentration seems not to have a large effect on the adsorption characteristics of the membrane. However, a maximum was reached at a concentration of 5 mass%.

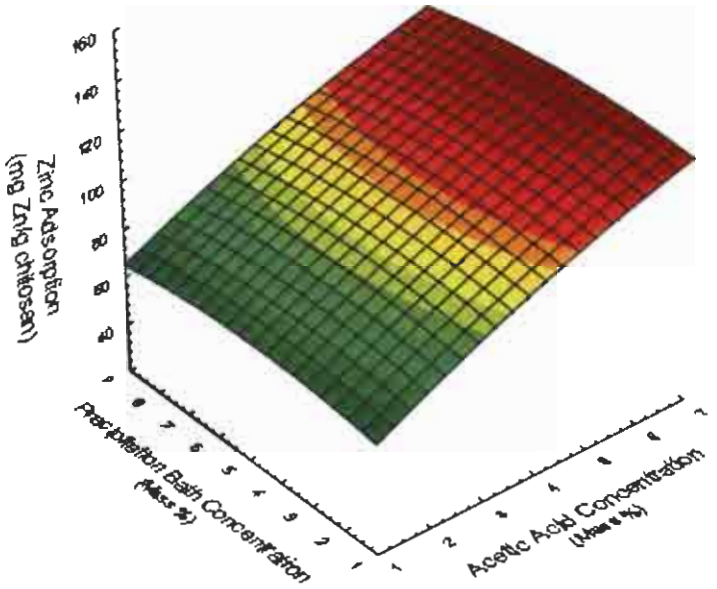

Figure 3.10: Effect of acetic acid concentration and precipitation bath (NaOH) concentration on zinc adsorption (Chitosan concentration = 7 mass%).

Figure 3.11 presents the effect of the chitosan concentration on the adsorption characteristics of the membrane (Table C-3.4, Appendix C-3). The adsorption capacity per gram of wet membrane strongly increases with the chitosan concentration in the acetic acid solution (Figure 3.11, secondary y-axis, green dots).

An increased chitosan concentration results in a higher adsorption due to higher final chitosan content in the membrane (Figure 4.2). The chitosan concentration on a dry basis (Section 4.3.1) does not change per gram of dry chitosan (Figure 3.11, primary y-axis, blue dots). Low adsorption capacities, below 2 mass% and above 7.5 mass%, results from membrane failure at these concentrations (Figure 3.9; these data points are not given in Figure 3.11).

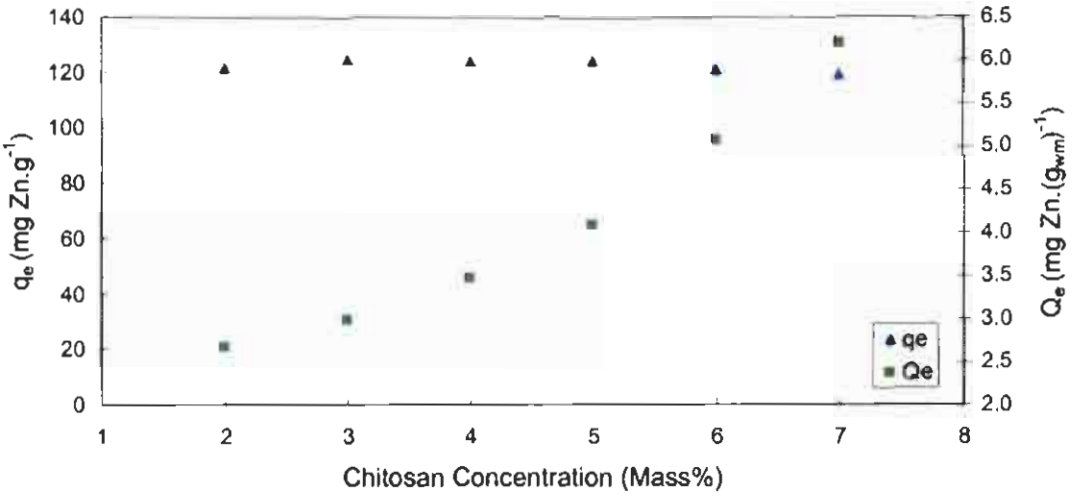

Figure 3.11: Effect of chitosan concentration on zinc adsorption.

3.4.5. Optimised conditions

An optimum sodium hydroxide concentration of 5 mass% was used. This resulted from the maximum adsorption achieved (Figure 3.10) and the decrease in flux (Figure 3.8) with increase in mass% at high acetic acid concentrations. The acetic acid concentration optimum was determined by a combination of the adsorption and flux results. For acetic acid, the flux decreased (Figure 3.8) relative to an increase in concentration, especially at a sodium hydroxide concentration of 5 mass% and higher. The adsorption increased with increasing acetic acid concentration (Figure 3.10).

Taking both opposite trends into account it was concluded to work with an optimum 4 mass% acetic acid solution, the best viscosity to cast mechanically stable membranes. Figure 3.9 shows that the increase in chitosan concentration has very little effect on the flux, however the zinc adsorption increases (Figure 3.11) with increasing chitosan concentration. Thus the optimum of 7 mass% was determined by the strength of the membrane.

3.5. Conclusions

The most important factor in the production of chitosan membranes, prepared by a phase inversion method, is the initial chitosan concentration in the acidic solution prior to membrane formation. The initial chitosan concentration is the major determinant of chitosan solution viscosity, which can either be too low, resulting in a mechanically weak membrane with a low adsorption capacity, or too high, forming membranes with cracks.

The viscosity of the chitosan solution is also dependent on the molecular weight of the chitosan, so that viscosity increases as the molecular weight increases. Since Chitosan A had the lowest molecular weight and could therefore be converted into a stable membrane with the highest percentage chitosan in its structure, it was chosen for further optimisation. For Chitosan A an optimum initial chitosan concentration of 7 mass% was determined.

A second important factor (in addition to viscosity) is the crosslinking time of the membrane, which has a negative effect on both the adsorption capacity and flux through the membrane. An optimal crosslinking time of 6 hours has been determined from a compromise between the loss in adsorption and flux and the improved stability of the membrane at a pH of 2. For this time the degree of crosslinking is 19%.

The concentration of acetic acid in the chitosan solution prior to membrane manufacturing and the concentration of sodium hydroxide in the precipitation bath had less significant effects on the adsorption and flux. However, after optimisation an acetic acid concentration of 4 mass% and a sodium hydroxide concentration of 5 mass% were determined.

Chapter 4: Characterisation of chitosan membranes

4.1. Introduction

Membrane processes cover a wide range of separation problems with a specific membrane functionality and structure being required for each application. Membranes can be divided in two main groups, porous and nonporous membranes. Porous membranes contain fixed pores, in the range of 1 to 5 000 nm, the dimensions of which mainly determine the selectivity, as the membrane discriminates between the sizes of different molecules. Nonporous membranes are used in gas- and vapour separation and in pervaporation. These are capable of separating molecules of approximately the same size. The term non-porous is however ambiguous as even these membranes contain voids on a molecular level.

It is often very difficult to relate the structural parameters (*e.g.* pore radius and pore distribution) directly to permeation parameters (*e.g.* flux and rejection) because the pore radius and shape are not well-defined. Nevertheless, a widely accepted method is to use a combination of well-defined characterisation techniques (*e.g.* Scanning Electron Microscope), which can give information about membrane morphology. This combination can be used as a first estimate in determining possible membrane modelling (Mulder, 1998).

Chitosan membranes are normally classified as non-porous membranes (Kawamura *et al.*, 1997) due to the gel properties of the membranes. The capillary pore model of water-swollen gel membranes assumes that the membrane is a network containing fixed, water-filled cylindrical channels/pores through which mass transport occurs and in which the pores can be described by free water volume (Krajewska, 1996). The free water volume however is not the total amount of water, but only the water removed from the membrane by spinning a wet membrane (*e.g.* in a centrifuge, ID of 5 cm, at 1000 rpm for 2 minutes). It is proposed that this water is free water, and the remaining water is termed fixed water.

With respect to membrane applications, it is important to relate the manufacturing conditions to the morphological properties of the membrane. In this chapter the manufactured chitosan membranes are characterised in order to determine the morphological properties of the membranes. Chitosan A was used for the reasons

as given in Section 3.4.1. Since the importance of chitosan concentration on membrane production was shown in chapter 3, the results of the investigation into the effect of chitosan concentration on the membrane characteristics are reported here.

In Section 4.2, the different techniques relevant to chitosan membrane characterisation are presented. The results of these characterisations are given in Section 4.3. Finally, conclusions from the characterisations with respect to the morphological structure are presented in Section 4.4.

4.2. Experimental procedure

4.2.1. Introduction

In order to determine the morphology of the manufactured Chitosan A membranes, different experiments have been carried out. These are described in the following section. For all experiments, chitosan membranes were manufactured in triplicate and the data present the average of the three values. The membranes were produced using the standard method as described in Section 3.3.2. The error was determined statistically and the coefficient of variation (the standard deviation as a percentage of the arithmetic mean) was less than 5%.

4.2.2 Methods used for determining the structure of the chitosan membranes:

4.2.2.1. Determination of the mass fraction chitosan in the membrane

The mass fraction of water was determined from the difference between the mass of a wet and a dry membrane. A wet membrane is hereby defined as the membrane obtained after manufacturing and after removing the cohesive water from the edges. A dry membrane is defined as the structure that remains after removing all the water from the membranes by heating the membrane at 60 °C in a ventilated oven for 24 hours. The mass fraction water (x_w) is calculated with:

$$x_w = \frac{m_{wm} - m_{dm}}{m_{wm}} \qquad \text{.....4.1}$$

The mass fraction chitosan in the membrane (x_c) can subsequently be calculated with:

$$x_c = 1 - x_w \qquad \text{.....4.2}$$

4.2.2.2. Determination of wet membrane density

The wet membrane density of the membranes was determined by a method as described by Kawamura *et al.* (1997). Before weighing, the cohesive water from the edges of the membrane was removed. The volume of the disk shaped membrane was determined from the membrane diameter and thickness. Finally, the density was calculated with:

$$\rho_{wm} = \frac{m_{wm}}{V_{wm}} \qquad \text{.....4.3}$$

4.2.2.3. Determination of fraction free water volume

Chitosan membranes are gel type membranes and are generally classified as being non-porous membranes. However, pores are present on a molecular level even in non-porous membranes. The fraction free water volume was determined using a method reported by Kawamura *et al.* (1997). It was assumed that the free water volume equals the volume water in the membrane that is not fixed to the membrane matrix. This free water can be removed easily by mechanical forces. It was determined by spinning a wet membrane in a centrifuge (Sorval Instrument, Model: RC5C at 1000 rpm, room temperature for 2 minutes) followed by collecting and weighing the released free water. The fraction free water volume was then be determined from:

$$\varepsilon = \frac{V_{fwp}}{V_{wm}} \qquad \text{.....4.4}$$

4.2.2.4. Determination of maximum pore radius

The maximum pore radius of the membrane was determined using the Bubble-point method as described by Mulder (1998). The procedure for bubble-point test is also described in American Society for Testing and Materials Standard (Method F316) as described by Lenntech (www.lentech.com). This method is based on measuring the minimum pressure required to permeate a gas bubble through the water filled membrane. In this way, the maximum pore radius was determined using the Young equation:

$$r_p = \frac{2 \cdot \gamma}{\Delta P} \cdot \cos\theta \qquad \text{.....4.5}$$

where θ is zero, since at the point of completely penetrating the membrane the radius of the gas bubble is equal to the pore radius.

The apparatus used to determine the maximum pore radius is shown in Figure 4.1. The pressure of nitrogen is gradually increased, with the use of a regulator until a gas bubble is visually present in the water on top of the membrane and at that point the pressure is taken from the pressure indicator (Hernandez *et al.*, 1996). Calvo *et al.* (1995) tested the accuracy of the bubble-point method relating to other methods and found it to be acceptable.

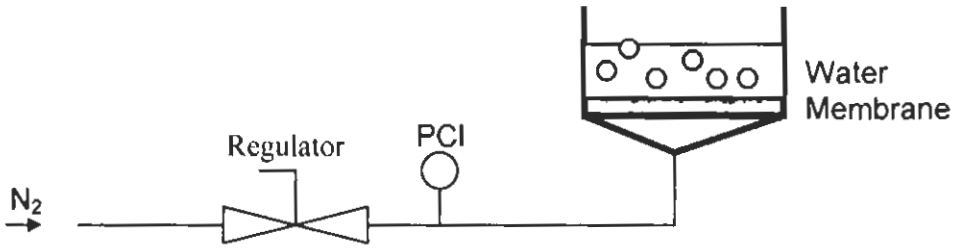

Figure 4.1: Schematic drawing of a bubble-point test apparatus.

4.2.2.5. Determination of the specific surface area

The specific surface area of the dried membrane was determined using the iodine adsorption number as described by Pawlowski (1971). In this method, the amount of iodine adsorbed by the dry membrane was measured according to the difference in iodine concentration before and after adsorption (iodine concentration is determined

by titration using a sodium thiosulphate solution). The amount of adsorbed iodine per gram adsorbent was then correlated to the surface area as described by Pawlowski (1971) and shown in Appendix D-1.1.

4.2.2.6. Determination of chitosan membrane structure after drying

Chitosan membranes were dried and the solid structure was examined using Scanning Electron Microscopy (SEM, FEI Quanta 200 ESEM) (more detailed information on sample preparation is given in Appendix D-1.2).

4.3. Results

4.3.1. The effect of chitosan concentration on the mass fraction chitosan in the membrane

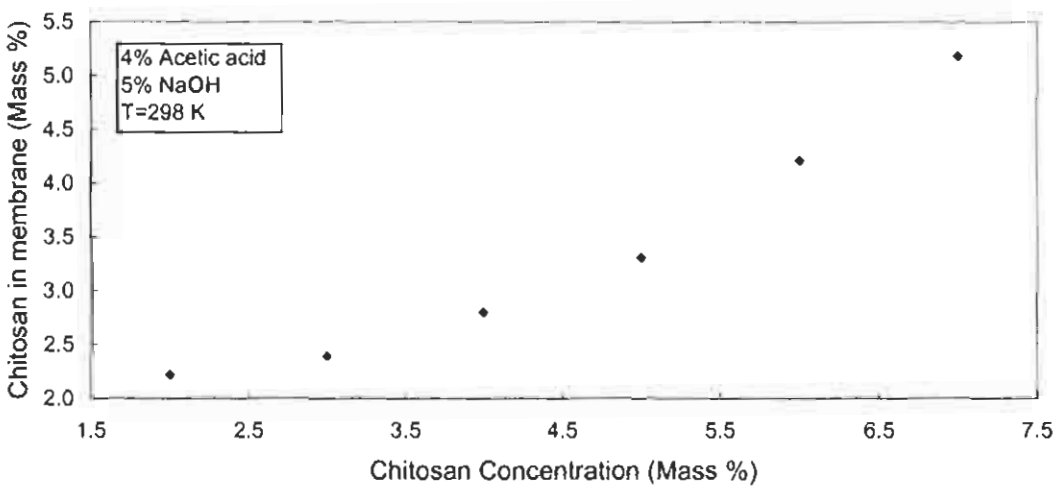

Figure 4.2: Effect of chitosan concentration on the % chitosan in the membrane.

In Figure 4.2, the mass fraction chitosan in the membrane (x_c) is given as a function of the chitosan concentration in the 4 mass% acetic acid solution during the manufacturing of the membrane (Table D-2.1, Appendix D-2). It is concluded that the mass fraction chitosan in the membrane increases with increasing chitosan concentration during membrane preparation. Generally, it can be seen that the water content of the membranes is high (95 – 98 mass%), values that are in agreement with Kawamura *et al.* (1997).

4.3.2. The effect of chitosan concentration on wet membrane density

The wet density is a specific property of gel-type membranes since it is directly related to some membrane properties (*e.g.* porosity) and thus to the transport properties of the membrane (Kawamura *et al.*, 1997). In Figure 4.3, the density of the membrane is given as a function of the chitosan concentration in the acidic solution used for the preparation of the membrane.

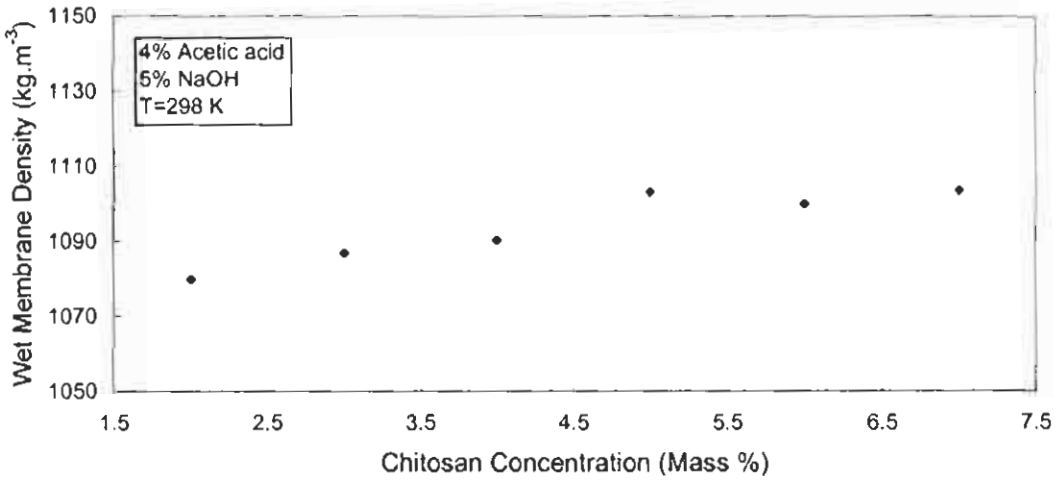

Figure 4.3: Effect of chitosan concentration on the wet membrane density.

It is clear from Figure 4.3 that the wet density only slightly increases with an increase in the chitosan concentration. As expected only a slight change in density is observed due to the fact that approximately 95% of the membrane consists of water (Figure 4.2). The increase in wet membrane density is a result of higher chitosan concentration and the corresponding decrease in free water volume. Kawamura *et al.* (1997), also observed this phenomenon (Table D-2.1, Appendix D-2).

4.3.3. The effect of chitosan concentration on the fraction free water volume

In Figure 4.4, the free water volume (as defined in Section 4.2.2.3) is given as a function of the chitosan concentration during membrane preparation (Table D-2.1, Appendix D-2). It can be seen from this figure, that the free water volume is only a slight function of the chitosan concentration and that its value is between 0.65 and 0.67. This value is significant lower than the total water content (see Section 4.3.1, between 0.95 and 0.98), indicating that some of the water in the chitosan membrane is part of the integral structure of the membrane. Therefore the free water volume of

the membrane can not be based on the mass difference between a wet membrane and a dry membrane as some of the water in the membrane, that would be removed by drying, is bonded to the chitosan and is part of the matrix (fixed water). The free water volume is equal to the free water in the membrane.

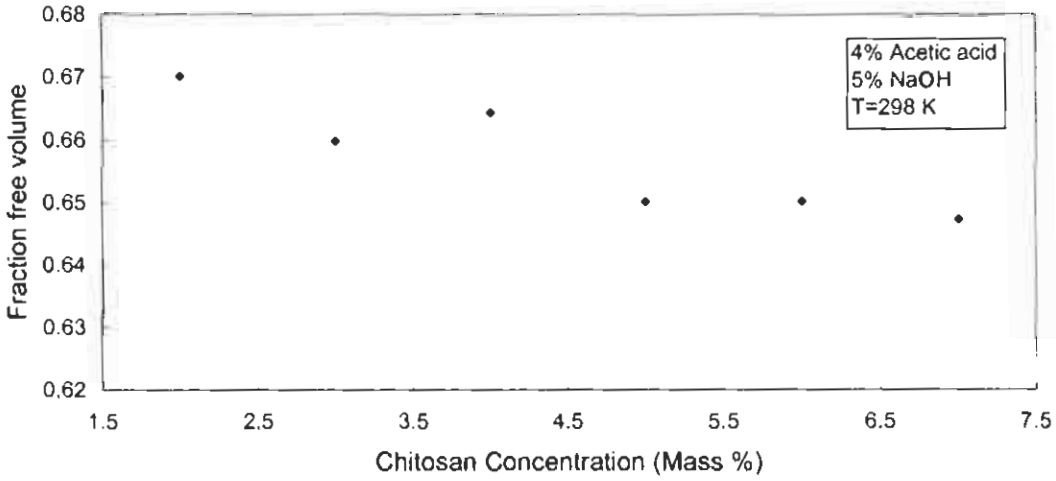

Figure 4.4: Effect of chitosan concentration on the free water volume of wet chitosan membranes.

4.3.4. The effect of chitosan concentration on the maximum pore radius

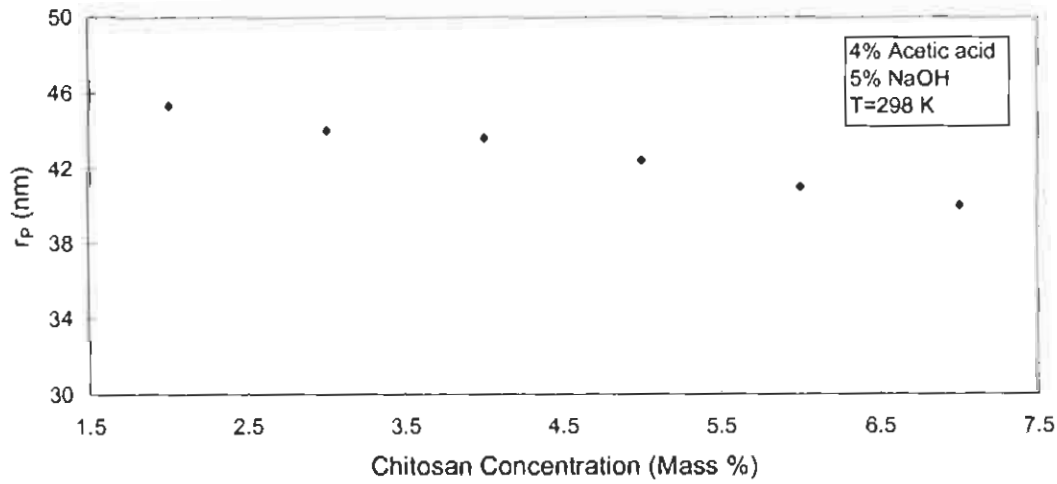

Figure 4.5: Effect of chitosan concentration on the maximum pore radius of the wet chitosan membranes.

Figure 4.5 gives the effect on maximum pore radius of the chitosan concentration during membrane preparation (Table D-2.2, Appendix D-2). The increase in chitosan concentration leads to a slight decrease in the maximum pore radius, which could be attributed to the fact that more space is occupied by chitosan macromolecules, resulting in a smaller pore radius. The maximum pore radius is in the range of 40-45 nm, which was also noted by Milot *et al.* (1997), a pore radius comparable to ultrafiltration (UF) membranes.

4.3.5. The effect of chitosan concentration on the specific surface area

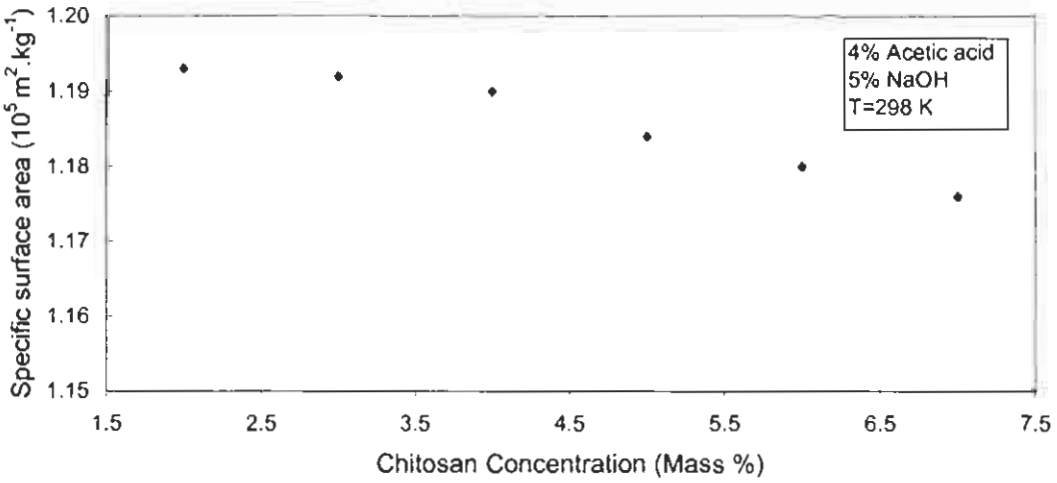

Figure 4.6: Effect of chitosan concentration on the specific surface area of dried chitosan membranes.

Figure 4.6 gives the relationship between the chitosan concentration and the specific surface area of the membrane on a dry basis (Table D-2.2, Appendix D-2). In this figure, a similar trend to that for the maximum pore radius (Figure 4.5) is observed. The increased chitosan concentration leads to a lower total porosity and thereby also to a lower specific surface area. This is however not a very strong effect. The specific surface area ranges from 1.175 – 1.195·10^5 $m^2.kg^{-1}$. This can be explained by the increase in wet membrane density (Figure 4.3).

4.3.6. Scanning Electron Microscope results

Figure 4.7 shows SEM-micrographs of three differently prepared membranes. A membrane prepared from a relatively low chitosan-acetic acid solution, shows a

mechanically weak structure (sponge-like, Figure 4.7a). As the membrane density increases with increasing chitosan concentration, at concentrations between 6.5 and 7.5 mass% a (mechanically) very strong membrane is produced (Figure 4.7b). Above a chitosan concentration of 8.0 mass% the membrane seems to exhibit cracks (Figure 4.7c). Permeation experiments show very high fluxes for these membranes (Figure 3.9), which suggests that the structure is cracked. From the SEM-study, it was concluded that a mechanically homogenous (strong) membrane is obtained if a chitosan concentration of 6.5 to 7.5 is used.

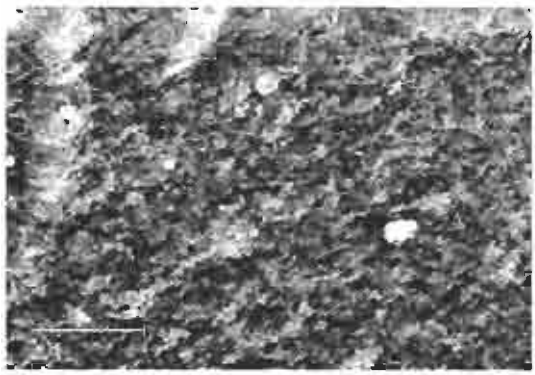

(a)

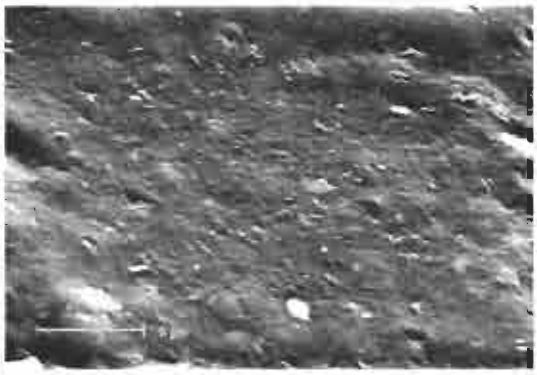

(b)

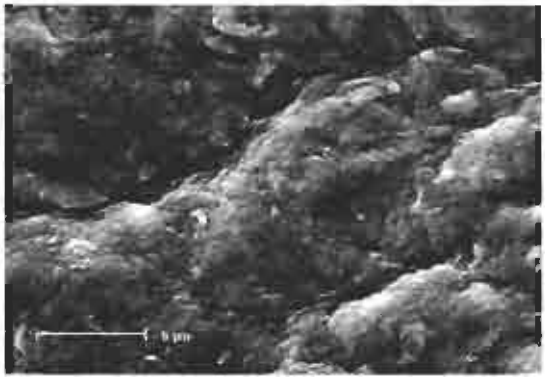

(c)

Sample No	(a)	(b)	(c)
Chitosan concentration (mass%)	2.5	7.5	8.22

Figure 4.7: Effect of Chitosan concentration during preparation on the dry membrane characteristics.

4.3.7. Proposed structure for chitosan membranes

After a thorough inspection of the manufactured chitosan membranes, the following structure for the chitosan is proposed. The membranes consist of a large fraction of water (95 – 98%) and it is assumed that not all water in the wet (gel) membrane is an

integrated part of the membrane. Water is thus present as both free and fixed water. The water filling the pores is termed free water in this study. The fixed water and the chitosan to which it is bonded forms the rigid network of the membrane.

When applying a pressure difference over the membrane, the free water can be transported through the porous network, while the fixed water remains bonded to the chitosan. The transport of free water through the membrane is similar to traditional MF and UF membranes.

For a dried membrane, a Scanning Electron Microscope analysis (cross-section view) revealed that the dried chitosan membrane has a porous honeycomb structure (Figure 4.8), thus free water volume exists. Due to the larger effect of crosslinking on the surface of the membrane the membrane pore size decreases from the middle of the membrane (≈1 μm) to the membrane surface (< 1 μm). The bubble point method, which showed a maximum pore radius of approximately 40 nm, confirms the smaller value at the surface. The pore radius classifies the chitosan membrane in the category of ultrafiltration (UF).

From Section 4.3.1, 4.3.3 and 4.3.7, it is concluded that a membrane, manufactured from a 7 mass% chitosan solution consists of 5 mass% chitosan, 30 mass% fixed water and 65 mass% free water.

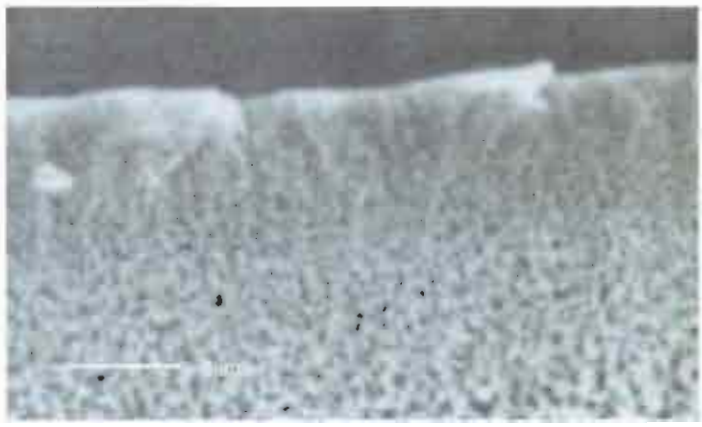

Figure 4.8: A cross-section view of dried chitosan membrane structure.

The combined data on the structure of the membrane supports the proposed structure for chitosan membranes. Therefore the transport properties of the chitosan membranes can be modelled as a porous membrane.

4.4. Conclusions

It was observed that the water content of the membranes was high (95 – 98 mass%) and decreased with an increase in chitosan concentration. The wet density slightly increased with an increase in the chitosan concentration and the free water volume, maximum pore radius, total porosity and specific surface area only slightly decreased.

The free water was found to be significantly lower than the total water content, indicating that some of the water in the chitosan membrane is part of the integral structure of the membrane. Therefore it was proposed that the water can be present as free water and as fixed water, in which the water filling the pores is termed free water, and the water bonded to form the network of the membrane is termed fixed water.

The physical properties of the chitosan membranes manufactured under optimum conditions are: a wet density of 1 100 kg.m^{-3}; a chitosan content of 5.2 mass%; a fraction free water volume of 0.65 kg.kg^{-1}; a maximum pore radius of 40 nm; and a total surface area of $1.15 \cdot 10^5$ m^2.kg^{-1}. Under these conditions, the resulting membrane consisted of 5 mass% chitosan, 30 mass% fixed water and 65 mass% free water.

The determined pore radius classified the chitosan membrane in the category of ultrafiltration (UF). The chitosan membrane can therefore be described according to a porous membrane.

Chapter 5: Transport properties of chitosan membranes

5.1. Introduction

The natural chelating marine polymer chitin, poly(N-acetyl-D-glucosamine), and in a more pronounced way its deacetylated derivative chitosan may be useful for the removal of heavy metal ions wastes from discharged water (Maruca *et al.*, 1982). Although detailed adsorption work has been published for chitosan beads (*e.g.* Kawamura *et al.*, 1997; Guibal *et al.*, 1998; Becker *et al.*, 2000; Wan Ngah *et al.*, 2002; Ng *et al.*, 2003), very little work has been done on (flat-sheet) chitosan membranes (Kaminski & Modrzejewska, 1997; Juang & Shiau, 2000; Krajewska, 2001; and Taoualit & Hadj-Boussaad, 2002). These studies were mainly focused on the adsorption characteristics of chitosan membranes, while this chapter deals with their transport properties. For the purpose of this study, the transport of water and zinc-ions through the chitosan membranes has been investigated, as knowledge of this transport is essential for design purposes and for assessing the effectiveness of membrane cleaning procedures (Gopal & April, 1998).

The driving force for transport to occur through membranes can either be pressure, concentration, electropotential, temperature difference or a combination of these. Chitosan membranes are porous membranes and transport therefore pressure driven. Pressure driven membrane processes can be classified into different types (Table 5.1) mainly associated with the applied pressure difference, flux and (average) pore size.

In Chapter 4, it was concluded that chitosan membranes can be regarded as porous membranes. Therefore, the modelling of transport has been carried out analogous to pressure driven membranes.

In Section 5.2, the relevant theoretical background is presented, while Section 5.3 describes the experimental set-up and procedures used. In Section 5.4, the results are presented and discussed and finally, the conclusions are listed in Section 5.5.

Table 5.1: Pressures and permeation in various pressure driven membrane processes (Mulder, 1998).

Membrane process	Applied pressure (bar)	Permeation ($L.m^{-2}.hr^{-1}$)	Pore sizes (nm)
Microfiltration (MF)	0.1-2.0	>50	50-10 000
Ultrafiltration (UF)	1.0-5.0	10-50	2-100
Nanofiltration (NF)	5.0-20.0	1.4-12	<2
Reverse osmosis (RO)	10.0-100.0	0.05-1.4	<2

5.2. Theoretical background

5.2.1 Transport Model

Transport through membranes can be described for any type of membrane by the laws of irreversible thermodynamics, where the solvent flux, J_v, and the solute flux, J_s, can be expressed by Eq. 5.1 and 5.2 respectively (Lakshminarayanaiah, 1969):

$$J_V = L_P \cdot (\Delta P - \sigma \cdot \Delta\pi) \quad \text{.....5.1}$$

$$J_S = c_S \cdot (1-\sigma) \cdot J_V + \omega \cdot \Delta\pi \quad \text{.....5.2}$$

The transport is described by three typical parameters: σ, the reflection coefficient, which is a measure of the separation properties of the membrane (σ = 0 means no separation, while σ = 1 represents an ideal separation); and L_p and ω, which are a measure of solvent and solute permeability respectively. Normally, the osmotic pressure difference (Δπ) in ultrafiltration processes is negligibly small, but for the application of zinc removal with chitosan membrane at high concentrations, it must be considered, as the osmotic pressure increases with solute concentration. If the solute is not completely retained by the membrane then the osmotic pressure difference is not Δπ but σ·Δπ.

This thermodynamic model considers the membrane as a black box, and the three parameters can be obtained from experiments. Using water (Δπ=0), Eq. 5.1 reduces to Eq. 5.3 and the solvent flux can be expressed in terms of the permeability coefficient (L_p) only:

$$J_V = L_P \cdot \Delta P \qquad \text{.....5.3}$$

Since L_P can be determined independently, σ and ω can now be determined using Eq. 5.1 and 5.2 for experiments with different salt concentrations. The permeability coefficient, however, can also be expressed in terms of the structural properties of the membrane. Although chitosan membranes are not completely similar to "traditional" membranes (membranes in which solutes or particles are rejected due to size exclusion or repulsion), chitosan membranes can be modelled as gel type membranes (Krajewska, 2001 and Taoualit & Hadj-Boussaad, 2002). In modelling transport through gels, two approaches are presented in the literature: the free volume model and the capillary pore model (Peppas & Reinhart, 1983). In the free volume model, the membrane is assumed to be a homogenous hydrated network. The diffusive transport of solutes occurs through water-filled spaces of the network by successive jumps through 'holes' (free water volume) that are larger than the solute. These spaces are not fixed in size and location. The effective free water volume for solute diffusion corresponds to the free water volume in the membrane (Mulder, 1998).

In the capillary pore model, the membrane is visualised as having fixed pores, with uniform radius, and the convective transport is described similarly to that of porous membranes.

In Chapter 4, the gel type chitosan membranes were classified according to their structure and pore radius. From the structure it was proposed that the water filling the pores is termed free water and occupies the free water volume. The fixed water and the chitosan form the network of the membrane. Based on this analogy, the chitosan membranes are modelled as porous membranes.

Different transport models have been developed to quantify the permeability coefficient (L_P) in terms of (average) pore size, porosity and tortuosity. Membranes consisting of a sponge-like structure are typical of organic membranes produced by the phase inversion technique. These membranes can best be described either by the Kozeny-Carman (Eq. 5.4) or the Hagen-Poiseuille (Eq. 5.5), equation (Davies & Dollimore, 1980 and Mulder, 1998).

$$L_p = \frac{\varepsilon^3}{K \cdot \eta \cdot S_{KC}^2 \cdot (1-\varepsilon)^2 \cdot x} \qquad \text{.....5.4}$$

$$L_p = \frac{\varepsilon \cdot r_p^2}{8 \cdot \eta \cdot \tau \cdot x} \qquad \text{.....5.5}$$

From Chapter 4, it was concluded that the pores are filled with free water; this free water is equivalent to the porosity (ε) of the membrane.

5.2.2 Concentration Polarisation

One of the general disadvantages of membrane processes is the occurrence of concentration polarisation. This phenomenon normally results in a significant flux decline over time, and is more severe for micro- and ultrafiltration than in other membrane processes. In general, concentration polarisation can be described as follows: when a solution is transported through a membrane, the solvent freely permeates through the membrane while the solute accumulates at the membrane-solution interface (Figure 5.1). Therefore, the concentration of the solute will be larger at the membrane interface than in the bulk of the solution.

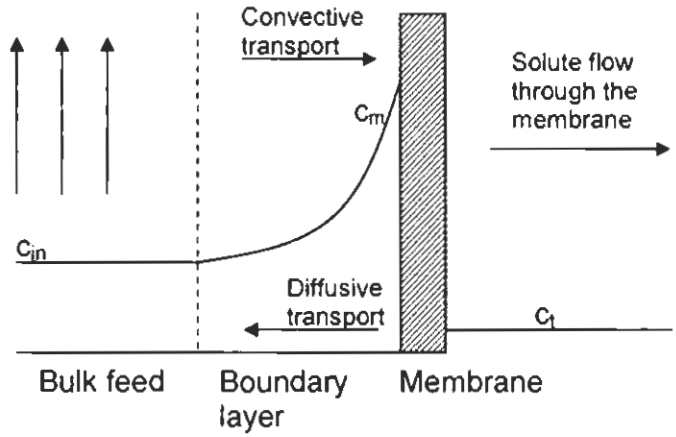

Figure 5.1: Concentration polarisation; concentration profile under steady state conditions (Mulder, 1998).

This concentration gradient causes a diffusive transport of the solute back to the bulk and, in a steady state operation, this diffusive transport equals the convective transport of the solute through the membrane. In the case of relatively low solute concentration and pressure differences, the transport is not affected by concentration

polarisation. However, at high solute concentrations and pressure differences, it can play an important role and even completely determine the transport rate through membranes.

In a case where concentration polarisation is completely determining the transport rate, the flux is independent of the pressure difference and is termed the limiting flux (J_{Vlim}). The limiting flux can be calculated with (Mulder, 1998)

$$J_{Vlim} = k \cdot \ln\left(\frac{c_m}{c_{in}}\right) \qquad \text{.....5.6}$$

in which c_{in} and c_m are the solute concentrations in the bulk and at the membrane interface, respectively; k is the external mass transfer coefficient in the liquid. Eq. 5.6 can be written in a linear form as shown in Eq. 5.7:

$$J_{Vlim} = k \cdot \ln c_m - k \cdot \ln c_{in} \qquad \text{.....5.7}$$

and can be used to determine c_m and k.

5.3. Experimental Procedure

5.3.1. Introduction

Chitosan membranes were used for this experimental work. Chitosan A was used for the reasons as given in Section 3.4.1. A number of laboratory experiments were carried out to determine the effect of different process parameters (pressure difference, zinc-ion concentration and pH) on the transport properties, with the membrane thickness varying from 0.8 to 1.5 mm. The membranes were produced by the phase inversion method as described in Section 3.3.2. A monovariant technique was used for this purpose. For all experiments, chitosan membranes were manufactured in triplicate and the data present the average of the three values. The statistical error was less than 7%.

5.3.2. Membrane permeability

The permeability through the membranes was measured for water and solutions of different heavy metal concentrations prepared from analytical grade $ZnSO_4 \cdot 7H_2O$

(99% pure $ZnSO_4 \cdot 7H_2O$ supplied by Merck) in de-ionised water (conductivity <0.5 $\mu S.cm^{-1}$). The experimental set-up is shown in Figure 5.2.

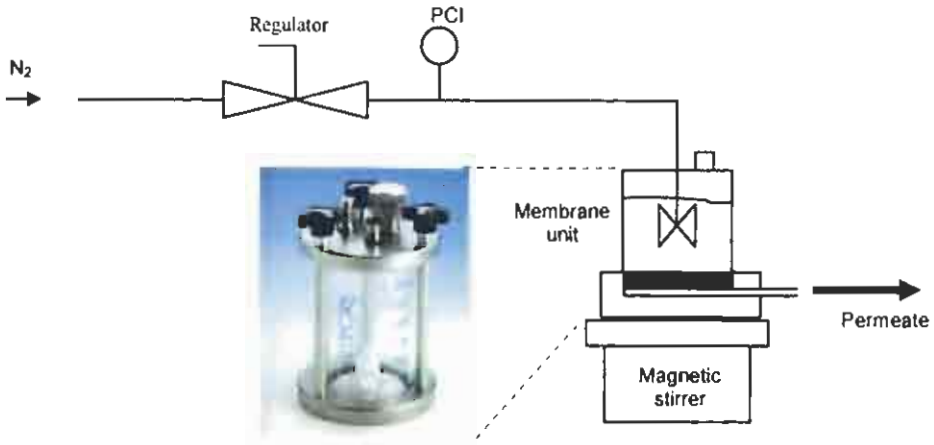

Figure 5.2: Experimental set-up for permeation studies.

The membrane module was purchased from Millipore, and is shown in Figure 5.2. A sintered stainless steel support, with an average mesh size of 0.1 mm was used. The transport resistance of the support is negligible when compared to the chitosan membrane, since the pore size of the support is relatively large.

To suppress permeation decline due to concentration polarisation the solution on top of the membrane was continuously stirred, using a magnetic stirrer at 100 rpm. The pH of the zinc salt solution was adjusted using sulphuric acid (98% pure supplied by Saarchem Ltd.) to obtain acidic conditions and sodium hydroxide (97% pure supplied by Saarchem Ltd.) for alkaline conditions. The temperature was controlled using a hot plate (Hydolph MR2002). The water or salt solution was poured into the membrane holder, and the temperature monitored until a constant temperature was obtained. Thereafter the nitrogen supply was opened to create the pressure difference over the membrane. The permeation is expressed as the volume flow through the membrane per unit area and time

$$J_V = \frac{V}{A \cdot t} \qquad \text{.....5.8}$$

5.4. Results and discussion

5.4.1. Determination of the permeability coefficient

Figure 5.3 shows the water permeation (J_P) as a function of pressure difference over the membrane at a temperature of 298K (Table E-1.1, Appendix E-1).

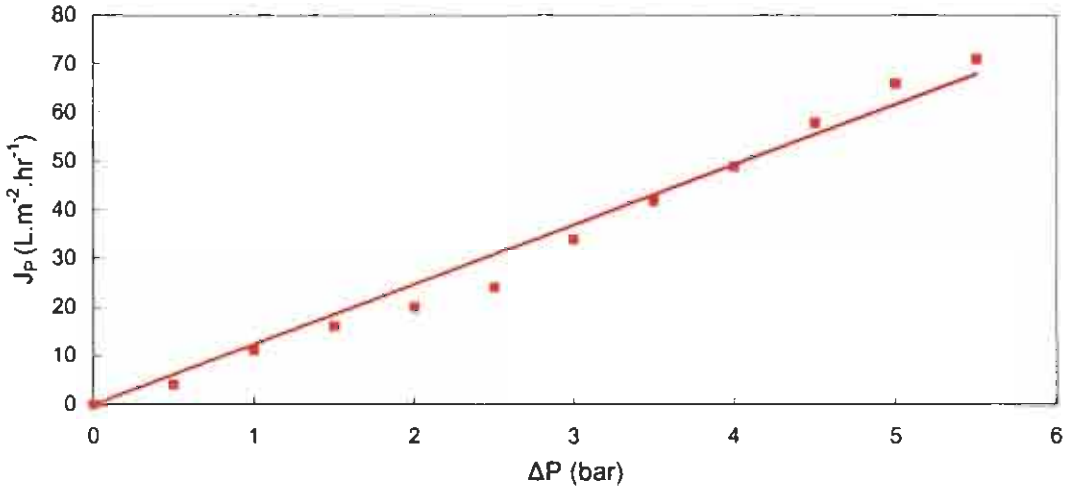

Figure 5.3: Permeation as a function of the pressure difference (Membrane thickness = 0.8 mm and T = 298K).

From the figure, a permeability coefficient of 12.4 L.m^{-2}.hr^{-1}.bar^{-1} is determined from the slope, which lies within the range (10-50 L.m^{-2}.hr^{-1}.bar^{-1}) of ultrafiltration pressure driven membrane processes.

The calculations for the Kozeny-Carman equation (Eq. 5.4) and the Hagen-Poiseuille equation (Eq. 5.5) were carried out with a porosity of 0.65 (Section 4.3.3) and a total surface area of $1.2 \cdot 10^5$ m^2.kg^{-1} (Section 4.3.5). Using the Kozeny-Carman equation and the determined permeability coefficient, the K value was calculated to be 4.83, which compares well with a K=5 value as conventionally used for micro- and ultrafiltration processes (Davies & Dollimore, 1980).

Using the Hagen-Poiseuille equation, the calculated permeability coefficient, and assuming that the tortuosity equals the reciprocal porosity (Neomagus *et al.*, 1998) the average pore radius was determined as 23 nm. Although the pore size distribution is not determined, this result compares well with the maximum pore radius of 40 nm as shown in Section 4.3.4 and the value of 23 nm falls also within the range of UF membranes (Table 5.1).

5.4.2. Determination of permeability- and retention coefficient

The solute permeability (ω) and the reflection coefficient (σ) can be obtained by performing several pressure difference experiments with a salt solution. By measuring the volumetric flux (J_v) and the solute flux (J_s), the two parameters can be obtained from the linearised form of Eq. 5.2:

$$\frac{J_s}{\Delta c} = (1-\sigma)\cdot J_v \cdot \frac{c_s}{\Delta c} + \omega \qquad \text{.....5.9}$$

which resembles

$$y = a \cdot x + b \qquad \text{.....5.10}$$

with $x = \frac{J_v \cdot c_s}{\Delta c}$ and $y = \frac{J_s}{\Delta c}$.

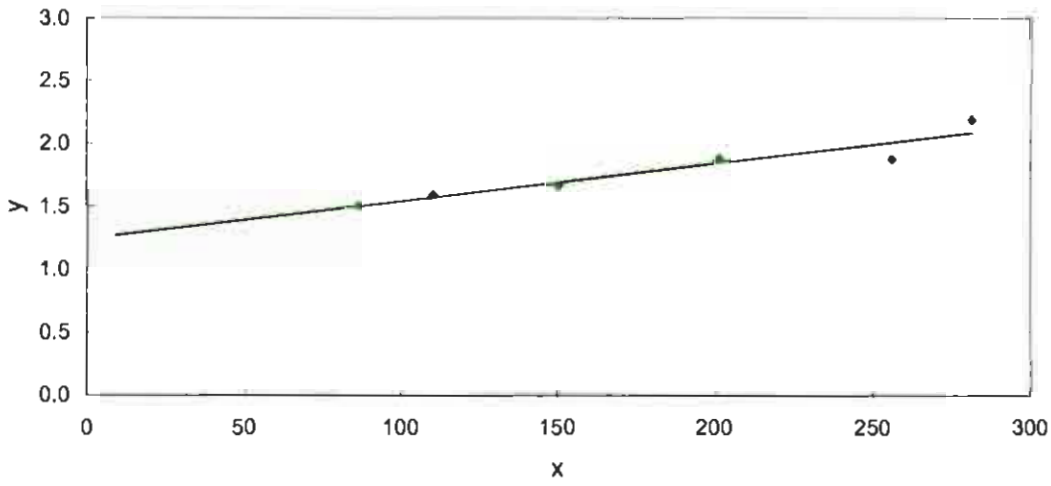

Figure 5.4: Determination of the solute permeability coefficient and the reflection coefficient.

By plotting x versus y the solute permeability (ω) is obtained from the intercept and the reflection coefficient (σ) from the slope of the resulting straight line. For these experiments, a 50 $mg.L^{-1}$ zinc solution was used (Table E-1.2, Appendix E-1).

Figure 5.4 gives the results from the experiments and, from slope and intercept, the general transport coefficients are determined as σ = 0.997 and ω = 1.24

$mg.m^{-2}.hr^{-1}.bar^{-1}$. The slope and intercept were taken from a straight line through the results at low pressures due to the effect of concentration polarisation at high pressures.

5.4.3. Determination of limiting flux

Experiments with higher solute concentrations, where the volumetric flow rate of the solvent is determined as a function of the pressure difference for different solute concentrations, were also carried out. The flow rate of the solvent is modelled with the thermodynamic model as represented in Eq. 5.1 and 5.3, using the solvent permeability coefficient as determined in Section 5.4.1 and the solute permeability- and retention coefficient as determined from Figure 5.4 (Table E-1.3, Appendix E-1). The results are given in Figure 5.5.

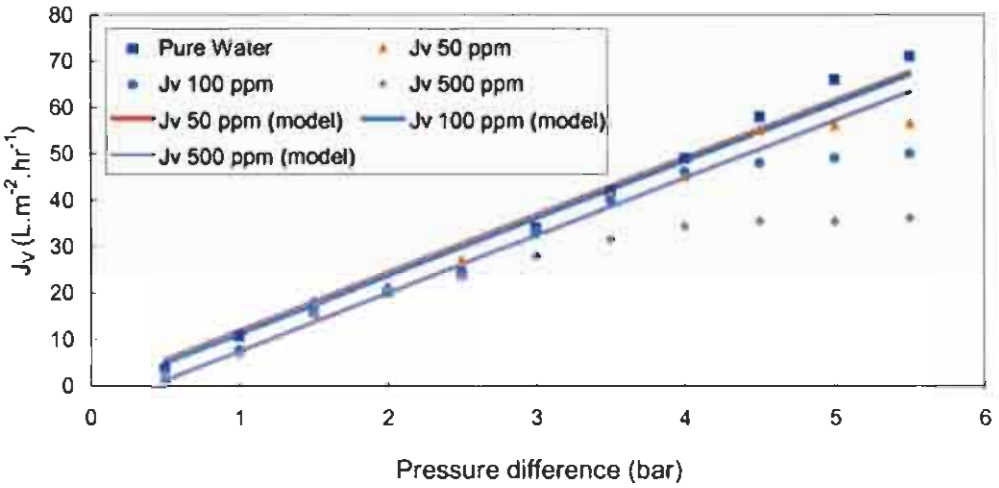

Figure 5.5: Relationship between experimental and calculated permeability using the transport model.

From this figure, it can be concluded that the volumetric flow rate of the solvent in the solution is well predicted by the model at low pressure differences, but deviates to higher fluxes at higher pressure differences. For the zinc feeds concentration polarisation, which is more pronounced at 500 $mg.L^{-1}$ than at 50 $mg.L^{-1}$, occurs as is evidenced by the drop in fluxes with pressure increase.

The solvent flow rate increases linearly with pressure difference at low pressure difference and reaches a maximum value at high pressure difference. At the point that the maximum is reached, the transport is mainly determined by concentration polarisation (see Section 5.2.2). This maximum observed permeability is termed the

limiting flux (J_{Vlim}) and is a function of the solute concentration. The limiting flux is plotted in Figure 5.6 for different concentrations of zinc (Table E-1.4, Appendix E-1).

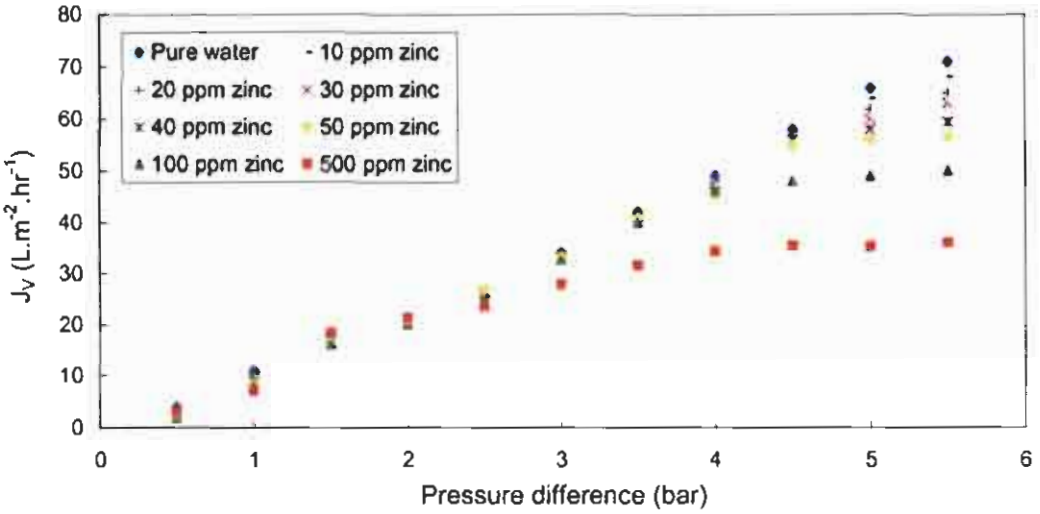

Figure 5.6: The relationship between permeability and applied pressure difference for different zinc concentrations (Membrane thickness = 0.8 mm).

Figure 5.6 shows that on increasing the feed concentration, the value of the limiting permeability decreases. The limiting flux depends on the concentration in the bulk of the feed (c_{in}), the membrane concentration (c_m), and the external mass transfer coefficient from the liquid to the membrane (k) according to Eq. 5.6. Figure 5.7 shows a plot of the limiting permeation against the logarithm of the bulk concentration, based on the data presented in Figure 5.6 (Table E-1.5, Appendix E-1), according to Eq. 5.7. From this figure, the mass transfer coefficient and the natural logarithm of the membrane interface concentration can be obtained from the slope and intercept respectively.

A value of 9.0 L.m^{-2}.hr^{-1} ($2.5 \cdot 10^{-6}$ m.s^{-1}) for the external mass transfer coefficient was determined, which is typical for water-ion systems (Perry, 1988). The membrane interface concentration was determined as $28 \cdot 10^3$ mg.L^{-1}. As mentioned by Mulder (1998) concentration polarisation is very severe in ultrafiltration due to high flux through the membrane and high membrane retention. This relatively high value can possibly be explained by the high concentration of the zinc in the membrane, due to adsorption.

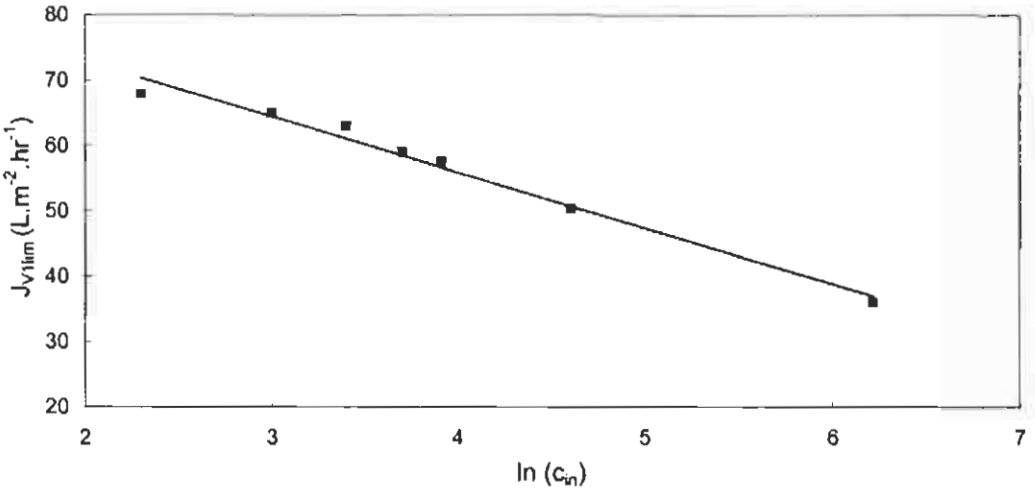

Figure 5.7: Limiting permeation plotted as a function of the logarithm of the bulk concentration (Pressure difference = 100 kPa).

5.4.4. Solute permeability

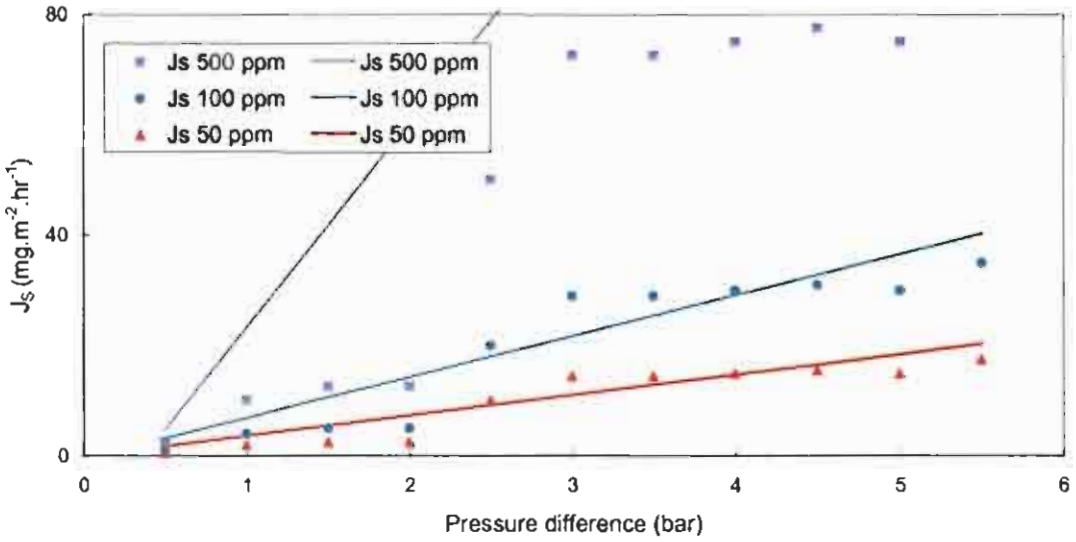

Figure 5.8: Relationship between experimental solute permeability and calculated permeability using the transport model.

Next to the solvent permeability, the solute permeability is also measured as a function of the applied pressure difference for different solute concentrations. The results are presented in Figure 5.8, where the experimental points are given by the dots and the model (Eqs. 5.2 and 5.3, using same parameters as in Section 5.4.2) is given by the lines (Table E-1.3, Appendix E-1). The model predicts the solute

permeation well at low solute concentrations (50 and 100 ppm), but overestimates the solute permeability at high concentrations (500 ppm), which is due to concentration polarisation which is not accounted for in the model (Lakshminarayanaiah, 1969).

5.4.5. Effect of membrane thickness

Figure 5.9 shows the effect of membrane thickness on the permeation using a 50 $mg.L^{-1}$ zinc solution (Table E-2.1, Appendix E-2). As expected, an increase in membrane thickness results in a decrease in permeation. The effect of membrane thickness is tested with the thermodynamic model as given in Eqs. 5.4 and 5.5, using the experimentally determined permeability coefficient.

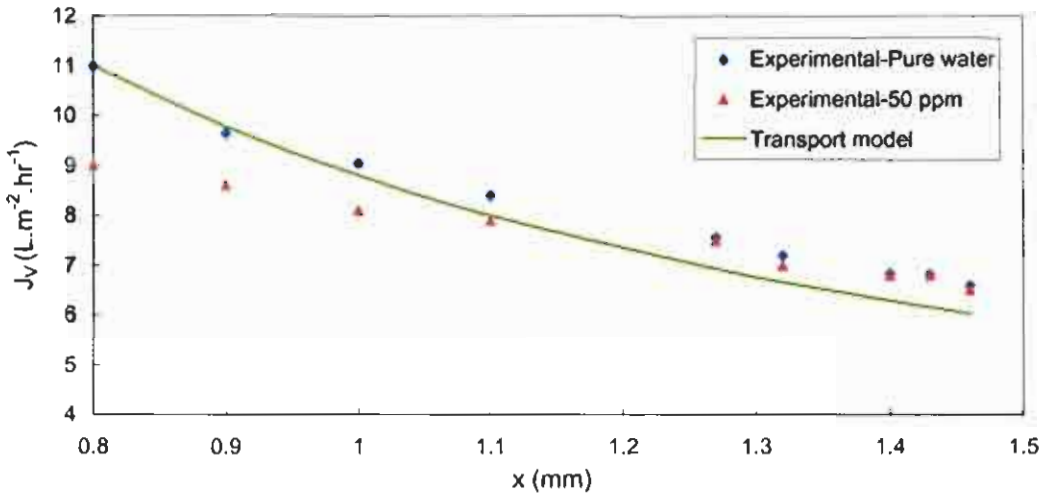

Figure 5.9: Figure of the relationship between permeability and membrane thickness (Pressure difference = 100 kPa).

The model predicts the experimental result well at a thickness close to 0.8 mm. At a thickness above 1.1 mm, the model underestimates the solvent flow rate. This can be explained by the preparation method of the membrane; the same crosslinking time has been used, independent of the membrane thickness, which results in the thick membranes being relatively more open than the thin membranes, thus improving the permeation properties.

5.4.6. The effect of pH on membrane permeability

A zinc salt solution, containing 500 $mg.L^{-1}$ Zn^{2+}, was prepared and the pH of the solution was varied using sulphuric acid to obtain an acidic environment and with

sodium hydroxide to obtain alkaline solutions. The permeability was determined using a 0.8 mm thick membrane. Pressure difference and temperature were kept constant at 100 kPa and 298 K respectively.

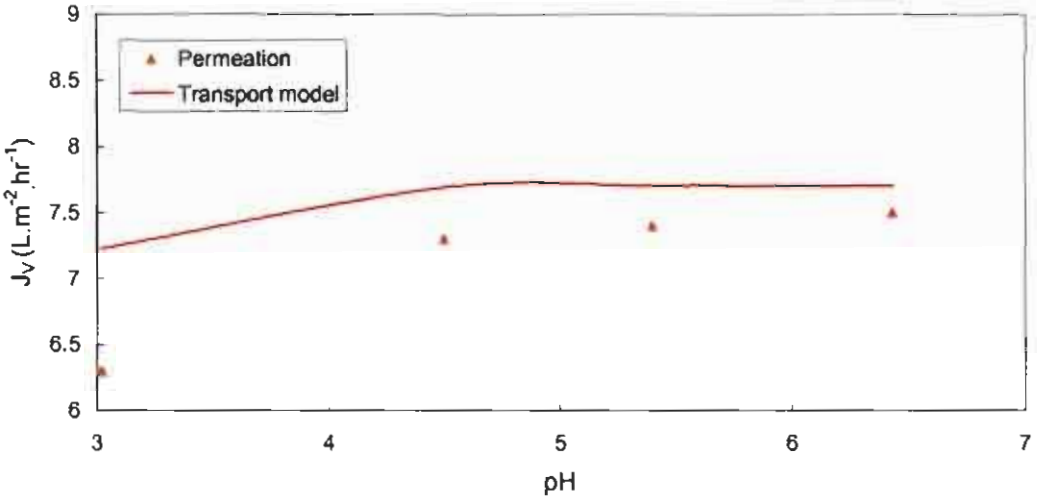

Figure 5.10: Effect of pH on membrane permeability, modelled by the osmotic model (Membrane thickness = 0.8 mm, and 500 ppm Zn with 100 kPa at room temperature).

Figure 5.10 gives the relation between the permeability and the pH (Table E-2.2, Appendix E-2). At low pH, the osmotic pressure of the solution is relatively high compared to the applied membrane pressure difference (40 kPa to 100 kPa). At sufficient low osmotic pressures (above pH = 4), the permeability remains constant with pH. It can therefore be concluded that within the workable adsorption pH range (efficient adsorption between 4 and 7) the pH has no significant effect on the permeability. The effect was modelled in Figure 5.10 using the transport model (Eq. 5.1) and a satisfactory comparison between model and experimental points was obtained.

5.4.7. The effect of temperature on membrane permeability

A zinc salt solution, containing 500 mg.L^{-1} Zn^{2+}, was prepared and the temperature of the solution was varied. The permeability was determined using a 0.8 mm thick membrane. Pressure difference was kept constant at 100 kPa.

Figure 5.11 shows the effect of temperature on the membrane permeability (Table E-2.3, Appendix E-2). The permeability only increases slightly with increasing

temperature, mainly due to a decrease in viscosity of the solution. The osmotic pressure model fits the results sufficiently.

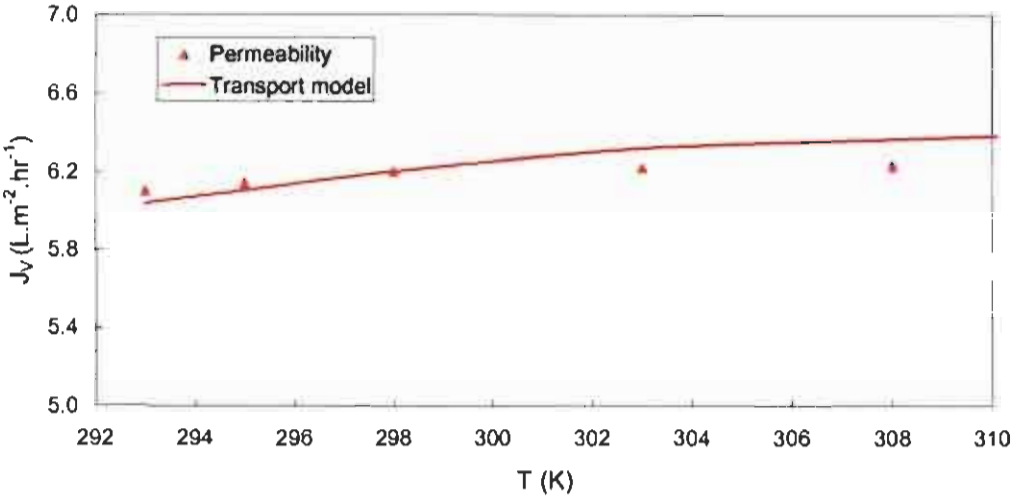

Figure 5.11: Figure of the relationship between permeability and temperature and is modelled by the transport model (Membrane thickness = 0.8 mm, and 500 ppm Zn with 100 kPa pressure difference).

5.5. Conclusions

A model, based on irreversible thermodynamics, using an experimentally determined permeability coefficient of 12.4 L.m^{-2}.hr^{-1}.bar^{-1}, solute permeability of 1.24 mg.m^{-2}.hr^{-1}.bar^{-1}; and a reflection coefficient of 0.997, described the transport of solvent and solute through the optimised chitosan membranes accurately at low solute concentrations. At high solute concentrations, the model deviates from the experimental values, mainly due to the occurrence of concentration polarisation. The effect of pH and temperature on the solvent flux could also be described adequately with this model.

From both structural and transport properties it can be concluded that the manufactured chitosan membranes can be modelled as ultrafiltration (UF) membranes with capillary pores. If the transport of water through the membrane is described with the Hagen-Poiseuille equation, an average pore radius of 23 nm is determined. Using the Kozeny-Carman equation, a value for K of 4.83 is determined.

Chapter 6: The adsorption of zinc-ions on chitosan membranes

6.1. Introduction

Polysaccharide biopolymers, isolated from aquatic organisms, are a new class of potentially inexpensive and environmentally benign solid adsorbents that exhibit a high selectivity towards metal ions. Several studies have produced results where chitosan binds with metal ions to form chitosan-metal complexes, generally with the aim of removing heavy metals from contaminated water (Eiden *et al.*, 1980, Jha *et al.*, 1988, McKay *et al.*, 1989, Rorrer *et al.*, 1993, Chui *et al.*, 1996, Guan *et al.*, 1996, Huang *et al.*, 1996, Kawamura *et al.*, 1997, Guibal *et al.*, 1998, Tomida *et al.*, 1998, Bassi *et al.*, 2000, Becker *et al.*, 2000, Chu, 2002, Wan Ngah *et al.*, 2002, Ng *et al.*, 2003, Cervera *et al.*, 2003, Varma *et al.*, 2003, Rojas *et al.*, 2004, and Ngah *et al.*, 2005). Specifically, chitosan has demonstrated a high affinity for the metals aluminium, cadmium, cobalt, chromium, copper, iron, gallium, mercury, indium, manganese, molybdenum, nickel, palladium, vanadium, zinc, as well as cyanide and metal-cyanide complexes.

In this chapter, the adsorption characteristics of chitosan membranes are studied, with an experimental focus on zinc adsorption. Both the adsorption equilibrium and the dynamics of adsorption have been studied. Desorption of zinc from the chitosan membranes has also been investigated.

In Section 6.2, the relevant adsorption theory is presented. In Section 6.3, the experimental set-up and experimental procedures are given and the results and discussions are presented in Section 6.4. In Section 6.4.1, the equilibrium results of the chitosan membranes are given in the form of adsorption isotherms. The dynamics of adsorption are presented in Section 6.4.2, where breakthrough curves are used to simulate a practical application of chitosan membranes in removing Zn(II) ions. The effect of process variables (pH and the presence of other ions) are given in Section 6.4.3. Since desorption of the metal from chitosan membranes can lead to an economic advantage (re-use of adsorbent, recovery of metal), this is subject to study in Section 6.4.4. Finally, the conclusions of the experimental work are presented in Section 6.5.

6.2. Literature survey

This section starts with general adsorption theory (Section 6.2.1) followed by the elucidation of the adsorption mechanism (Section 6.2.2). In Section 6.2.3 a summary of the most relevant adsorption studies are given and the adsorption, mainly using Langmuir theory, is quantified. In Section 6.2.4 the desorption of ions from chitosan membranes is discussed.

6.2.1. General adsorption theory

Adsorption is defined as the process where an adsorbate attaches to the surface of an adsorbent, either via chemical (covalent) or physical (Van der Waals) bonds. The enthalpy of physisorption is 20-100 $kJ.mol^{-1}$ (Atkins, 1987). Chemical adsorption is associated with a larger heat of adsorption (200-500 $kJ.mol^{-1}$, (Atkins, 1987)) and is generally an exothermic process (Tien, 1994). The strength of the bond with the adsorbent is one of the most important factors of the adsorption process (Swart *et al.*, 1999). A strong bond between adsorbate and adsorbent enhances the adsorption capacity, but makes desorption of the adsorbate from the adsorbent more difficult. Mechanistically, it has been suggested by Tien (1994) that the adsorption of an adsorbate from a solution (*e.g.* metal ions) onto an adsorbent occurs in three steps:

1. External transport from the bulk of the liquid to the adsorbent;
2. Internal transport to an vacant adsorption site; and
3. Adsorption onto this vacant adsorption site.

When the liquid is well mixed, the first step is fast and the second step is generally rate determining.

In the specific case that ions are adsorbed from an aqueous solution onto an adsorbent, the equilibrium of the adsorbate between the two phases can be determined from the amount of solute that is adsorbed as a function of the solute concentration, which is called an isotherm. There are two widely accepted adsorption isotherm models available in literature, one proposed by Langmuir, the other by Freundlich (Tien, 1994). The most frequent used model to describe metal ion adsorption on chitosan is the Langmuir isotherm model (*e.g.* Eiden *et al.*, 1980, Yang and Zail, 1984, McKay *et al.*, 1989, Kawamura *et al.*, 1997, Guibal *et al.*, 1998, Bassi *et al.*, 2000, Wan Ngah *et al.*, 2002, and Ng *et al.*, 2003). The Langmuir model

assumes uniform energies of adsorption on the surface and no transmigration of sorbent in the plane of the surface This model is valid for monolayer sorption on a surface containing a finite number of sites (Volesky, 1989), and is represented by:

$$q_e = \frac{b \cdot C_e}{1 + b \cdot C_e} \cdot q_m \qquad \text{.....6.1}$$

in which b represents the affinity parameter (a measure of the strength of the bond between adsorbate and adsorbent) and q_m, the maximum adsorption capacity.
The equilibrium characterisation of an adsorbent (*e.g.* chitosan) material is crucial for a quantitative assessment of the performance of the adsorbent and for process design (Volesky, 1989). Factors that influence the adsorption characteristics in the case of the adsorption of heavy metal ions from an aqueous solution are: temperature; presence of other ions; oxidation number of the metal-ion; and the pH of the solution (Maruca *et al.*, 1982). One of the more widely used methods to describe the effect of temperature on the adsorption parameter b in the Langmuir equation, can be given by the Van 't Hoff equation:

$$b = b_o \cdot \exp\left(-\frac{\Delta H_{ads}}{R \cdot T}\right) \qquad \text{.....6.2}$$

The second frequently used isotherm model, is the Freundlich model, which is a semi-empirical relation between the adsorbate-concentration and the adsorbed concentration. The general form of this model is:

$$q_e = K_F \cdot C_e^{1/n} \qquad \text{.....6.3}$$

in which K_F and n are empirical constants.

6.2.2. Mechanism of adsorption

The mechanism of adsorption of heavy metal ions from water onto chitosan has been studied intensively. Kondo *et al.* (1996) studied the adsorption of heavy metals onto chitosan modified by D-galactose and found that the mechanism is a chelating physisorption mechanism in which the amine and hydroxyl groups of the chitosan are

the active groups. Kaminski and Modrzejewska (1997) observed similar results for unmodified chitosan and presented an adsorption mechanism (*e.g.* for copper and zinc) as presented in Figure 6.1. This mechanism is however very controversial and still debatable, which is reported by Guzman *et al.* (2003), in studying the influence of metal speciation on the sorption mechanism and uptake capacities of copper.

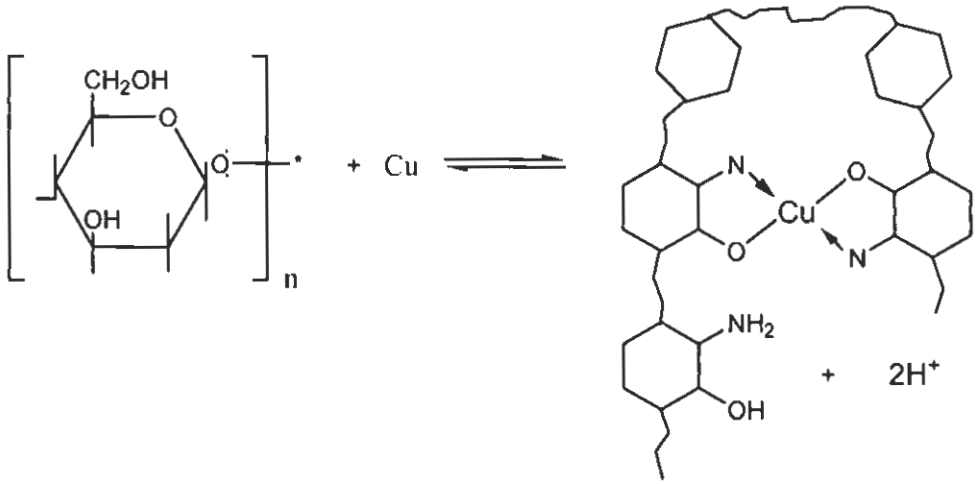

Figure 6.1: Formation of chitosan chelates with copper ions (as suggested by Kaminski & Modrzejewska, 1997).

The activity of the amine group has been studied by Jansson-Charrier *et al.* (1995) using carbon nuclear magnetic resonance for uranium adsorbed on chitosan and found that the amine sites are the main adsorption sites. A comparison of Fourier transform infra-red spectra of chitosan and chitosan doped with rare earth metals, indicated complex formation between the metal ions and the amino groups of the chitosan (Grant, 2000). X-ray photoelectron spectroscopy analysis supports this (Jiang *et al.*, 1997), and indicates that these bonds are weak and possibly ionic in nature. The influence of the combined effect of amine and hydroxyl groups is studied in more detail by Nam and Lee (1998) and Rhazi *et al.* (2002). Since the presence of amine groups is one of the most important characteristics of chitosan, the number of amine sites in the biopolymer (hence the degree of deacetylation) is of great importance.

The adsorption mechanism is influenced by the pH of the metal-ion solution, the speciation of the metal ions (Guibal *et al.*, 1999a) and the ionic strength of the solution (Juang & Shao, 2002). In general, an increase in pH provides an increased

metal adsorption capacity (Juang & Shao, 2002), mainly due to the decrease of the surface charge of chitosan with increasing pH. Since chelation is an equilibrium reaction, the equilibrium can be shifted and altered by species such as protons and hydroxide ions that interact with metals and chelants (Nam & Lee, 1998). If protons are introduced into a solution containing metal, the hydrogen ions will compete with the metal ions and at sufficient low pH, the metal ions will be desorbed from the chitosan (Conway *et al.*, 1999). Grant (2000) showed that the maximum adsorption capacity for copper, cadmium and lead was between a pH of 6 and 7.

6.2.3. Metal adsorption on chitosan

One of the first quantitative studies on the adsorption of zinc on chitosan flakes with different particle sizes was carried out by McKay *et al.* (1989). The authors showed that the monolayer sorption capacity of the biopolymer chitosan was dependent on the particle size and determined a maximum capacity for mercury (815 $mg.g^{-1}$), copper (222 $mg.g^{-1}$), zinc (164 $mg.g^{-1}$) and nickel (75 $mg.g^{-1}$), at room temperature and at a particle size between 710-1000 μm. Langmuir adsorption isotherms for zinc ions showed a maximum adsorption capacity of between 98 $mg.g^{-1}$ (particle size between 210 – 355 μm) and 164 $mg.g^{-1}$ (particle size between 710 – 1000 μm), an affinity parameter (b) of 0.007-0.013 $L.mg^{-1}$, and an adsorption equilibrium constant of 1.21-1.27 $L.g^{-1}$ for the zinc ions. Temperature studies indicated that the maximum adsorption capacity decreased with increasing temperature, and resulted in an adsorption enthalpy value of –18 $kJ.mol^{-1}$.

Kawamura *et al.* (1997) reported adsorption values on the adsorption of zinc ions on polyaminated highly porous chitosan beads. They found an adsorption capacity of 1 mg zinc.(g wet chitosan)$^{-1}$. However, the water content was not given so that the capacity on a dry basis is not known.

Peter (1995) reported a maximum adsorption capacity of 104 $mg.g^{-1}$ for zinc on 97% deacetylated chitosan (the formulation and source of chitosan are not given) at a pH of 7.4 and a temperature of 30 °C.

Bassi *et al.* (2000) proved that in commercially available chitosan (chitosan flakes supplied by Sigma, with a DDA of 85%) the order of metal ion adsorption decreased as follows: copper (1 $mg.g^{-1}$) > lead (0.20 $mg.g^{-1}$) > cadmium (0.113 $mg.g^{-1}$) > zinc (0.06 $mg.g^{-1}$) when starting with a 10 $mg.L^{-1}$ metal solution. The metal adsorption uptake was found to be pH-dependent, with a maximum between pH 6 and pH 7.

Equilibrium studies correlated well with the Langmuir isotherm equation, with a maximum adsorption capacity of 11.7 $mg.g^{-1}$ and an affinity parameter (b) of 0.97 $L.mg^{-1}$ for the zinc ions.

The large difference in results between McKay *et al.* (1989) and Bassi *et al.* (2000) can be explained by the difference in chitosan flake particle size, process conditions and the degree of deacetylation.

Becker *et al.* (2000) studied the adsorption of zinc on 6 different modified chitosan (DDA = 83%) beads. The maximum adsorption capacity was about 100 $mg.g^{-1}$ (slightly dependent of the sort of derivative) for zinc sulphate at a pH of 6. The authors found that the sulphate anion can enhance the adsorption. The chloride and nitrate anions were also used, and a strong influence on the adsorption of the modified chitosan was shown, reducing the capacity to almost zero in some cases. Elson *et al.* (1980) also experienced the increasing effect of sulphate and Kurita *et al.* (1998) the decreasing adsorption effect of chlorides. However, Jha *et al.* (1988) found that the cations calcium, and magnesium, and the anions bicarbonate and chlorides present in tap water did not influence cadmium uptake by chitosan flakes.

Vold *et al.* (2003) studied the selective adsorption of copper, zinc, cadmium and nickel on further deacetylated commercial chitosan and observed a high selectivity to copper compared to zinc, cadmium and nickel between a pH of 5 and 6.

Osifo (2005) investigated the adsorption of zinc onto chitosan beads at a pH of 5, and found an adsorption capacity of 52 $mg.g^{-1}$.

Lima and Airoldi (2004) carried out a detailed investigation on chitosan-divalent cation interactions using cobalt, nickel, copper and zinc ions. The authors used chitosan flakes with a particle size of between 80 and 200 mesh, and showed a preferred adsorption of copper (18 $mg.g^{-1}$) above cobalt (14 $mg.g^{-1}$), nickel (13 $mg.g^{-1}$) and zinc (9 $mg.g^{-1}$). The adsorption enthalpies of these metals were also determined and were found to be -40 $kJ.mol^{-1}$ for copper and -27 $kJ.mol^{-1}$ for cobalt, nickel and zinc.

6.2.4. Desorption of ions from chitosan membranes

In contrast to the numerous studies on the adsorption of heavy metals on chitosan, little work has been published on the desorption of heavy metals from chitosan, although this is a very important issue with regard to the introduction of chitosan technology in practical application (Guibal, 2004). The advantage of desorption is

twofold: the adsorbent can be re-used and the metal could possibly be recovered and used again. Metals are most often removed from chelating molecules by decreasing the pH that enhances the exchange of metal ions by hydronium ions (Volesky, 1989, Coughlin *et al.* 1990). Volesky (1989) also reported that most biomass-based systems will not withstand long-term recycling, and frequently a loss of activity (especially for solid adsorbents) is observed. The loss of activity is due to chemical degradation, chemical fouling, thermal degradation and mechanical destruction. Both chemical degradation and mechanical destruction were studied on chitosan beads by Jha *et al.* (1988). The authors reported a 91.2% recovery of cadmium using a 0.01 N HCl-solution. After two cycles, the adsorption capacity of chitosan was reduced to 69%, whereas the recovery of the cadmium with 0.01 N HCl reduced from 89.3% in the second cycle to 81.3% in the third. The loss in capacity is attributed to incomplete desorption of the metal from the adsorbent and the mass loss of the chitosan associated with the acid treatment.

6.3. Experimental procedures

For the experimental work, chitosan membranes manufactured according to the procedure described in Section 3.3.2 were used (diameter 47 mm, thickness 0.8 - 1.5 mm). Chitosan A was used for the reasons as given in Section 3.4.1. For all experiments, the standard 0.8 mm membranes were used, unless otherwise noted. All experiments were conducted in triplicate and the data present the average of the three values. The statistical error was less than 9.3%.

The membranes adsorption was tested using a solution of heavy metals prepared from analytical grade chemicals in de-ionised water, and the same equipment and procedures detailed in Section 4.3.

During the adsorption equilibrium experiments, the solution was re-circulated until, after three cycles equilibrium was reached. This corresponds with a contact time in the order of tens of hours, mainly depending on the applied pressure difference. The adsorption loading (q_e) of the membrane was calculated in mg of zinc adsorbed per gram of dry chitosan in the membrane:

$$q_e = \frac{\left(C_{in} - C_e\right) \cdot V}{m} \qquad \text{.....6.4}$$

Zinc samples were collected in acid washed plastic bottles. The pH of the solutions was measured with a Jenway 3310 pH meter (Model no. 5205). A quantitative determination of metal elements present in the filtrate was determined using Atomic Absorption Spectrophotometry (Aanalyst 200 Model no. B3150070).

In metal ion adsorption studies, it is important to know the speciation of the metal (Guibal, 2004). In the case of zinc, the speciation was calculated using the simulation program OLI (www.olis.com). A typical example of the speciation of 100 $mg.L^{-1}$ zinc in an aqueous solution is given in Figure 6.2. From this figure, it can be seen that, under the experimental conditions worked in this study (pH ≤ 6), more than 99.8% of the zinc is in the Zn^{2+} configuration while the formation of other species (e.g. $Zn(OH)^{+}$) is negligible.

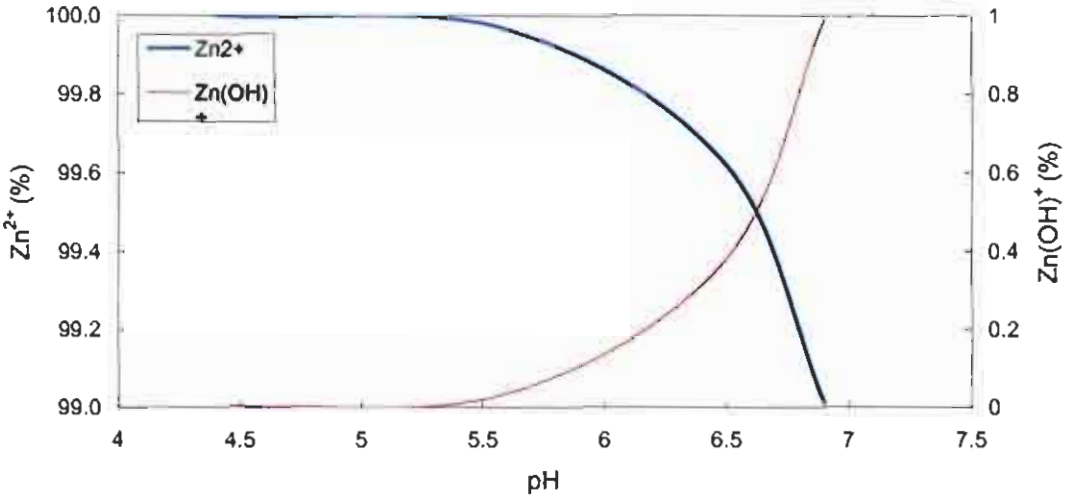

Figure 6.2: Figure describing zinc-species (100 $mg.L^{-1}$) in aqueous solutions.

Another aspect that is important in this study, is to work outside the precipitation limits of zinc hydroxide ($Zn(OH)_2$). For this reason, the effect of the pH on precipitation of $Zn(OH)_2$ at different concentrations of zinc (C_{in}) is studied. The pH of the solution was changed using a dilute solution of sodium hydroxide and the results are shown in Figure 6.3.

From this figure, it can be seen that a decrease in zinc concentration occurs at a pH value of 6 and higher if working with a zinc solution of 500 ppm and below. Above a pH of 6, the zinc precipitates as zinc hydroxide as also described by Pourbaix (1974). It can be concluded that the adsorption experiments must be conducted at a pH of 6 or below for high zinc concentrations, otherwise the decrease in Zn(II) concentration

will be a combination of chitosan zinc adsorption and precipitation (Table F-1.1, Appendix F-1).

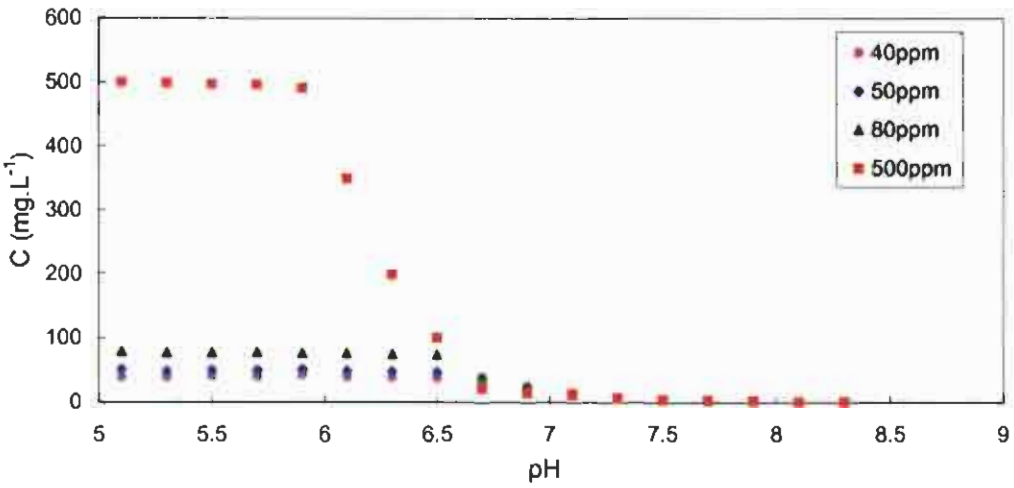

Figure 6.3: Effect of pH on the concentration of zinc in solution.

6.4. Results and discussion

In Section 6.4.1 the equilibrium results are presented, and in Section 6.4.2 the dynamic properties of the membranes are discussed. This is followed by the effect of external factors on the adsorption process (Section 6.4.3) and finally an experimental desorption study is presented in Section 6.4.4.

6.4.1. Equilibrium studies

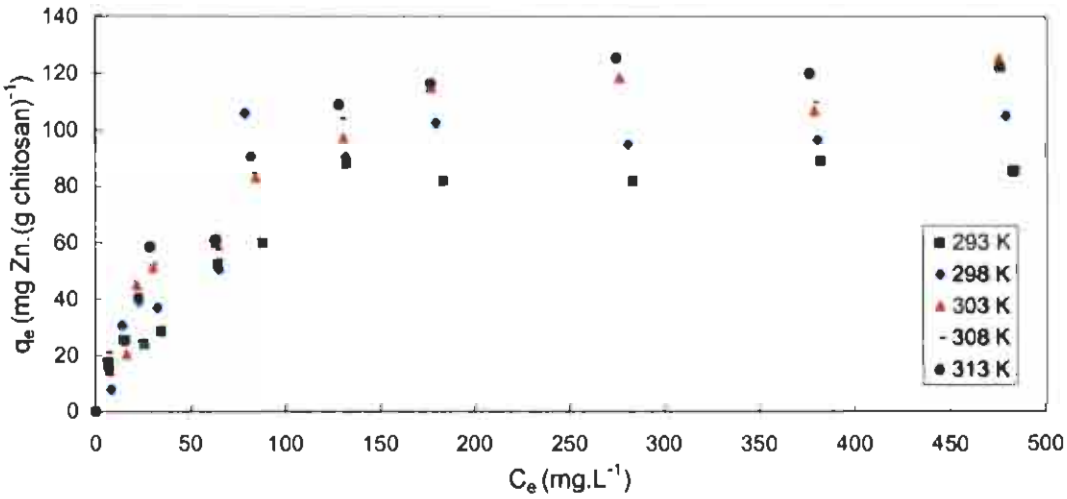

Figure 6.4: Equilibrium adsorption of zinc onto chitosan membranes.

The results for the equilibrium adsorption of chitosan membranes for zinc are shown in Figure 6.4 at a pH of 6 (Table F-2.1, Appendix F-2). It was also observed that the pH of the permeate was slightly higher than that of the feed solution (an average increase of 0.2 was observed). Experiments were conducted at temperatures between 293 K and 313 K, with 5 K intervals. The shape of the adsorption isotherm shows a rapid initial increase in adsorption capacity resulting from chitosan's high affinity for the zinc cation.

The adsorption results were fitted using both the Langmuir (Eq. 6.1 with R^2 range of 0.9664 to 0.9897) and Freundlich (Eq. 6.3 with R^2 range of 0.8945 to 0.9055) isotherms, indicating that the Langmuir model fitted the results more accurately. To fit the parameters associated with the Langmuir model, Eq. 6.1 was rearranged to:

$$\frac{C_e}{q} = \frac{1}{K_L} + \frac{b \cdot C_e}{K_L} \qquad \text{.....6.5}$$

Hence a plot of C_e/q versus C_e is linear with the intercept equal to the inverse of K_L, and the slope equal to the product of b and the inverse of K_L. The linearised form of the Langmuir model is given in Figure 6.5 (Table F-2.2, Appendix F-2).

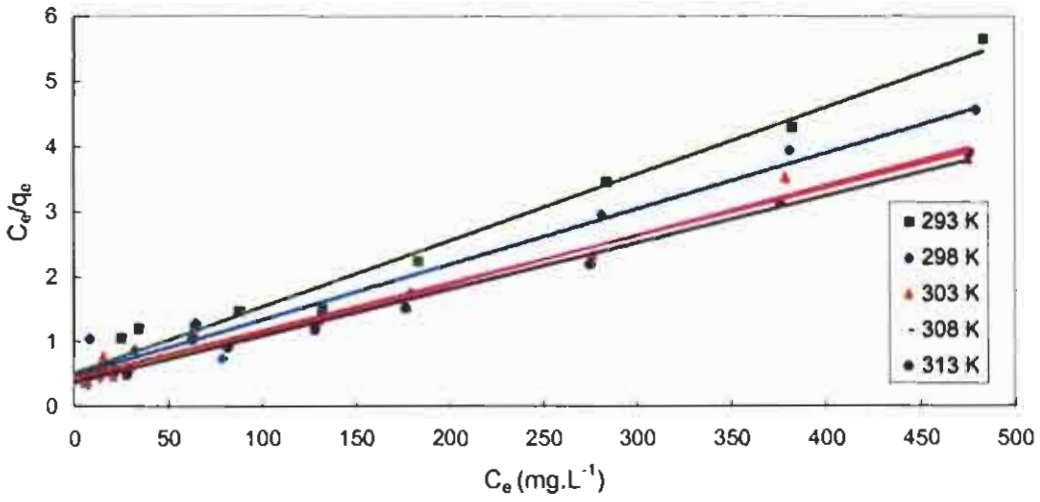

Figure 6.5: Experimental data modelling using Langmuir equation for equilibrium concentration.

The Langmuir equilibrium constants were calculated from this figure and are given in Table 6.1. From this table, it can be concluded that the maximum adsorption

capacity (q_{max}) increases with temperature to a value of 135 $mg.g^{-1}$ for a temperature of 303 K and above. This temperature related increase could possibly be explained by the fact that chitosan membranes are gel type membranes where the free water volume plays an important role (Krajewska, 2001). An increase in temperature results in swelling of the membrane and thus an increase in free water volume (Matsuyama *et al.*, 1997), which could make the adsorption sites more accessible and result in a higher adsorption capacity. This effect, however, is only evident at a temperature of 303 K after which the adsorption capacity remains constant.

Table 6.1: Langmuir constants for zinc adsorption at different temperatures.

Temperature (K)	q_{max} (mg Zn.g chitosan^{-1})	b ($L.mg^{-1}$)	K_L ($L.g^{-1}$)
293	105	0.012	1.22
298	122	0.013	1.61
303	135	0.016	2.18
308	136	0.018	2.44
313	135	0.020	2.68

The determined adsorption capacity is higher than reported by Peter (1995) and Becker *et al.* (2000) for chitosan beads and Bassi *et al.* (2000) for chitosan flakes, who found capacities of about 100 $mg.g^{-1}$ or smaller, under similar process conditions. Bassi *et al.* (2000) reported an affinity parameter of 0.97 $L.mg^{-1}$ for the zinc ions. McKay *et al.* (1989) reported an adsorption capacity of 164 $mg.g^{-1}$ for chitosan powder, with an Langmuir affinity parameter of 0.007-0.013 $L.mg^{-1}$, but the process conditions (*i.e.* pH) were not given.

Osifo (2005) measured an adsorption capacity of 52 $mg.g^{-1}$, at a pH of 5, using chitosan beads of the same raw material as has been used in this study. This comparison between beads and membranes suggests that the use of membranes can be advantageous over beads with regard to the adsorption capacity. The forced contact between water and chitosan in the membrane (due to the convective transport of the water through the membrane) not only improves the transport rate, but might also improve the contact between the metal ion and the functional groups of chitosan, resulting in a higher adsorption capacity.

The influence of temperature on the affinity parameter (b, see Table 6.1) was used to determine the enthalpy of adsorption using the linear form of the Van 't Hoff equation (Eq. 6.2):

$$\ln(b) = \ln(b_o) - \frac{\Delta H_{ads}}{R \cdot T} \qquad \text{.....6.6}$$

Hence a plot of the natural logarithm of b versus the reciprocal temperature results in a line from which the enthalpy of adsorption (20 kJ.mol^{-1}) can be calculated from the slope (Fig 6.6) (Table F-2.3, Appendix F-2).

The observed adsorption enthalpy suggests an endothermic adsorption, i.e. a rise in temperature will favour the adsorption. Lima and Airoldi (2004) and McKay *et al.* (1989) found negative values (-27.7 kJ.mol^{-1} for beads and -17.7 kJ.mol^{-1} for powder) for the adsorption enthalpy of zinc on chitosan. Most adsorption processes are exothermic (Tien, 1994), however, McKay *et al.* (1989) reported positive adsorption enthalpies for the adsorption of copper and mercury on chitosan powder. This behaviour could possibly also be attributed to the influence of the temperature on the free water volume of the chitosan, as was discussed with the increase in the adsorption capacity relative to temperature.

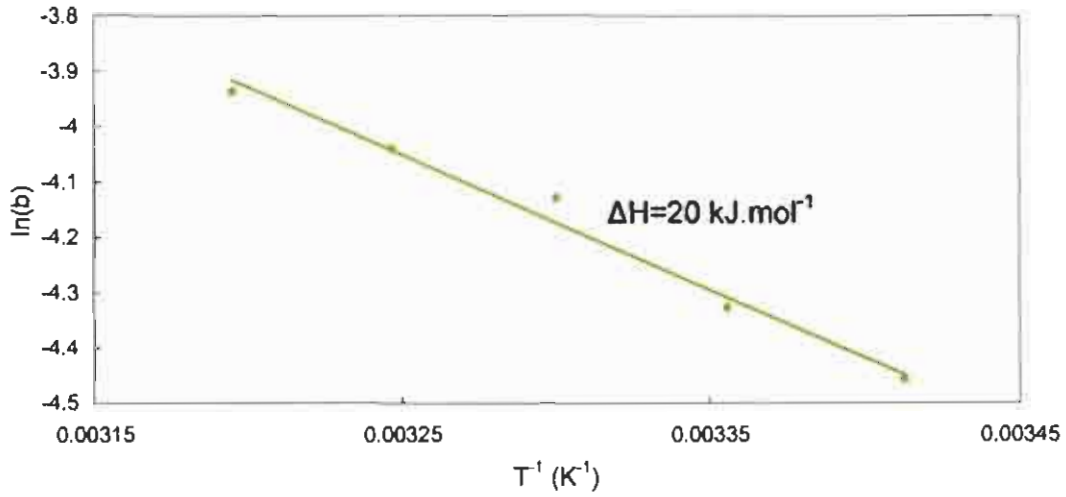

Figure 6.6: Van 't Hoff plot of Zinc adsorption on chitosan membranes.

The capacity of chitosan membranes is compared to other formulations of chitosan and also to other adsorbents in Table 6.2 (only the maximum values found in literature are given). From this table, it can be seen that chitosan membranes have a

large adsorption capacity compared to the other chitosan formulations and adsorbents.

Table 6.2: Chitosan membrane adsorption compared to the highest adsorption capacities on other adsorbent materials for zinc.

Material	Adsorption capacity ($mg.g^{-1}$)	Reference
Chitosan membranes	122	This study
Chitosan powder	164	McKay *et al*, 1989
Chitosan flakes	83	Levan *et al*, 1998
Chitosan beads	52	Osifo, 2004
Chitin	18	Chui *et al*, 1996
Activated sludge	25	Sekar *et al*. 2004
Lignin	95	Atkinson *et al*. 1998
Activated carbon (GAC-C)	18	Atkinson *et al*. 1998
Peat moss	13	Atkinson *et al*. 1998
Bentonite	53	Atkinson *et al*. 1998

The maximum adsorption capacity was also determined for the heavy metals copper and nickel on chitosan membranes at a pH of 6 and a temperature of 298K. Table 6.3 shows the adsorption value of these metals, compared to zinc and the theoretical maximum value, assuming that 2 chitosan amino groups bind with 1 metal ion (Figure 6.1) and that the crosslinked monomers are not active. This theoretical value can than be calculated with:

$$q_{theoretical} = \frac{1}{2}\left(\frac{Mw_{metal\ adsorbed}}{Mw_{chitosan\ monomer}}\right)\cdot(1-DOC)\cdot(DDA) \qquad .....6.7$$

From Table 6.3, it can be concluded that chitosan shows the largest adsorption capacity for copper, zinc and nickel, a series that was also observed by Bassi *et al.* (2000), Osifo (2004) and Lima and Airoldi (2004). McKay *et al.* (1989) determined a higher value of copper compared to nickel and zinc, and observed a higher capacity for nickel than zinc.

Table 6.3: Theoretical and experimental adsorption capacity for some metals onto SA chitosan (pH=6).

Metal	Experimental q_e ($mg.g^{-1}$)	$q_{theoretical}$ ($mg.g^{-1}$)
Zinc	122	126
Copper	182	123
Nickel	100	114

6.4.2. Dynamic studies

The dynamics of adsorption is also an important factor in the design of adsorption columns, therefore the adsorption rate was studied using breakthrough curves. A zinc solution was pumped through the membrane and the zinc concentration in the effluent of the membrane measured as a function of time. Breakthrough experiments were carried out with different zinc concentrations, membrane thicknesses and pressure differences.

6.4.2.1. The effect of flux on adsorption

These experiments were conducted under non-equilibrium conditions, with the solution only being circulated once through the membrane. This was done in order to determine whether high flux ratios influence adsorption capacity. Figure 6.7 illustrates the effect of flux on the membrane adsorption (Table F-3.1, Appendix F-3). As the flux depends on the pressure difference, this was changed until a specific flux was reached, and the adsorption at this specific flux was then determined.

It is clear that the adsorption loading decreases with an increase in flux. This is caused by the reduction in adsorption time. Thus, the process is a kinetic process, the higher the flux the lower the adsorption. Therefore it can be concluded that internal diffusion plays a role in the dynamics of adsorption.

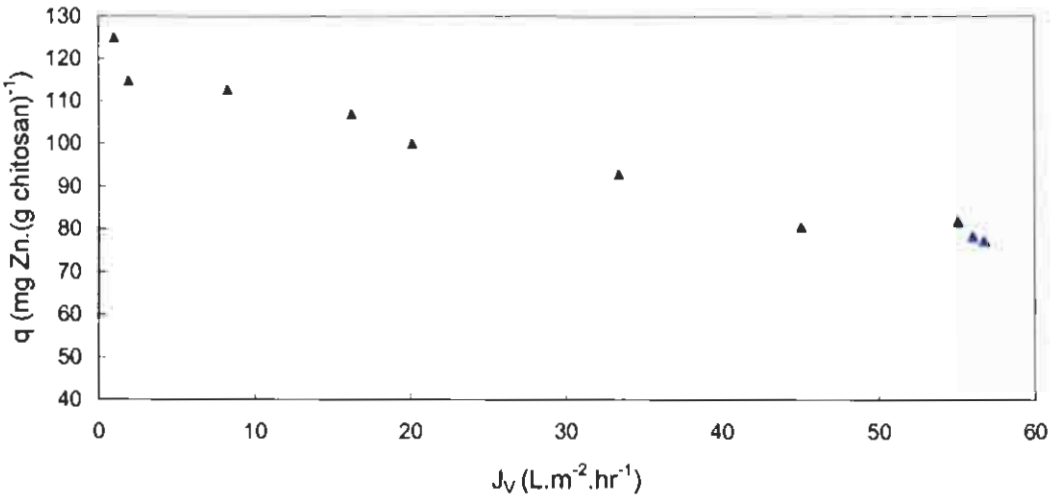

Figure 6.7: The relationship between zinc adsorption to membrane flux (Non-equilibrium, pH=6 and 50 mg.L^{-1} Zn).

6.4.2.2. Breakthrough studies of chitosan membranes

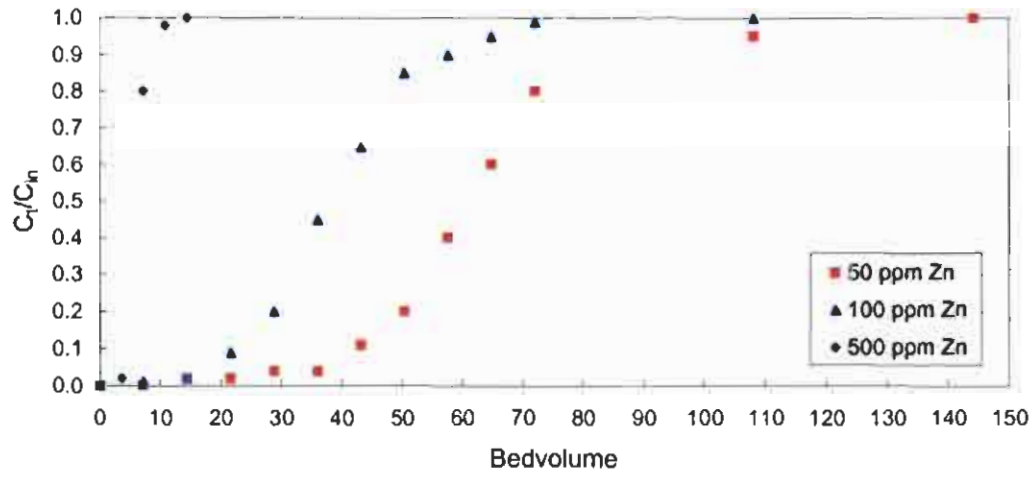

Figure 6.8: The breakthrough profile of zinc solutions (pH = 6).

In Figure 6.8, the experimental breakthrough curves of 50, 100 and 500 ppm zinc solutions for an applied pressure difference of 100 kPa and a pH of 6 are given (Table F-3.2, Appendix F-3). In this figure, the dimensionless concentration (c_t/c_{in}) is given as a function of the number of bedvolumes penetrated through the membrane. If the breakthrough is defined at a concentration of 10% of the inlet concentration (c_t/c_{in}=0.1), thus the moment when the concentration of zinc in the permeate reaches 10% of the zinc concentration in the feed, the number of bedvolumes can be

determined as the breakthrough from Figure 6.8. These values are given in Table 6.4. The low bedvolume value for the 500 $mg.L^{-1}$ zinc solution suggests that chitosan membranes are not very well suited for applications with relatively high metal ion concentrations.

Table 6.4: Bedvolumes at which breakthrough occurs (pH=6) and the permeate concentration.

Metal concentration ($mg.L^{-1}$)	Breakthrough bedvolumes	C_t ($mg.L^{-1}$)
50	43	5.5
100	22	9.0
500	5	10.0

From a mass balance, it could be calculated that breakthrough occurred at 30% capacity of the membrane, independent of the solute concentration.

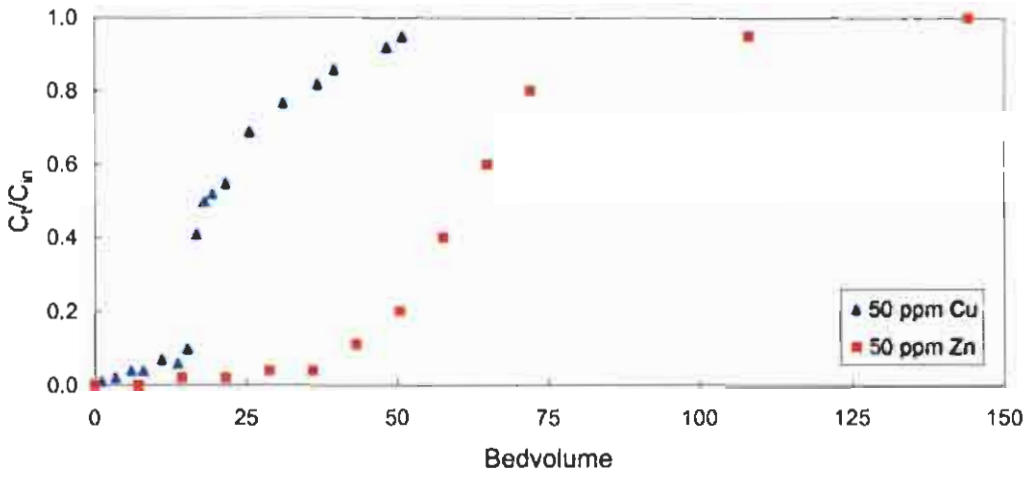

Figure 6.9: The breakthrough profile of zinc solutions for membrane adsorption (pH = 6) compared to copper solutions for bead adsorption (Grant, 2000).

In Figure 6.9, the breakthrough curve of 50 $mg.L^{-1}$ zinc solution and chitosan membrane is compared to the breakthrough curve for copper as obtained by Grant (2000) using chitosan beads (3.8 mm), prepared from the same raw material as used in this study. It can be seen that more bedvolumes can be treated with membranes than with beads, even knowing that copper is a better adsorbate than zinc (Table

6.3). This behaviour can again be attributed to the improved contact between water and adsorbent, due to the convective transport through the membrane.

Due to the limited literature available on the breakthrough of zinc, the breakthrough curves were compared with the breakthrough of zinc on activated carbon. Mohan and Chander (2001) investigated the adsorption of zinc ions on different activated carbons at a pH of 6 and a 50 $mg.L^{-1}$ starting solution and observed a breakthrough after 20 bedvolumes.

6.4.3. Other factors influencing the adsorption

6.4.3.1. The effect of cations and anions on membrane adsorption

To investigate the effect of other contaminants on the chitosan adsorption, a reference solution of 500 $mg.L^{-1}$ zinc ($ZnSO_4 \cdot 7H_2O$) was used. The reference solution was divided into 9 samples and these samples were again divided into three sets of samples. All contaminants were compared to the reference solution (Table 6.5). The first set of samples was used to determine the effect of nitrates and chlorides on the adsorption capacity; the second set to test the effect of calcium, sodium, potassium and magnesium; and the third set, to test the effect of sulphates. The solutions were treated under 100 kPa pressure difference and 298 K, using a 0.8 mm membrane (Table F-4.1, Appendix F-4).

From Table 6.5, it can be concluded that nitrates and to a lesser extend chlorides have a negative influence on the adsorption capacity as was described by Becker *et al.* (2000). In the case of nitrates, competitive adsorption could possibly occur, since it is reported that nitrates do adsorb on chitosan in a pH range of 3 to 5 and to a lesser extend at pH 6 (Jaafari *et al.*, 2004). The reduction in adsorption capacity due to chlorides was also reported by Kurita *et al.* (1998) and was explained by the formation of various zinc chloro complexes. Typical rinse water contains low levels of nitrates but high levels of chlorides, which can have a negative effect on the adsorption of chitosan membranes.

Taking into account the effect of chlorides on the adsorption capacity, the effect of sodium, potassium, magnesium and calcium do not result in large differences in adsorption capacity and do not prevent adsorption of the zinc metal ions when simultaneously present. This was also observed by Jha *et al.* (1988), who found that

the presence of calcium and magnesium did not influence the adsorption of cadmium.

There is a slight increase in adsorption capacity with an increase in sulphate concentration. In accordance with sulphate-induced structure modifications in chitosan, chitosan in a sulphate media shows enhanced capacity for transition metal ions (Elson *et al.*, 1980). Elson *et al.* (1980) reported a reduction of sulphate levels after metal adsorption studies

Table 6.5: The effect of cations and anions on membrane adsorption.

Set	Contaminant	Concentration ($mg.L^{-1}$)								$\frac{q}{q_{ref}}$
		Zn	SO_4	NO_3	Cl	K	Mg	Na	Ca	
Ref.	$ZnSO_4.7H_2O$	500	735	-	-	-	-	-	-	100%
1	$ZnSO_4.7H_2O$	50	73.5	-	-	-	-	-	-	103%
	$Zn(NO_3)_2.6H_2O$	50	-	95	-	-	-	-	-	84%
	$ZnCl_2$	50	-	-	54	-	-	-	-	91%
2	KCl	-	-	-	50	55	-	-	-	97%
	$MgCl_2.2H_2O$	-	-	-	50	-	17	-	-	92%
	NaCl	-	-	-	50	-	-	32	-	94%
	$CaCl_2.2H_2O$	-	-	-	50	-	-	-	28	91%
3	$CaCl_2.2H_2O$	-	-	-	88	-	-	-	50	85%
	$CaSO_4.2H_2O$	-	120	-	-	-	-	-	50	95%

6.4.3.2. The effect of pH on adsorption

To test the effect of pH on adsorption, a salt solution mixture, containing 500 $mg.L^{-1}$ Zn^{2+}, was prepared. The pH was changed with sulphuric acid solution to obtain acidic concentration, and with sodium hydroxide to obtain alkaline solutions.

Figure 6.10 gives the relationship between the adsorption capacity and the pH (Table F-4.2, Appendix F-4). From this figure, it can be seen that there is a slight increase in the amount of Zn^{2+} taken up by chitosan as the pH varies between 4.5 and 6.4, showing that the maximum adsorption capacity is reached, and a further decrease in pH results in a slight decrease in adsorption. This decrease can be explained by chelants possessing acid-base characteristics, and chelation being an equilibrium reaction, so that the equilibrium can be shifted and altered by species such as protons and hydroxide ions that interact with chelants (Conway *et al.*, 1999). If

protons are introduced into a metal containing solution, the hydrogen ions will compete with the metal ions and at sufficient low pH, the metal ions will be desorbed from the chitosan (Conway *et al.*, 1999).

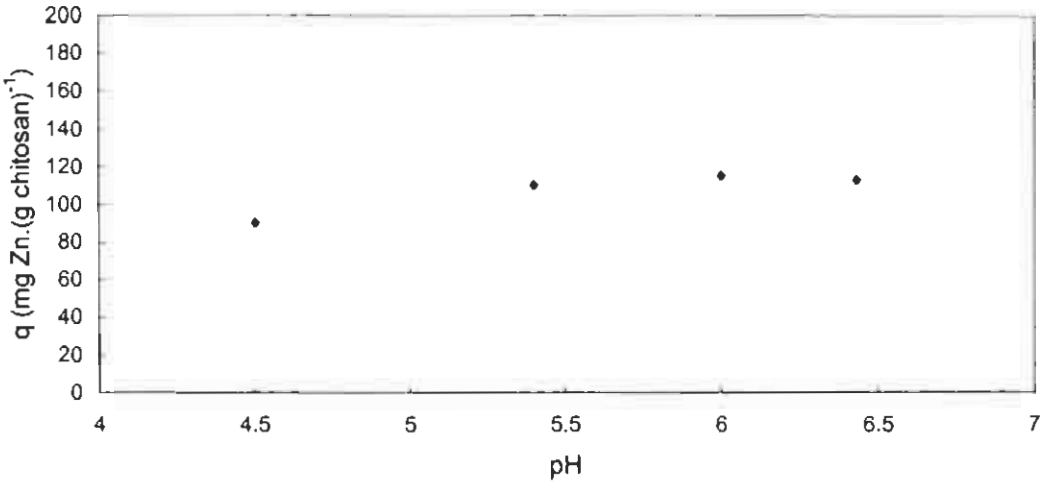

Figure 6.10: The relationship between zinc adsorption and pH (Membrane thickness = 0.8 mm, and 500 mg.L^{-1} Zn).

6.4.4. Desorption and recovery

The membranes prepared for desorption studies were first subjected to adsorption. During the adsorption process, each membrane was treated with 500 mg.L^{-1} zinc solution at a pH of 6. The concentration of the zinc solution before and after treatment was analysed to determine the equilibrium adsorption capacity. Desorption was carried out by treating the membranes in separate experiments with distilled water and solutions of hydrochloric acid (pH = 2 and 4), and sulphuric acid (pH=2 and 4). The membranes were immersed for 6 hours. A volume of 200 mL water and acid respectively was used per treatment.

Table 6.6 (Table F-5.1,2, Appendix F-5) summarises the percentage of zinc that was desorbed (calculated on the amount that was adsorbed) and the percentage membrane loss (calculated on the original mass) during the regeneration treatment. No significant amounts of ions were desorbed by water. The percentage desorption by sulphuric acid (90%) is more than the percentage desorption by hydrochloric acid (85%).

With the use of hydrochloric acid, the membrane loss (up to 5%) associated with the desorption process is higher than sulphuric acid (up to 3%). Therefore, sulphuric acid is a better recovering agent than hydrochloric acid. It has been shown by Milot

et al. (1997) that chitosan is less soluble in sulphuric acid than in hydrochloric and nitric or organic acids. Thus, to investigate the amount of cycles a membrane can undergo before destruction of the mechanical strength of the membrane, sulphuric acid was used.

Table 6.6: Adsorption and desorption.

Desorption medium	pH	Desorption (% of adsorption)	Mass loss (% of the original)
Water	7.4	2%	0%
HCl	2	85%	5%
HCl	4	70%	2%
H_2SO_4	2	90%	3%
H_2SO_4	4	81%	1%

Multi cycle experiments were carried out with the most efficient desorption agent (H_2SO_4, pH=2). After the second cycle the adsorption capacity was reduced to 75% (based on the original membrane mass) with a desorption percentage of 70% (based on the new adsorption capacity) and a mass loss of 11% (based on the original membrane mass). At best, the membrane can be regenerated twice, whereafter the structural integrity of the membrane was lost. For chitosan beads, Jha *et al.* (1988) reported a desorption capacity of 91.2% (based on the original bead mass) during the first cycle, a reduction of adsorption to 69% (based on the new adsorption capacity) and a desorption of 89.3% (based on the new mass) after cycle two using hydrochloric acid.

6.5. Conclusions and Recommendations

Equilibrium isotherm studies revealed that the adsorption of zinc onto chitosan can be described by a Langmuir equation with a maximum zinc adsorption capacity of 135 $mg.g^{-1}$ of chitosan for 303-313 K. It was also determined that the adsorption process is endothermic with an adsorption enthalpy of 20 $kJ.mol^{-1}$.

Breakthrough curves were affected by the initial concentration of zinc in the solution and indicated that chitosan membranes perform better than other formulations of chitosan. The membranes adsorbed the metal ion zinc almost completely when working at low initial concentrations (<50 $mg.L^{-1}$). Further studies proved that the

adsorption process is also determined by kinetics, with a decrease in adsorption (125-85 $mg.g^{-1}$) as the flux increases (2-55 $L.m^{-2}.hr^{-1}$). The flux is inversely proportional to the membrane thickness.

It was also shown that the adsorption of metal ions by chitosan membranes is affected by co-ions, and the pH of the solution. The adsorption is limited by nitrates and enhanced by sulphates. The optimum pH for adsorption of zinc onto chitosan membranes is a pH of 6.

This adsorption process results in a membrane with a high zinc concentration in its structure, from which metals can be recovered by washing the chitosan membranes with an acidic solution. As the pH of the elution solution was decreased from a pH of 6 to a pH of 2, zinc was removed, up to 90%. This regeneration caused a decrease in the adsorption capability of the chitosan mainly due to a mass loss of the membrane (up to 11%). After 2 regeneration cycles the structural integrity of the membrane was lost and the membrane could not be used anymore.

Chapter 7: Conclusions & prospects

7.1 Conclusions

Chitosan flakes, with an average diameter of 1.5 mm, were produced from the waste material from South African shellfish material and were characterised. The yield in the production of chitin flakes (>0.75 mm) was 26%, and the successive conversion to chitosan resulted in a yield of 18%. The molecular weight of the chitosan was found to depend on the source of the raw material, while the DDA of the chitosan produced did not differ significantly. The structure and molecular weight of the chitosan, produced from the cape rock lobster (Chitosan A), with an average molecular weight of 144 200 kg.kmole^{-1} compared very well with the industrial grade chitosan, with an average molecular weight of M_w = 150 000 kg.kmole^{-1}, however the DDA of the produced chitosan was lower than that of the industrial grade chitosan (77% and 98% respectively).

Chitosan membranes were manufactured via a phase inversion method, a process in which the most important factor is the initial chitosan concentration in the acidic solution prior to membrane formation. The chitosan concentration mainly determines the viscosity of the solution, which can either by being too low, result in a mechanically weak membrane with a low adsorption capacity, or by being too high, result in membranes with cracks. The viscosity of the chitosan solution is also dependent on the molecular weight of the chitosan, where the viscosity increases as the molecular weight increases. Since Chitosan A had the lowest molecular weight, it could be converted into a stable membrane with the highest percentage chitosan and, hence, adsorption capacity. Chitosan A was chosen for further optimisation. If a Chitosan A membrane is manufactured from a 7 mass% chitosan in a 4 mass% acetic acid solution, precipitated in a 4 mass% sodium hydroxide solution, and crosslinked for 6 hours, optimum characteristics, in terms of adsorption, flux through the membrane, stability and mechanical strength were obtained.

During characterisation of the chitosan membranes, it was found that the water content of the membranes was high (95 – 98 mass%) and decreased with an increase in the chitosan concentration, prior to membrane formation. The free water volume is significantly lower than the total water content, indicating that water can be present as free water and as fixed water. The physical properties of the chitosan

membranes manufactured under optimum conditions are: a wet density of 1100 $kg.m^{-3}$; a chitosan content 5.2 mass%; a fraction free water volume of 65 mass%; a fraction fixed water of 30 mass%; a maximum pore radius of 40 nm; and a total surface area of $1.15 \cdot 10^5$ $m^2.kg^{-1}$.

A transport model based on irreversible thermodynamics, using an experimentally determined permeability coefficient of 12.4 $L.m^{-2}.hr^{-1}.bar^{-1}$, a solute permeability of 1.24 $mg.m^{-2}.hr^{-1}.bar^{-1}$ and a reflection coefficient of 0.997, describes the transport of solvent and solute through the optimised chitosan membranes accurately at low solute concentrations. At high solute concentrations, the model deviates from the experimental values, mainly due to the occurrence of concentration polarisation. The effect of pH and temperature on the solvent flux could also be described adequately with this model.

From both structural and transport properties it can be concluded that the manufactured chitosan membranes can be modelled as ultrafiltration (UF) membranes with capillary pores. If the transport of water through the membrane is described with the Hagen-Poiseuille equation, an average pore radius of 23 nm is determined. Using the Kozeny-Carman equation, a K value of 4.83 is determined.

Equilibrium isotherm studies revealed that the adsorption of zinc onto chitosan can be described by a Langmuir equation with a maximum zinc adsorption capacity of 135 $mg.g^{-1}$ of chitosan for 303-313 K. It was also determined that the adsorption process is endothermic with an adsorption enthalpy of 20 $kJ.mol^{-1}$.

Breakthrough curves were affected by the initial concentration of zinc in the solution and indicated that chitosan membranes perform better than other formulations of chitosan. The membranes adsorbed the metal ion zinc almost completely when working at low initial concentrations (<50 $mg.L^{-1}$). Further studies proved that the adsorption process is a kinetic process, with a decrease in adsorption (125 - 85 $mg.g^{-1}$) as the flux increases (2-55 $L.m^{-2}.hr^{-1}$).

It was also shown that the adsorption of metal ions by chitosan membranes is affected by co-ions, and the pH of the solution. The adsorption is limited by nitrates and enhanced by sulphates. The optimum pH for adsorption of zinc on chitosan membranes, outside the limits of precipitation of zinc hydroxide, is a pH of 6.

This adsorption process results in a membrane with a high zinc concentration in its structure, from which metals can be recovered by washing the chitosan membranes with an acidic solution. As the pH of the elution solution was decreased from a pH of

6 to a pH of 2, up to 90% of the adsorbed zinc was removed. This regeneration caused a decrease in the adsorption capability of the chitosan mainly due to a mass loss of the membrane (up to 11%). After 2 regeneration cycles the structural integrity of the membrane was lost and the membrane could not be used anymore.

7.2 Prospects

The growing need for new sources of low-cost adsorbent, the increased problems of waste disposal, and the increasing cost of synthetic resins undoubtly make chitosan one of the most attractive materials for wastewater treatment.

Because chitosan is produced from fishery wastes that can be obtained from fishery industries for free, especially in Asian countries such as Thailand, Japan and China where large fishing industries exists, it can be classified as a low cost alternative adsorbent. In South Africa, the fishing industry is decentralised and obtaining large amounts of raw material from one supplier is not possible, however raw material on small scale can be obtained from restaurants.

The use of chitosan for waste water remediation, in contrast to simple ion exchange, takes advantage of removing only toxic metal ions while the harmless ions move on into the environment. In some cases, chitosan can even be highly specific for a certain metal of particular interest. It also has the advantages of being non-contaminating, as chitosan is a natural, non-toxic and biodegradable material. Another advantage is that because no chemicals or reagents are added to the system it does not increase the hardness and scaling properties of the water, as is the case with lime dosing. The pH of the treated water also increases slightly with treatment, therefore making it less corrosive.

The disadvantage to the use of chitosan is limited to the production of chitin and chitosan. Here large amounts of chemicals are used during deproteinisation, demineralisation, and deacetylation (0.5 kg of 8 mass% sodium hydroxide solution for every 1 kg flakes was used, 10% hydrochloric acid, and 45 kg of 50 mass% sodium hydroxide solution per kg of chitin, respectively) at relatively high temperatures. Although the spent sodium hydroxide and hydrochloric acid were used to neutralise each other, the process remains hazardous and environmental spills must be avoided. The rather complex production process also makes the price of chitosan material relatively high.

The membrane process was favourable with regard to cleanliness and efficiency. The membrane process is also superior, from an adsorption capacity point of view to other chitosan formulations. Another advantage to using membranes for end point water treatment is the filtration of any suspended solids that can still be available after precipitation of the supernatant liquid.

Based on the relative high price of chitosan and this preliminary investigation on the technical feasibility of chitosan gel membranes in the removal of zinc ions from wastewater, a polishing treatment for small-size units would be a niche area. However, for the membrane process to be industrially feasible the membrane stability has to be improved, so that the number of regeneration cycles increase.

References

1. ATKINS, P.W. 1987. Physical Chemistry. Oxford: Oxford University Press. 857.

2. ATKINSON, B.W. & BUX, F. & KASAN, H.C. 1998. Waste activated sludge remediation of metal-plating effluents. *Water SA.* 24(4): 355-359.

3. BABEL, S. & KURNIAWAN, T.A. 2003. Low-cost adsorbents for heavy metals uptake from contaminated water: a review. *Journal of Hazardous Materials.* B97: 219-224.

4. BASSI, R. & PRASHER, S.O. & SIMPSON, B.K. 2000. Removal of Selected Metal Ions from Aqueous Solutions Using Chitosan Flakes. *Separation Science and Technology.* 35(4): 547-560.

5. BAXTER, A. & DILLO, M. & TAYLOR, K.D.A. & ROBERTS, G.A.F. 1992. Improved method for IR determination of the degree of N-acetylation of chitosan. *International Journal of Biological Macromolecules.* 14: 166-169.

6. BECKER, T. & SCHLAAK, M. & STRASDEIT, H. 2000. Adsorption of nickel(II) and cadmium(II) by new chitosan derivatives. *Reactive and Functional Polymers.* 44(3), July 2000: 289-298.

7. BUX, F. & SWALAHA, F.M. & KASAN, H.C. 1994. Microbiological transformation of metal contaminated effluents. *Pretoria: Water Research Commission.* Report No. 357/1/94.

8. CALVO, J.I. & HERNANDEZ, A. & PRADANOS, P. & MARTINEZ, L. & BOWEN, W.R. 1995. Pore Size Distributions in Microporous Membranes. *Journal of Colloid and Interface Science.* 176: 467-478.

9. CERISIER, S.D.M. 1994. The electrochemical generation of ferric ions in cooling water as an alternative for ferric chloride dosing to effect flocculation. Potchefstroom: PU for CHE. (Dissertation – M.Eng.) 145.

10. CERVERA, L. & ARNAL, C. & DE LA GUARDIA, M. 2003. Removal of heavy metals by using adsorption on alumina or chitosan. *Analytical and Bioanalytical Chemistry.* 375(6), March 2003: 820-825.

11. CHEN, J. & YIACOUMI, S. 1997. Biosorption of metal ions from aqueous solutions. *Separation Science and Technology.* 32(1-4): 51-69.

12. CHU, K.H. 2002. Removal of copper from aqueous solution by chitosan in prawn shell: adsorption equilibrium and kinetics. *Journal of Hazardous Materials.* B90(2002): 77-95.

13. CHUI, V.W.D. & MOK, K.W. & LUONG, B.P. & NG, C.Y. & MA, K.K. 1996. Removal and Recovery of Copper(II), Chromium(III), and Nickel(II) from Solutions Using Crude Shrimp Chitin Packed in Small Columns. *Environmental International.* 22(4): 463-468.

14. COLLINS, E.A. 1973. Experiments in Polymer Science. USA: Wiley. 429.

15. CONWAY, M. & HOLOMAN, S. & JONES, L. & LEENHOUTS, R. & WILLIAMSON, G. 1999. Selecting and Using Chelating Agents. *Chemical Engineering.* March 1999: 86-90.

16. COUGHLIN, R.W. & DESHAIES, M.R. & DAVIS, E.M. 1990. Chitosan in crab shell wastes purifies electroplating wastewater. *Environmental Progress.* 9(1): 35-39.

17. DAVIES, L. & DOLLIMORE, D. 1980. Theoretical and experimental values for the parameter k of the Kozeny-Carman equation, as applied to sedimenting suspensions. *Journal of Physics.* 13(11): 2013-2020.

18. EIDEN, C.A. & JEWELL, C.A. & WIGHTMAN, J.P. 1980. Interaction of Lead and Chromium with Chitin and Chitosan. *Journal of Applied Polymer Sciences.* 25: 1587-1599.

19. ELSON, C.M. & DAVIES, D.H. & HAYES, E.R. 1980. Removal of arsenic from contaminated drinking water by a chitosan/chitin mixture. *Water research.* 14: 1307-1311.

20. GHANDI, P. 1997. Obtaining Copper-Free Water. *WATER/Engineering & Management.* February 1997: 18-21.

21. GOPAL, V. & APRIL, G.C. 1998. Heavy metal decontamination from dilute aqueous solutions using membrane-electrode process. *Chemical Technology.* Nov/Dec 98: 3-5.

22. GRANT, H.W. 2000. Modelling the Kinetics of Cation Removal from Simulated Waste Water using Chitosan Beads. Potchefstroom : PU for CHE. (Dissertation – M.Eng.) 104.

23. GUAN, Y.L. & SHAO, L. & LIU, J. & YAO, K.D. 1996. pH effect on Correlation Between Water State and Swelling Kinetics of Crosslinked Chitosan. *Journal of Applied Polymer Sciences.* 62: 1253-1258.

24. GUIBAL, E. & MILOT, C. & ROUSSY, J. 1998. Molybdate Sorption by Crosslinked Chitosan Beads: Dynamic Studies. *Water Environment Research.* 71: 10-17.

25. GUIBAL, E. & MILOT, C. & ROUSSY, J. 1999a. Influence of Hydrolysis Mechanisms on Molybdate Sorption Isotherms Using Chitosan. *International Journal of Biological Macromolecuels.* 1-26.

26. GUIBAL, E. & MILOT, C. & ETERRADOSSI, O. & GAUFFIER, C. & DOMARD, A. 1999b. Study of molybdate ion sorption on chitosan gel beads by different spectrometric analyses. *International Journal of Biological Macromolecuels.* 24: 49-59.

27. GUIBAL, E. 2004. Interactions of metal ions with chitosan-based sorbents: a review. *Separation and Purification Technology.* 38: 43-74.

28. GUZMAN, J. & SAUCEDO, I. & REVILLA, J. & NAVARRO, R. & GUIBAL, E. 2003. Copper sorption by chitosan in the presence of citrate ions: influence of metal speciation on sorption mechanism and uptake capacities. *International Journal of Biological Macromolecules.* 33: 57-65.

29. HERNANDEZ, A. & CALVO, J.I. & PRADANOS, P. & TEJERINA, F. 1996. Pore size distribution in microporous membranes: A critical analysis of the bubble point extended method. *Journal of Membrane Science.* 112: 1-12

30. HORAN, N.J. 1991. Theory and operation of Biological Waste Treatment systems. Chichester : Wiley. 298.

31. HUANG, C. & CHUNG, Y. & LIOU, M. 1996. Adsorption of Cu(II) and Ni(II) by pelletized biopolymer. *Journal of Hazardous Materials.* 45: 265-277.

32. HUDSON, S.M. & SMITH, C. 1998. Biopolymers from Renewable Resources. Berlin: Springer. 96.

33. INOUE, K. & HIRAKAWA, H. & ISHIKAWA, Y. & YAMAGUCHI, T. & NAGATA, J. & OHTO, K. & YOSHIZUKA, K. 1996. Adsorption of Metal Ions on Gallium(III)-Templated Oxine Type of Chemically Modified Chitosan. *Separation Science and Technology.* 32(16): 2273-2285.

34. JAAFARI, K. & RUIZ, T. & ELMALEH, S. & COMA, J. & BENKHOUJA, K. 2004. Simulation of a fixed bed adsorber packed with protonated cross-linked chitosan gel beads to remove nitrate from contaminated water. *Chemical Engineering Journal.* 99: 153-160.

35. JANSEN, K.C. 2002. Adsorption and desorption of Cu2+ on chitosan beads. Potchefstroom : PU for CHE. (Internal report) 70. (unpublished.)

36. JANSSON-CHARRIER, M. & SAUCEDO, I. & GUIBAL, E. & LE CLOIREC, P. 1995. Approach of uranium sorption mechanisms on chitosan and glutamate glucan by IR and C-NMR analysis. *Reactive & Functional polymers.* 27: 209-221.

37. JHA, I.N. & IYENGAR, L. & PRABHAKARA RAO, A.V.S. 1988. Removal of Cadmium Using Chitosan. *Journal of Environmental Engineering.* 114(4): 963-974.

38. JIANG, H. & LIANG, J. & GRANT, J.T. & SU, W. & BUNNING, T.J. & COOPER, T.M. & ADAMS, W. 1997. Characterization of chitosan and rare-earth-metal-ion doped chitosan films. *Macromolecule chemistry and physics.* 198: 1561-1578.

39. JUANG, R. & SHIAU, R. 2000. Metal removal from aqueous solutions using chitosan-enhanced membrane filtration. *Journal of Membrane Science.* 165(2), February 2000: 159-167.

40. JUANG, R. & SHAO, H. 2002. A simplified equilibrium model for sorption of heavy metal ions from aqueous solutions on chitosan. *Water Research.* 36: 2999-3008.

41. KAMINSKI, W. & MODRZEJEWSKA, Z. 1997. Application of Chitosan Membranes in Separation of Heavy Metal Ions. *Separations Science and Technology.* 32(16): 2659-2668.

42. KANDAH, M. 2001. Zinc adsorption from aqueous solutions using disposal sheep manure waste (SMW). *Chemical engineering journal.* 84: 543-549.

43. KAWAMURA, Y. & YOSHIDA, H. & ASAI, S. 1997. Effects of Chitosan Concentration and Precipitation Bath Concentration on the Material Properties of Porous Cross-linked Chitosan Beads. *Separation Science and Technology.* 32(12): 1959-1974.

44. KEMMER, F.N. 1989. The NALCO Water Handbook. New York: McGraw-Hill Book Company. 365.

45. KHALID, N. & AHMAD, S. 1998. Removal of Lead from aqueous solutions Using Rice Husk. *Separation Science and Technology.* 33(15): 2349-2362.

46. KONDO, K. & SUMI, H. & MATSUMOTO, M. 1996. Adsorption Characteristics of Metal Ions on Chitosan Chemically Modified by D-Galactose. *Separation Science and Technology.* 31(12): 1771-1775.

47. KOTZE, J.S. 2001. Characterization of chitosan by size exclusion chromatography using a Malls detector. Potchefstroom : PU for CHE. (Dissertation – M.Eng.) 121.

48. KOYAMA, Y. & TANIGUCHI, A. 1986. Studies on Chitin X. Homogeneous Cross-linking of Chitosan for Enhanced Cupric Ion Adsorption. *Journal of Applied Polymer Science.* 31: 1951-1954.

49. KRAJEWSKA, B. 1996. Pore structure of gel chitosan membranes. III. Pressure-driven mass transport measurements. *Polymer Gels and Networks.* 4(1996): 55-63.

50. KRAJEWSKA, B. 2001. Diffusion of metal ions through gel chitosan membranes. *Reactive & Functional Polymers.* 47(2001): 37-47.

51. KURITA, K. & SHIMADA, K. & NISHIYAMA, Y. & SHIMOJO, M. & NISHIMURA, A. 1998. Nonnatural branched polysaccharides: Synthesis and properties of chitin and chitosan having a-Mannoside branches. *Macromolecules.* 31: 4764-4769.

52. KYOON NO, H. & MEYERS, S.P. 1997. Preparation of chitin and chitosan. In: R.A.A. Muzzarelli and M.G. Peters (eds). *Chitin Handbook.* Atec: European chitin society. 475-489.

53. LAIDLER, K.J. & MEISER, J.H. 1916. Physical Chemistry. California: Cummings Publishing Company Inc. 919.

54. LAKSHMINARAYANAIAH, I. 1969. Transport phenomena in membranes. USA: Academic Press, Orlando. 300.

55. LE DUNG, P. & MILAS, M. & RINAUDO, M. & DESBRIERES, J. 1994. Water Soluble Derivatives Obtained by Controlled Chemical Modifications of Chitosan. *Carbohydrate Polymers.* 24: 209-214.

56. LEVAN, M.D. & KNAEBAL, K.S. & SIRCAR, S. & WANKAT, P.C. 1998. Adsorption and ion exchange : Fundamentals and applications. *AIChE Symposium Series.* 84(264): 23-82.

57. LEWIS, T. 1999. Innovative Use of Activated Carbon for Recovering Heavy Metals. *Lewis Environmental Services.* August 1999: 1-2.

58. LIMA, I.S. & AIROLDI, C. 2004. A thermodynamic investigation on chitosan-divalent cation interactions. *Thermochimica acta.* 421: 125-131.

59. MARUCA, R. & SUDER, B. & WIGHTMAN, J.P. 1982. Interaction of Heavy Metals with Chitin and Chitosan. *Journal of Applied Polymer Science.* 27: 4827-4837.

60. MATHEICKAL, J.T. & YU, Q. 1999. Biosorption of lead(II) and copper(II) from aqueous solutions by pre-treated biomass of Australian marine algae. *Bioresource technology*. 69: 223-229

61. MATSUYAMA, H. & TERAMOTO, M. & URANO, H. 1997. Analysis of solute diffusion in poly(vinyl alcohol) hydrogel membrane. *Journal of Membrane Science*. 126(1): 151-160.

62. MCKAY, G. & BLAIR, H.S. & FINDON, A. 1989. Equilibrium studies for the sorption of metal ions onto Chitosan. *Indian Journal of Chemistry*. 28A: 356-360.

63. MILOT, C. & MCBRIEN, J. & ALLEN, S. & GUIBAL, E. 1997. Influence of Physicochemical and Structural Characteristics of Chitosan Flakes on Molybdate Sorption. *Journal of Applied and Polymer Science*. 68: 571-581.

64. MOHAN, D. & CHANDER, S. 2001. Single component and multi-component adsorption of metal ions by activated carbons. *Physicochemical and Engineering Aspects*. 177: 183-196.

65. MULDER, M. 1998. Basic Principles of Membrane Technology. 2nd ed. The Netherlands : Kluwer Academic Publishers. 564.

66. MURRAY, K.A. 1991. Wastewater Treatment and Pollution Control. South Africa : Beria Printers. 456.

67. MUZZARELLI, R.A.A. 1977. Chitin. Oxford : Pergamon Press Ltd. 309.

68. NAM, S.Y. & LEE, Y.M. 1998. Pervaporation performance of surface crosslinked chitosan membranes. *Journal of Membrane Science*. 153: 155-162.

69. NEOMAGUS, H.W.J.P. & VAN SWAAIJ, W.P.M. & VERSTEEG, G.F. 1998. The catalytic oxidation of H_2S in a stainless steel membrane reactor with separate feed of reactants. *Journal of Membrane Science*. 148(1998): 147-160.

70. NG, J.C.Y. & CHEUNG, W.H. & MCKAY, G. 2003. Equilibrium studies for the sorption of lead from effluents using chitosan. *Chemosphere*. 52(6), August 2003: 1021-1030.

71. NGAH, W.S. & GHANI, S. & KAMARI, A. 2005. Adsorption behaviour of Fe(II) and Fe(III) ions in aqueous solution on chitosan and cross-linked chitosan beads. *Bioresource Technology*. 96(4): 443-450.

72. NKALANGA, C.B. 2003. Removal of heavy metals from industrial waste water using chitosan coated aluminium oxide. (Paper delivered as part of the International Conference on Engineering Technology Research at the Vaal Triangle Technikon on 14 August 2002.) Vanderbijlpark. (unpublished.)

73. OSIFO, P.O. 2005. Adsorption of transitional elements onto chitosan beads. (Internal report) Potchefstroom : PU for CHE. (unpublished.)

74. PAWLOWSKI, B.S. 1971. Determination of the iodine number of activated carbon. (Paper as part of analytical manual for SATECH.) Sasolburg. 23. (unpublished.)

75. PEPPAS, N.A. & REINHART, C.T. 1983. Solute diffusion in swollen membranes. *Membrane Science*. 15: 275.

76. PERRY, R.H. 1988. Perry's Chemical Engineers' Handbook. Japan: Kosaido Printing Co., Ltd.

77. PETER, M.G. 1995. Applications and Environmental Aspects of Chitin and Chitosan. *J.M.S.-Pure Applied Chemistry*. A32(4): 629-640.

78. POURBAIX, M. 1974. Atlas of electrochemical equilibria in aqueous solutions. Texas: National Association of Corrosion Engineers. 313.

79. PULLES, W. & HOWIE, D. & OTTO, D. & EASTON, J. 1995. A manual on Mine Water Treatment and Management Practices in South Africa. Pretoria : Water Research Commission. 527.

80. RHAZI, M. & DESBRIERES, J. & TOLAIMATE, A. & RINAUDO, M. & VOTTERO, P. & ALAGUI, A. 2002. Contribution to the study of complexation of copper by chitosan and oligomers. *Polymer.* 43:1267-1276.

81. ROBERTS, G.A. 1992. Chitin Chemistry. UK: The Macmillan Press, London.

82. ROJAS, G. & SILVA, J. & FLORES, J.A. & RODRIGUEZ, A. & LY, M. & MALDONADO, H. 2004. Adsorption of chromium onto cross-linked chitosan. *Separation and Purification Technology.* 44(1): 31-36.

83. RORRER, G.L. & YANG HSIEN, T. & WAY, J.D. 1993. Synthesis of Porous-Magnetic Chitosan Beads for Removal of Cadmium Ions from Waste Water. *Industrial Engineering Chemistry. Res.* 32: 2170-2178.

84. SA. 1998a. Requirements for the purification of waste water or effluent. *Government Gazette.* 9225: 119.

85. SA. 1998b. South African Standard Specification for Drinking Water. *Pretoria: The South African Bureau of Standards.* (SABS 241:1999)

86. SCHOEMAN, J.J. & STEYN, A. 1995. Evaluation of Membrane Technology for Electroplating Effluent Treatment. *Pretoria : Water Research Commission.* Report No, 275/1/95.

87. SEKAR, M. & SAKTHI, V. & RENGARAJ, S. 2004. Kinetics and equilibrium adsorption study of lead(II) onto activated carbon prepared from coconut shell. *Journal of Colloid and Interface Science.* 279(2): 307-313.

88. SWART, P. & MAARTENS, A. & ENGELBRECHT, J. & ALLIE, Z. & JACOBS, E.P. 1999. Developing biological techniques for cross-flow filtration membranes. *SA Waterbulletin*. June 1999: 7.

89. TAOUALIT, N. & HADJ-BOUSSAAD, D.E. 2002. Metallic species (Ag^{+} and Cu^{2+} ions) transfer through a membrane-gel. *Desalination*. 144(2002): 273-277.

90. TIEN, C. 1994. Adsorption Calculations and Modelling. USA : Butterworth-Heinemann. 244.

91. TOMIDA, T. & KATOH, M. & INOUE, T. & MINAMINO, T.Y. & MASUDA, S. 1998. Transient Analysis of Mass-Transfer Rate in Recovering Metal Ions Using a Microporous Hollow Fibre Membrane and a Water-Soluble Chelating Polymer. *Separation Science and Technology*. 33(15): 2281-2293.

92. VAN VEELEN, M. 1999. Changes in Water Resource Management and the effect on the water industry. *Chemical Technology*. July/August 1999: 4-5.

93. VARMA, A.J. & DESHPANDE, S.V. & KENNEDY, J.F. 2003. Metal complexation by chitosan and its derivatives: a review. *Carbohydrate Polymers*. August 2003: 1-7.

94. VOGEL, A.I. 1991. Textbook of Quantitative Chemical Analysis. New York: Longman Scientific&Technical. 465.

95. VOLD, I.M.G. & VARUM, K.M. & GUIBAL, E. & SMIDSROD, O. 2003. Binding of ions to chitosan – selectivity studies. *Carbohydrate Polymers*. 54: 471-477.

96. VOLESKY, B. 1989. Biosorption of Heavy Metals. Boston: CRC Press. 396.

97. WAN NGAH, W.S. & ENDUD, C.S. & MAYANAR, R. 2002. Removal of copper(II) ions from aqueous solution onto chitosan and cross-linked chitosan beads. *Reactive & Functional Polymers*. 50(2002): 181-190.

98. YANG, T.C. & ZAIL, R.R. 1984. Absorption of Metals by Natural Polymers Generated from Seafood Processing Wastes. *Industrial Engineering Chemistry*. 23: 168-172.

99. YOUNG, R.J. 1980. Introduction to polymers. New York: Chapman and Hall. 331.

Appendix A: Introduction

A-1: Water Services Act and the National Water Act

The National Water Act (SA, 1998a) described two water management concepts.

- The first is the concept that there is no private ownership of water only the right to use water can be acquired.
- The second concept is that the aquatic ecology is part of the resource, and should be protected as such. For this purpose it is defined as the quantity and quality of water that is required to protect aquatic ecosystems in order to secure ecologically sustainable development and use of a water resource (Van Veelen, 1999).

The Water Services Act (SA, 1998a) describes the rules under which water supply has to be provided. This act regulates drinking water standards, industrial water use and sets standards for the disposal and control of sewer water. The Water Services Authority uses the limited effluent standards as set by the government for final treated effluent and has the authority to accept or reject industrial effluent (Van Veelen, 1999).

Tables A-1.1 and A-1.2 show the South African Bureau of Standards (SABS) specifications for drinking water guidelines and the specifications for effluent discharge respectively as proposed by the National Water Act and the Water Services Act (SA, 1998a).

Table A-1.1: SABS physical, organoleptic, chemical and microbiological requirement for drinking water.

Determinants	Units	Upper limits and ranges		
		Ideal	Acceptable	Max. allowable
Physical and organoleptic requirements				
Colour	$mg.L^{-1}$ Pt	15	20	50
Conductivity at 298K	$mS.m^{-1}$	70	150	370
Dissolved solids	$mg.L^{-1}$	450	1000	2400
Odour	TON	1	5	10
pH value at 298K	pH unit	6-9	5-9.5	4-10
Taste	FTN	1	5	10
Turbidity	NTU	0.1	1	10
Chemical requirements: Macro-determinants				
Ammonia as N	$mg.L^{-1}$	0.2	1	2
Calcium as Ca	$mg.L^{-1}$	80	150	300
Chloride as Cl	$mg.L^{-1}$	100	200	600
Fluoride as F	$mg.L^{-1}$	0.7	1	1.5
Magnesium as Mg	$mg.L^{-1}$	30	70	100
Nitrate + Nitrite as N	$mg.L^{-1}$	6	10	20
Potassium as K	$mg.L^{-1}$	25	50	100
Sodium as Na	$mg.L^{-1}$	100	200	400
Sulphate as SO_4	$mg.L^{-1}$	200	400	600
Zinc as Zn	$mg.L^{-1}$	3	5	10

Table A-1.1(continuing): SABS physical, organoleptic, chemical and microbiological requirement for drinking water.

Determinants	Units	Upper limits and ranges		
		Ideal	Acceptable	Max. allowable
Chemical requirements:				
Micro-determinants				
Aluminium as Al	$\mu g.L^{-1}$	150	300	500
Antimony as Sb	$\mu g.L^{-1}$	5	10	50
Arsenic as As	$\mu g.L^{-1}$	10	50	200
Cadmium as Cd	$\mu g.L^{-1}$	3	5	20
Chromium as Cr	$\mu g.L^{-1}$	50	100	500
Cobalt as Co	$\mu g.L^{-1}$	250	500	1000
Copper as Cu	$\mu g.L^{-1}$	500	1000	2000
Cyanide as CN	$\mu g.L^{-1}$	70	70	70
Iron as Fe	$\mu g.L^{-1}$	10	200	2000
Lead as Pb	$\mu g.L^{-1}$	10	50	100
Manganese as Mn	$\mu g.L^{-1}$	50	100	1000
Mercury as Hg	$\mu g.L^{-1}$	1	2	5
Nickel as Ni	$\mu g.L^{-1}$	50	150	350
Selenium as Se	$\mu g.L^{-1}$	10	20	50
Vanadium as V	$\mu g.L^{-1}$	100	200	500
Chemical requirements:				
Organic determinants				
Dissolved organic carbon as C	$mg.L^{-1}$	5	10	20
Total trihalomethanes	$\mu g.L^{-1}$	100	200	300
Phenols	$\mu g.L^{-1}$	5	10	70

Table A-1.1(continuing): SABS physical, organoleptic, chemical and microbiological requirement for drinking water.

Determinants	Units	Upper limits and ranges		
		Ideal	Acceptable	Maximum
Microbiological requirement				
Heterotrophic plate count	count.$(mL)^{-1}$	100	1000	10000
Total coliform	count.$(100mL)^{-1}$	0	10	100
Faecal coliform	count.$(100mL)^{-1}$	0	1	10
Somatic coliphages	count.$(10mL)^{-1}$	0	1	10
Enteric viruses	count.$(100L)^{-1}$	0	1	10
Protozoan parasites	count.$(100L)^{-1}$	0	1	10

(SA, 1998b)

Table A-1.2: Specifications for industrial effluent discharge.

Determinants	Standard
Colour, odour or taste	Shall not contain any substance in a concentration capable of producing any colour, odour or taste
pH	Shall be between 5.5 and 9.5
Dissolved oxygen	Shall be at least 75% saturation
Typical coliforms	0 count.$(100\ mL)^{-1}$
Temperature	Shall be a maximum of 308K
Chemical oxygen demand	Not to exceed 75 $mg.L^{-1}$ after applying chloride correction
Oxygen absorbed	The oxygen adsorbed from acid in 4 hours shall not exceed 10 $mg.L^{-1}$
Conductivity	Not to be increased by more than 75 $mS.m^{-1}$ above that of the intake water, with an maximum for any effluent of 250 $mS.m^{-1}$
Suspended solids	Not to exceed 25 $mg.L^{-1}$
Sodium	Not to be increased by more than 90 $mg.L^{-1}$ above that of the intake water
Soap, oil or grease	Not to exceed 2.5 $mg.L^{-1}$

Table A-1.2(continuing): Specifications for industrial effluent discharge.

Determinants	Maximum concentration	Units
Residual chlorine as Cl	0.1	$mg.L^{-1}$
Ammonia as N	10	$mg.L^{-1}$
Arsenic as As	0.5	$mg.L^{-1}$
Nitrates as N	1.5	$mg.L^{-1}$
Boron as B	1	$mg.L^{-1}$
Chromium(a) as Cr	0.5	$mg.L^{-1}$
Copper(a) as Cu	1	$mg.L^{-1}$
Phenolic as phenol	0.1	$mg.L^{-1}$
Lead(a) as Pb	0.1	$mg.L^{-1}$
Cyanides as CN	0.5	$mg.L^{-1}$
Sulphides as S	1	$mg.L^{-1}$
Fluoride as F	1	$mg.L^{-1}$
Zinc as Zn	5	$mg.L^{-1}$
Manganese as Mn	0.4	$mg.L^{-1}$
Cadmium(a) as Cd	0.05	$mg.L^{-1}$
Mercury(a) as Hg	0.02	$mg.L^{-1}$
Nickel as Ni	1	$mg.L^{-1}$
Selenium as Se	0.05	$mg.L^{-1}$
Other	The wastewater or effluent shall contain no other constituents in concentrations which are poisonous or injurious to humans, animals, fish other than trout, or other forms of aquatic life, or which are deleterious to agricultural use. (a)The sum of the concentrations of Ca, Cr, Cu, Hg and Pb shall not exceed 1 $mg.L^{-1}$	

(SA, 1998a and Murray, 1991)

A-2: Industrial water effluent

Table A-2.1: Example of typical coal mine water effluent analysis in South Africa.

Metal species	**Units**	**Inlet**
Conductivity	$mS.m^{-1}$	401
Total hardness	$mg.L^{-1}$	2383
Calcium hardness	$mg.L^{-1}$	438
Magnesium hardness	$mg.L^{-1}$	310.6
Cl^-	$mg.L^{-1}$	31.8
Na^+	$mg.L^{-1}$	110
K^+	$mg.L^{-1}$	9.4
pH		2.88
SO_4^{2-}	$mg.L^{-1}$	3600
Fe	$mg.L^{-1}$	74.7
Mn	$mg.L^{-1}$	23.76
Zn	$mg.L^{-1}$	514
Cu	$mg.L^{-1}$	29.4
Al	$mg.L^{-1}$	36.6
Total suspended solids		4501

Table A-2.2: Example of final effluent metal composition acquired after treatment from a metal-plating plant.

Metal species	Units	Concentration
Cadmium as Cd	$mg.L^{-1}$	1.7
Chromium as Cr	$mg.L^{-1}$	14.1
Copper as Cu	$mg.L^{-1}$	10.5
Mercury as Hg	$mg.L^{-1}$	0
Nickel as Ni	$mg.L^{-1}$	8.5
Zinc as Zn	$mg.L^{-1}$	43.4

(Schoeman & Steyn, 1995)

Table A-2.3: Typical rinse water composition from the nickel plating industry in South Africa.

Metal species	Units	Inlet
Sodium	$mg.L^{-1}$	174
Potassium	$mg.L^{-1}$	3
Calcium	$mg.L^{-1}$	23
Magnesium	$mg.L^{-1}$	16
Ammonium + Nitrogen	$mg.L^{-1}$	7.3
Nitrate + Nitrite	$mg.L^{-1}$	<0.2
Sulphate	$mg.L^{-1}$	2969
Chlorides	$mg.L^{-1}$	184
COD	$mg.L^{-1}$	664
Nickel	$mg.L^{-1}$	1370
Iron	$mg.L^{-1}$	2.17
TDS	$mg.L^{-1}$	4612
pH		1.8
Conductivity	$mS.m^{-1}$	1010

(Schoeman & Steyn, 1995)

Table A-2.4: Typical rinse water composition from the chromium plating industry in South Africa.

Metal species	**Units**	**Inlet**
Sodium	$mg.L^{-1}$	159
Potassium	$mg.L^{-1}$	5.3
Calcium	$mg.L^{-1}$	42
Magnesium	$mg.L^{-1}$	8.9
Nitrate + Nitrite	$mg.L^{-1}$	3.49
Sulphate	$mg.L^{-1}$	11.5
Chlorides	$mg.L^{-1}$	19
COD	$mg.L^{-1}$	49
Nickel	$mg.L^{-1}$	24.9
Iron	$mg.L^{-1}$	1.7
Chromium	$mg.L^{-1}$	740
TDS	$mg.L^{-1}$	1480
pH		3.5
Conductivity	$mS.m^{-1}$	121

(Schoeman & Steyn, 1995)

Table A-2.5: Typical rinse water composition from the zinc plating industry in South Africa.

Metal species	**Units**	**Inlet**
Sodium	$mg.L^{-1}$	339
Potassium	$mg.L^{-1}$	6.7
Calcium	$mg.L^{-1}$	45.2
Magnesium	$mg.L^{-1}$	24.2
Ammonium	$mg.L^{-1}$	3427
Nitrate + Nitrite	$mg.L^{-1}$	5.2
Sulphate	$mg.L^{-1}$	166.29
Chlorides	$mg.L^{-1}$	9648
COD	$mg.L^{-1}$	4480
Zinc	$mg.L^{-1}$	1740
Iron	$mg.L^{-1}$	0.04
TDS	$mg.L^{-1}$	20716
pH		6.6
Conductivity	$mS.m^{-1}$	3870

(Schoeman & Steyn, 1995)

Table A-2.6: Typical rinse water composition from the cadmium plating industry in South Africa.

Metal species	**Units**	**Inlet**
Sodium	$mg.L^{-1}$	707
Potassium	$mg.L^{-1}$	2
Calcium	$mg.L^{-1}$	2
Magnesium	$mg.L^{-1}$	1
Ammonium + nitrogen	$mg.L^{-1}$	2.7
Nitrate + Nitrite	$mg.L^{-1}$	0.3
Sulphate	$mg.L^{-1}$	37
Chlorides	$mg.L^{-1}$	668
COD	$mg.L^{-1}$	510
Cadmium	$mg.L^{-1}$	95
Iron	$mg.L^{-1}$	9.1
TDS	$mg.L^{-1}$	2416
pH		11

(Schoeman & Steyn, 1995)

Table A-2.7: Methods currently in use for heavy metal recovery at electroplating industries.

Method	**Metal application**	**Advantages**	**Disadvantages**
Hydroxide and sulphide precipitation	All metals	1. Cheap 2. High concentrations	1. Moderate purity 2. Large precipitation dams
Ion exchange	Ni, Cr, Cu rinse water	1. High effectivity 2. Remove to low concentrations	1. Not for high concentrations 2. High cost factor
Reverse osmosis	Ni, Cr, Cu, Zn rinse water	1. Can be used for moderate concentrations 2. Moderate energy consumption 3. High purity 4. Moderate stability	1. Only lines with heated plating baths can be treated, others need supplement evaporation 2. High fouling
Electrodialysis	Ni, Au, Pt, Sn, Cu, Ag, Pd, Cd, Zn rinse water	1. High concentrations 2. Moderate energy 3. High stability	1. Fouling 2. Moderate purity

(Schoeman & Steyn, 1995)

Table A-2.8: Effectiveness analyses between reverse osmosis (RO) and electrodialysis (ED).

Metal species	**Method**	**Inlet** $mg.L^{-1}$	**Outlet** $mg.L^{-1}$	**Effectiveness**
Ni	RO	1266	21	98%
	ED	3488	898	74%
Cr	RO	1016	92	91%
Zn	RO	930	130	86%
Cd	RO	95	0.16	99%

(Schoeman & Steyn, 1995)

Appendix B: Chitosan production and characterisation

B-1: Analytical Techniques

B-1.1: Molecular weight

To determine the molecular weight the chitosan was thoroughly washed with de-ionised water and dried for 12 hours at 70°C. The chitosan was dissolved in a solvent (0.2M Ammonium Acetate, buffered at pH 4.5 with acetic acid) in a water bath at constant temperature for 10 days. The samples were then filtered through 0.22 μ m membrane filter. The samples, with a volume of 100 μL were injected at a flow rate of 0.8 $ml.min^{-1}$ (40 min/sample).

A Size Exclusion Chromatography/Multiple Angle Laser Light Scattering (SEC/MALLS) technique was used to characterise the molecular weight of the chitosan using TSK GW columns (Size Exclusion Columns: TSK-G5000PW, G6000PW) with an on-line double detection system including a Waters R410 differential refractometer and a Dawn Wyatt multi-angle laser light scattering photometer.

B-1.2: Degree of deacetylation

To determine the degree of deacetylation (DDA) of the chitosan samples, infrared spectroscopy (IR-spectroscopy) was chosen. It is preferable to use fine particles for IR analysis and therefore the chitosan was crushed in a crusher (Dickie and Stockler Pty.) for 10 minutes. Then thoroughly rinsed with de-ionised water (to remove any NaOH residue, which could influence the IR spectrum) and dried for 12 hours at 70°C. Exactly 2 mg of chitosan was weighed and mixed with 300 mg of dry KBr. A chitosan/KBr pill was then pressed under a pressure of 200 $kg.cm^{-2}$. The pill was stored open at 100°C in an oven before IR analysis. The analyses were done as quickly as possible (20 seconds) from the time the pill was removed from the oven until the IR spectrum was recorded. The IR spectra were recorded using a Nicolet (Magna-IR 550) infrared spectrometer employing OMNIC software to construct absorbance spectra. The absorbance peaks used for the calculation of the DDA are the 1650 cm^{-1} (N-acetyl groups) and the 3450 cm^{-1} (hydroxyl band). Figure B-1

shows the IR spectrum for chitosan, derived from the average of three spectra, from where the adsorption fractions were measured.

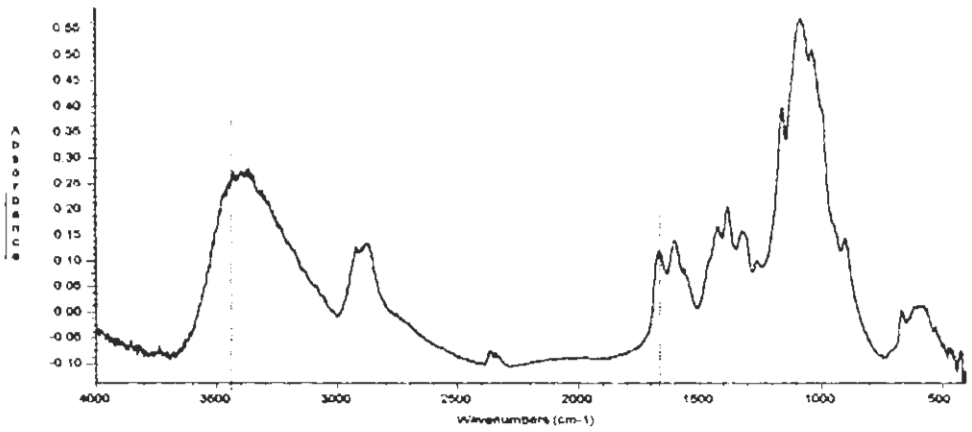

Figure B-1: IR spectrum for chitosan.

The DDA was determined from the infraspectrum obtained for chitosan using the method of Baxter *et al.* (1992) represented by the following expression:

$$\%DDA = 100 - \frac{A_{1655}}{A_{3450}} * 115 \qquad \text{.....B-1}$$

Appendix C: Membrane preparation

C-1. Statistical Design

The most important parameters that influence the membrane manufacturing process were the chitosan concentration, acetic acid concentration and the precipitation bath concentration. The influence of these parameters on both transport and adsorption characteristics of the membrane was measured. The range values for the factors were determined for the experimental design (minimum and maximum values were assigned for the different parameters), and a set of experiments was designed. The experimental profile of the 16 experiments is a normalised 5-point form as reflected in Table C-1.1 and Table C-1.2.

Table C-1.1: 5-point experimental profile.

Factors	**Levels**					**Units**
	-1.29	-1.00	0	1.00	1.29	
[Chitosan]	1.78	2.50	5.00	7.50	8.22	Mass%
[Acetic Acid]	1.43	2.00	4.00	6.00	6.57	Mass%
[Precipitation Bath]	1.78	2.50	5.00	7.50	8.22	Mass%

Table C-1.2: Experimental 16 profile.

Run	[Chitosan]	[Acetic acid]	[Precipitation bath]
1	-1	-1	-1
2	-1	-1	1
3	-1	1	-1
4	-1	1	1
5	1	-1	-1
6	1	-1	1
7	1	1	-1
8	1	1	1
9	-1.29	0	0
10	1.29	0	0
11	0	-1.29	0
12	0	1.29	0
13	0	0	-1.29
14	0	0	1.29
15	0	0	0
16	0	0	0

C-2: Analytical Techniques

C-2.1: Viscosity

The viscosity of the solution was determined after the dissolution of chitosan into acetic acid. The apparatus used for the viscosity measurement was the Ostwald Viscometer shown in Figure C-2.1.

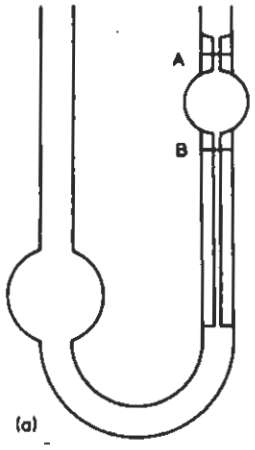

Figure C-2.1: The Ostwald viscometer (Laidler & Meiser, 1916).

The viscosity was determined by measuring the time it took for a given volume of the solution to flow through the viscosity meter from A to B. The time it takes the solution level to drop is called the efflux time (Perry, 1988). Several measurements were made and the averages calculated to obtain the viscosity.

Measurements of efflux times for solutions of the polymers solution were made for different chitosan concentrations and acetic acid concentrations. For comparison, the efflux time for the pure solvent, with no polymer dissolved in it, was measured. The efflux time of the pure solvent is labelled t_0. The first thing to do is calculating the viscosity of the polymer solutions to the viscosity of the pure solvent, in this case distilled water. This is done by taking the efflux time of the polymer solution at a given concentration t (from statistical design) and dividing it by the corresponding t_0 (the efflux time for the pure solvent). The temperature was kept constant by using a water bath at 25°C. The result is the relative viscosity (η_r) (Young, 1980):

$$\eta_r = \frac{t}{t_0} \qquad \text{.....C-1}$$

The viscosity was then calculated by multiplying the relative viscosity with the viscosity of the pure solvent.

C-2.2: Atomic Adsorption Spectrophotometer

The calibration curve procedure was followed whereby standard concentration solution of zinc purchased from Merck was used to plot the curve. Six standard solutions from Merck were used to plot the calibration graph in the region of 0 to 500 $mg.L^{-1}$. The samples were introduced in raw form to the Atomic Adsorption Spectrophotometer, without any dilution or concentration (Vogel, 1991).

C-3: Experimental data

In this section, the production of several different chitosan membranes is reported. For the production, different types of chitosan (Chitosan A-F) that vary in molecular weight, and DDA were used. In addition, the process variables for manufacturing the membrane (chitosan-, acetic acid- and NaOH concentration) were also varied.

Figure C-3.1 shows a homogeneous solution of chitosan. The minimum time necessary to dissolve chitosan into acetic acid solution was determined by using the maximum chitosan concentration (9 mass%) and dissolving it in the minimum concentration acetic acid (1 mass%). The solution was visually inspected until it was evident that all chitosan was dissolved.

Figure C-3.1: Homogeneous solution of a 9 mass% chitosan solution in a 1 mass% acetic acid solution at 24 hours.

Table C-3.1: Effect of chitosan molecular weight and DDA on the viscosity of a solution of 7% chitosan in 4% acetic acid.

Molecular weight $\cdot 10^3$ **(kg.kmole^{-1})**	**DDA** **(%)**	**Viscosity** **(Pa.s)**
60.0	>98	0.05
144.2	77	0.18
150.0	>98	0.25
201.3	78	0.35
298.9	79	0.50
400.0	>98	0.65

Table C-3.2: The effect of crosslinking time on the flux and adsorption of chitosan membranes at 50 kPa pressure difference.

Experimental conditions	
Chitosan type	A
Volume	0.25 L solution
Membrane area	0.00174 m^2
Membrane mass	0.076 g
Temperature	298 K
pH	5
Crosslinking	2.5 mass% glutaraldehyde rate of 1.5 cc per gram wet membrane

Results					
Crosslinking time (hrs)	Flux time (minutes)	C_{in} ($mg.L^{-1}$)	C_e ($mg.L^{-1}$)	q_e ($mg.g^{-1}$)	J_V ($L.m^{-2}.hr^{-1}$)
0	873	498	453	149	9.9
3	1017	498	458	131	8.5
6	1417	498	461	122	6.1
9	1921	498	475	76	4.5
12	2882	498	481	55	3.0
15	2789	498	481	56	3.1
18	2981	498	483	49	2.9
21	2981	498	484	46	2.9
24	2882	498	484	45	3.0

Table C-3.3: The effect of chitosan concentration on the flux through Chitosan A membranes at 50 kPa pressure difference.

Experimental conditions	
Chitosan type	A
Volume	0.25 L solution
Membrane area	0.00174 m^2
Temperature	298 K
pH	5
Crosslinking	2.5 mass% glutaraldehyde rate of 1.5 cc per gram wet membrane (6 hours)

Results		
[Chitosan] (mass%)	Flux time (minutes)	J_v ($L.m^{-2}.hr^{-1}$)
1.80	344	25.1
2.00	848	10.2
2.25	1351	6.4
2.50	1330	6.5
3.75	1441	6.0
5.00	1491	5.8
6.25	1517	5.7
7.50	1394	6.2
8.00	873	9.9
8.20	211	41.0

Table C-3.4: The effect of chitosan concentration on the adsorption by chitosan membranes at 50 kPa pressure difference.

Experimental conditions	
Chitosan type	A
Volume	0.25 L solution
Membrane area	0.00174 m^2
Temperature	298 K
pH	5
Crosslinking	2.5 mass% glutaraldehyde rate of 1.5 cc per gram wet membrane (6 hours)

Results						
[Chitosan] (mass%)	m_{wm} (g)	m (g)	C_{in} ($mg.L^{-1}$)	C_e ($mg.L^{-1}$)	q_e ($mg.g^{-1}$)	Q_e ($mg.g^{-1}$)
2	1.499	0.033	503	487	121.290	2.7
3	1.509	0.036	503	485	124.275	3.0
4	1.513	0.042	503	482	123.933	3.5
5	1.531	0.051	503	478	123.709	4.1
6	1.527	0.064	503	472	120.857	5.1
7	1.531	0.080	503	465	119.332	6.2

Appendix D: Characterisation of chitosan membranes

D-1: Analytical Techniques

D-1.1: Method of determining the Specific Surface Area

1. Grind a representative sample of dry chitosan membrane. The grinded sample is then sieved to obtain a sample of approximately 45 μm size .
2. Oven-dry the sample at 150°C for 3 hours and cool to room temperature in a desiccator.
3. Accurately weigh 1 gram of the dried sample.
4. Quantitatively transfer the weighed sample into a clean, dry closed, 250 mL iodine flask.
5. Pipette 10 mL of 5% hydrochloric acid solution into the flask.
6. Gently swirl the flask until the chitosan is completely wetted.
7. Place the flask on the hot plate and bring the contents to a boil and allow to boil gently for exactly 30 seconds.
8. Remove the flask from the hot plate and allow the contents to cool to room temperature.
9. Pipette 100 mL of 0.5N iodine solution into the flask.
10. Immediately close the flask, and shake contents vigorously for 30 seconds, then filter by gravity into a beaker.
11. Discard the first 20 mL of filtrate and collect the remainder into the beaker.
12. Mix the filtrate by swirling the beaker.
13. Pipette 50 mL of the filtrate into a clean 250 mL iodine flask.
14. Titrate with a standardised 0.01N sodium thiosulphate solution until the solution is a very pale yellow.
15. Ad 2 mL of starch indicator solution.
16. Continue the titration, dropwise, with sodium thiosulphate until 1 drop produces a colourless solution.
17. Record the volume of sodium thiosulfate used.
18. Use the diagram below to find the total surface area.

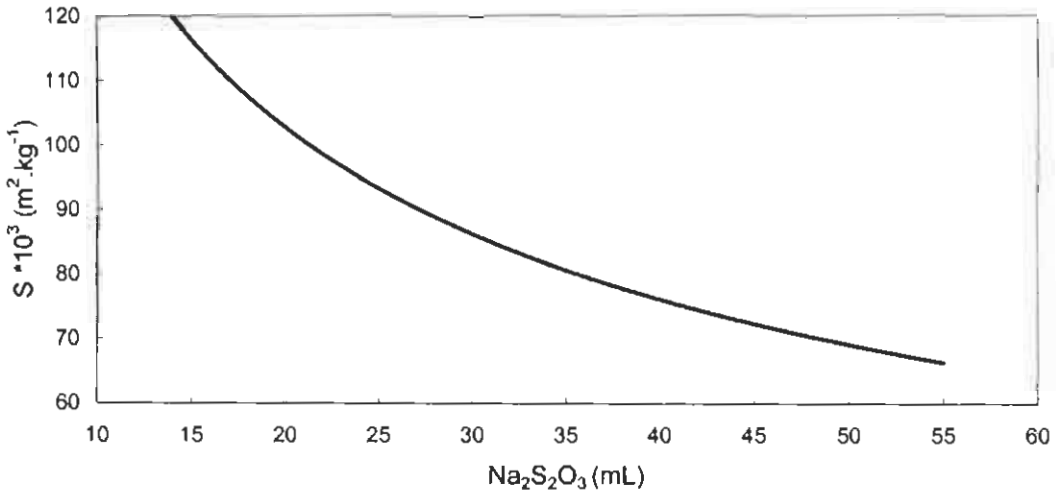

Figure D-2.1: Relationship between specific surface area and the millilitre of sodium thiosulphate titrated (Pawlowski, 1971).

D-1.2: Scanning Electron Microscope

The Scanning Electron Microscope analysis is one of the methods that can be used for dry membrane characterisation. The resolution is about 10 nanometers. The following steps in sample preparation were followed:

1. Because the specimen contains large amounts of water, evaporation of water will cause problems under vacuum; therefore the sample needs to be dehydrated. To dehydrate the sample it is emerged for short times in a graded series of ethanol. The concentration of the ethanol is gradually increased.
2. The samples were then critical point dried using CO_2.
3. The samples were then directly mounted onto the sample stub of the Scanning Electron Microscope using double-sided carbon tape.
4. The specimen was coated with a gold conductive layer to increase the conductivity. This is necessary to reduce thermal damage, and to increase the electron emission and mechanical stability.
5. After this treatment the specimens were ready for scanning.

D-2: Experimental data

In this section the effect of chitosan concentration on the wet membrane density, chitosan in the membrane, fraction free water volume, pore radius and the specific surface area at optimum conditions of 4 mass% acetic acid and 5 mass% sodium hydroxide was investigated.

Table D-2.1: Effect of chitosan concentration on wet membrane density, percentage chitosan in the membrane and the fraction free water volume.

Experimental conditions	
Chitosan type	A
Crosslinking	2.5 mass% glutaraldehyde rate of 1.5 cc per gram wet membrane (6 hours)
[Acetic acid]	4 mass%
[Sodium hydroxide]	5 mass%
Wet volume	$2.464 \cdot 10^{-6}$ m^3

Results							
[Chitosan] (mass%)	m_{wm} (mg)	m_{dm} (mg)	m_{wm}-m_{dm} (mg)	m_{fwp} (mg)	ρ_{wm} ($kg.m^{-3}$)	x_c ($kg.kg^{-1}$)	ε ($m^3.m^{-3}$)
2	2661	59	2602	1783	1080	0.022	0.67
3	2678	64	2614	1767	1087	0.024	0.66
4	2686	75	2611	1784	1090	0.028	0.66
5	2718	90	2628	1767	1103	0.033	0.65
6	2710	114	2596	1762	1100	0.042	0.65
7	2719	141	2578	1760	1103	0.052	0.65

Table D-2.2: The effect of chitosan concentration on the maximum pore radius and the specific surface area of Chitosan A.

Experimental conditions	
Chitosan type	A
Crosslinking	2.5 mass% glutaraldehyde rate of 1.5 cc per gram wet membrane (6 hours)
[Acetic acid]	4 mass%
[Sodium hydroxide]	5 mass%
Surface tension	0.001 $N.m^{-1}$
P_2	981 Pa

Results					
[Chitosan] (mass%)	Tiosulphate (mL)	P_1 (Pa)	ΔP (Pa)	r_P (nm)	Specific surface area $\cdot 10^5$ ($m^2.kg^{-1}$)
2	13.7	1025	44	45.3	1.193
3	13.8	1028	47	44.0	1.192
4	14.0	1028	47	43.6	1.190
5	14.5	1028	47	42.4	1.184
6	14.6	1030	49	41.0	1.180
7	15.0	1031	50	40.0	1.176

Appendix E: Transport properties of chitosan membranes

E-1. Experimental data

In this section the effect of different process parameters (pressure difference, zinc-ion concentration) on the transport properties are investigated. The average values are presented throughout the appendix.

Table E-1.1: The effect of pressure difference on the membrane water permeability (Membrane thickness = 0.8 mm and T = 298K).

Experimental conditions		
Volume	0.25 L solution	
Membrane area	0.001735 m^2	
Membrane thickness	0.8 mm	
Mass	0.076 g chitosan	
Temperature	298 K	
pH	6	
Results		
ΔP (bar)	Permeability time (min)	J_P ($L.m^{-2}.hr^{-1}$)
0.0	0	0
0.5	2161	4
1.0	786	11
1.5	540	16
2.0	432	20
2.5	360	24
3.0	254	34
3.5	206	42
4.0	176	49
4.5	149	58
5.0	131	66
5.5	122	71

Table E-1.2: Obtaining the solute permeability coefficient and the reflection coefficient.

Experimental conditions	
Volume	0.25 L solution
Membrane area	0.001735 m^2
Membrane thickness	0.8 mm
Mass	0.076 g chitosan
Temperature	298 K
pH	6
C_S	50 $mg.L^{-1}$

Results							
ΔP (bar)	Flux time (min)	J_V ($L.m^{-2}.hr^{-1}$)	C_e ($mg.L^{-1}$)	ΔC ($mg.L^{-1}$)	J_S ($mg.m^{-2}.hr^{-1}$)	$\frac{J_S}{\Delta C}$	$\frac{J_V \cdot C_S}{\Delta C}$
2.0	4550	1.9	39.7	10.3	2.5	0.2	9.2
2.5	1042	8.3	40.0	10.0	10.0	1.0	41.5
3.0	534	16.2	40.6	9.4	12.5	1.3	86.1
3.5	430	20.1	40.9	9.1	12.5	1.4	110.5
4.0	320	27.0	41.0	9.0	50.0	5.6	150.1
4.5	259	33.4	41.7	8.3	72.5	8.7	201.1
5.0	211	41.0	42.0	8.0	72.5	9.1	256.1
5.5	192	45.0	42.0	8.0	75.0	9.4	281.4

Table E-1.3: Relationship between experimental permeability and calculated permeability using the transport model.

Experimental conditions	
Volume	0.25 L solution
Membrane area	0.001735 m^2
Membrane thickness	0.8 mm
Mass	0.076 g chitosan
Temperature	298 K
pH	6
Solute permeability	0.715 $mg.m^{-2}.hr^{-1}$
Reflection coefficient	0.994

Results							
ΔP (bar)	Experimental volume permeability J_V ($L.m^{-2}.hr^{-1}$)				Transport model J_V ($L.m^{-2}.hr^{-1}$)		
	Clean water	Zinc concentration ($mg.L^{-1}$)			Zinc concentration ($mg.L^{-1}$)		
		500	100	50	500	100	50
π					0.375	0.075	0.040
0.5	4	3.0	1.8	1.9	1.5	5.2	5.7
1.0	11	7.0	8.0	8.3	7.7	11.4	11.9
1.5	16	18.4	16.5	16.2	13.9	17.6	18.1
2.0	20	21.3	20.3	20.1	20.0	23.8	24.3
2.5	24	23.4	25.0	27.0	26.2	30.0	30.4
3.0	34	27.9	32.8	33.4	32.4	36.1	36.6
3.5	42	31.5	39.9	40.9	38.6	42.3	42.8
4.0	49	34.3	46.1	45.0	44.8	48.5	49.0
4.5	58	35.4	48.0	55.0	50.9	54.7	55.2
5.0	66	35.3	49.0	56.0	57.1	60.9	61.3
5.5	71	36.0	50.0	56.5	63.3	67.0	67.5

Table E-1.3 (continue): Relationship between experimentally verified permeability and calculated permeability using the transport model.

Results						
ΔP (bar)	Experimental solute permeability J_S ($mg.m^{-2}.hr^{-1}$)			Transport model J_S ($mg.m^{-2}.hr^{-1}$)		
	Zinc concentration ($mg.L^{-1}$)			Zinc concentration ($mg.L^{-1}$)		
	500	100	50	500	100	50
0.5	2.5	1	0.5	4.8	3.2	1.7
1.0	10.0	4	2.0	23.3	6.9	3.6
1.5	12.5	5	2.5	41.8	10.6	5.5
2.0	12.5	5	2.5	60.4	14.3	7.3
2.5	50.0	20	10.0	78.9	18.0	9.2
3.0	72.5	29	14.5	97.5	21.7	11.0
3.5	72.5	29	14.5	116.0	25.4	12.9
4.0	75.0	30	15.0	134.5	29.2	14.7
4.5	77.5	31	15.5	153.1	32.9	16.6
5.0	75.0	30	15.0	171.6	36.6	18.4
5.5	87.5	35	17.5	190.2	40.3	20.3

Table E-1.4: The relationship between permeability and applied pressure difference for different zinc concentrations.

Experimental conditions								
Volume	0.25 L solution							
Membrane area	0.001735 m^2							
Membrane thickness	0.8 mm							
Mass	0.076 g chitosan							
Temperature	298 K							
pH	6							
Results								
Zn ($mg.L^{-1}$)	0	10	20	30	40	50	100	500
ΔP (bar)	J_V ($L.m^{-2}.hr^{-1}$)							
0.5	4.0	3.6	3.2	2.8	2.3	1.9	1.8	3.0
1.0	11.0	10.5	9.9	9.4	8.8	8.3	8.0	7.0
1.5	16.0	16.0	16.1	16.1	16.2	16.2	16.5	18.4
2.0	20.0	20.0	20.0	20.1	20.0	20.1	20.3	21.3
2.5	24.0	25.0	25.2	25.8	26.4	27.0	25.0	23.4
3.0	34.0	34.0	33.8	33.6	33.5	33.4	32.8	27.9
3.5	42.0	42.0	41.6	41.0	41.0	40.9	39.9	31.5
4.0	49.0	48.0	47.4	47.0	46.0	45.0	46.1	34.3
4.5	58.0	57.5	57.0	56.0	56.0	55.0	48.0	35.4
5.0	66.0	64.0	62.0	60.0	58.0	56.0	49.0	35.3
5.5	71.0	68.2	65.0	63.0	59.4	56.5	50.0	36

Table E-1.5: Calculations to determine the limiting flux.

C_b	$\ln(C_b)$	J_{V1lim}
10	2.3	68.0
20	3.0	65.0
30	3.4	63.0
40	3.7	59.0
50	3.9	57.6
100	4.6	50.4
500	6.2	36.0

E-2. Modelling

Table E-2.1: Effect of membrane thickness on the membrane transport properties.

Experimental conditions	
Volume	0.25 L solution
Membrane area	0.001735 m^2
Membrane thickness	0.8 mm
Mass	0.076 g chitosan
Temperature	298 K
pH	6
Porosity (ε)	0.65
Specific surface area	120 000 $m^2.kg^{-1}$
	132 000 000 $m^2.m^{-3}$
K	5.443
Viscosity	0.001 Pa.s
Pore radius	22 nm
Tau	1.538

Results				
Membrane thickness (mm)	J_V ($L.m^{-2}.hr^{-1}$)			
	Water	Zinc (50 $mg.L^{-1}$)	Kozeny-Carman	Hagen-Poiseuille
0.80	10.1	9.0	11.0	11.5
0.90	9.6	8.6	9.8	10.2
1.00	9.0	8.1	8.8	9.2
1.10	8.4	7.9	8.0	8.4
1.27	7.6	7.5	6.9	7.2
1.32	7.2	7.0	6.7	7.0
1.40	6.8	6.8	6.3	6.6
1.43	6.8	6.8	6.2	6.4
1.46	6.6	6.5	6.0	6.3

Table E-2.2: The effect of pH on membrane permeability.

Experimental conditions	
Volume	0.25 L solution
Membrane area	0.001735 m^2
Membrane thickness	0.8 mm
Mass	0.076 g chitosan
Temperature	298 K
Pressure	100 000 Pa

Results		
pH	Permeability ($L.m^{-2}.hr^{-1}$)	Transport model ($L.m^{-2}.hr^{-1}$)
3.02	6.3	7.23
4.50	7.3	7.69
5.40	7.4	7.70
6.43	7.5	7.70

Table E-2.3: The effect of temperature on membrane permeability

Experimental conditions	
Volume	0.25 L solution
Membrane area	0.001735 m^2
Membrane thickness	0.8 mm
Mass	0.076 g chitosan
Temperature	298 K
pH	6
Pressure	100 000 Pa

Results		
T (K)	Permeability ($L.m^{-2}.hr^{-1}$)	Viscosity ($kg.hr^{-1}.m^{-1}$)
293	6.1	3.8
295	6.1	3.7
298	6.2	3.4
303	6.2	3.1
308	6.2	2.7
313	6.3	2.5

Appendix F: The adsorption of zinc-ions on chitosan membranes

F-1. Precipitation

An important aspect in this study, is to work outside the precipitation limits of zinc hydroxide ($Zn(OH)_2$). For this reason, the effect of the pH on precipitation of $Zn(OH)_2$ at different concentrations of zinc (C_{in}= 500, 80, 50 and 40 $mg.L^{-1}$) is studied. The pH of the solution was changed using a dilute solution of sodium hydroxide. The average values are presented throughout the appendix.

Table F-1.1: The effect of pH on the concentration of zinc in solution.

pH	Final zinc concentrations ($mg.L^{-1}$) at various pH values (C_{in})			
	500.0	80.0	50.0	40.0
4.9	498.5	77.9	49.7	40.3
5.1	499.4	79.1	51.1	39.0
5.3	498.2	77.3	48.5	38.9
5.5	496.6	77.4	50.2	41.1
5.7	495.5	78.1	49.8	40.3
5.9	490.2	76.7	51.4	43.0
6.1	349.0	76.1	48.8	39.7
6.3	199.0	74.8	48.0	39.0
6.5	100.3	73.8	47.0	38.0
6.7	20.6	38.8	38.0	37.7
6.9	14.6	19.5	23.4	24.7
7.1	12.4	12.1	12.8	13.0
7.3	6.5	6.5	6.5	6.5
7.5	3.3	3.3	3.3	3.3
7.7	2.6	2.6	2.6	2.6
7.9	2.0	1.9	1.9	2.0
8.1	0.7	0.6	0.6	0.7
8.3	0.6	0.7	0.5	0.7

F-2. Equilibrium studies

Table F-2.1: Equilibrium adsorption of zinc onto chitosan membranes.

Experimental conditions										
Volume	1 L solution									
Membrane thickness	0.8 mm									
pH	6									
Results										
C_{in} ($mg.L^{-1}$)	C_e ($mg.L^{-1}$)					q_e ($mg.g^{-1}$)				
	Temperature (K)					Temperature (K)				
	293	298	303	308	313	293	298	303	308	313
0	0.0	0.0	0.0	0.0	0.0	0.0	0.0	0	0.0	0.0
10	6.5	8.4	7.1	5.8	6.9	17.5	8.0	14.5	21.0	15.5
20	14.9	13.9	15.9	14.8	15.0	25.5	30.5	20.5	26.0	25.0
30	25.2	22.2	21.0	21.2	21.9	24.0	39.0	45.0	44.0	40.5
40	34.3	32.6	29.8	29.5	28.3	28.5	37.0	51.0	52.5	58.5
75	64.5	64.9	63.0	63.5	62.8	52.5	50.5	60.0	57.5	61.0
100	88.0	78.8	83.4	83.0	81.9	60.0	106.0	83.0	85.0	90.5
150	132.4	131.9	130.5	129.2	128.2	88.0	90.5	97.5	104.0	109.0
200	183.6	179.5	177.0	176.6	176.7	82.0	102.5	115.0	117.0	116.5
300	283.6	281.0	276.3	276.4	174.9	82.0	95.0	118.5	118.0	125.5
400	382.2	380.7	378.6	378.0	376.0	89.0	96.5	107.0	110.0	120.0
500	482.9	479.0	475.0	475.9	475.6	85.5	105.0	125.0	120.5	122.0

Table F-2.2: Data modelling using Langmuir equation for equilibrium concentration.

Experimental conditions	
Volume	1 L solution
Membrane thickness	0.8 mm
pH	6

Results

C_{in} ($mg.L^{-1}$)	C_e/q_e					Langmuir plot				
	Temperature (K)					Temperature (K)				
	293	298	303	308	313	293	298	303	308	313
0	0.0	0.0	0.0	0.0	0.0	0.0	0.0	0.0	0.0	0.0
10	0.4	1.1	0.3	0.3	0.4	7.4	12.2	13.9	11.5	13.5
20	0.6	0.5	0.6	0.6	0.6	15.5	18.9	27.5	26.0	26.3
30	1.1	0.6	0.5	0.5	0.5	23.8	27.7	34.1	34.4	35.2
40	1.2	0.9	0.6	0.6	0.5	29.9	36.7	43.8	43.5	42.3
75	1.2	1.3	1.1	1.1	1.0	44.9	56.3	68.0	68.3	67.9
100	1.5	0.7	1.0	1.0	0.9	53.0	62.2	77.4	77.3	76.8
150	1.5	1.5	1.2	1.2	1.2	63.6	77.5	91.5	91.2	91.0
200	2.2	1.8	1.5	1.5	1.5	71.5	85.8	100.0	99.9	100.0
300	3.5	3.0	2.3	2.3	2.2	80.5	96.1	110.3	110.3	110.2
400	4.3	3.9	3.4	3.4	3.1	85.7	101.8	116.1	116.0	115.9
500	5.6	4.6	3.9	3.9	3.9	89.1	105.4	119.5	119.5	119.5

The influence of temperature (Figure F-2.1) on the affinity parameter was used to determine the enthalpy of adsorption using the linear form of the Van 't Hoff equation:

$$\ln(b) = \ln(b_o) - \frac{\Delta H_{ads}}{R \cdot T} \qquad \text{.....F2-1}$$

A plot of the natural logarithm of b versus the reciprocal temperature results in a line from which the enthalpy of adsorption can be calculated.

Table F-2.3: The effect of temperature on adsorption; and calculation of the adsorption enthalpy.

Experimental conditions				
Membrane thickness 0.8 mm				
pH 6				
Results				
T (K)	q_e ($mg.g^{-1}$)	1/T	b	ln(b)
293	90.1	0.00341	0.0116	-4.46
298	104.9	0.00336	0.0132	-4.33
303	119.9	0.00330	0.0161	-4.13
308	125.3	0.00325	0.0176	-4.04
313	126.0	0.00319	0.0195	-3.94

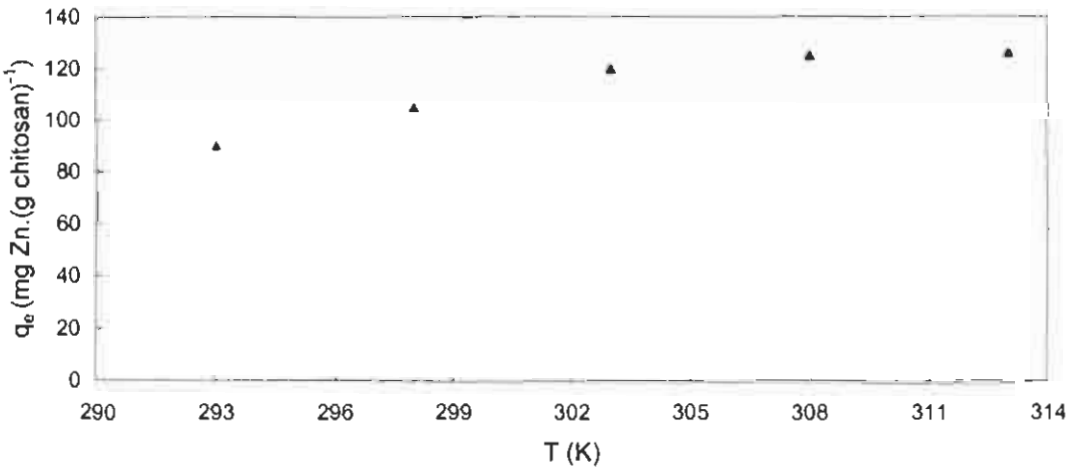

Figure F-2.1: The effect of temperature on the adsorption capacity.

F-3. Dynamic studies

These experiments were conducted at non-equilibrium conditions, the solution was only circulated once through the membrane. This is done in order to determine whether high flux ratios influence adsorption capacity. The flux depends on the pressure difference, therefore, the pressure difference was changed until a specific flux was reached, the adsorption at this specific flux was determined.

Table F-3.1: The relationship between zinc adsorption to membrane flux (Non-equilibrium, pH=6 and 50 $mg.L^{-1}$ Zn).

Experimental conditions			
Volume	0.25 L		
Membrane thickness	0.8 mm		
Temperature	298 K		
pH	6		
C_{in}	50		
Results			
ΔP (bar)	J_V ($L.m^{-2}.hr^{-1}$)	C_t ($mg.L^{-1}$)	q ($mg.g^{-1}$)
0.08	1.0	12.0	125.0
0.15	1.9	15.1	114.8
0.67	8.3	15.8	112.5
1.31	16.2	17.5	106.9
1.63	20.1	19.6	100.0
2.70	33.4	21.7	93.1
3.64	45.0	25.5	80.6
4.46	55.0	25.1	81.9
4.47	56.0	26.2	78.3
4.49	56.7	26.5	77.3

Table F-3.2: The effect of concentration on the breakthrough profile for zinc solutions.

Experimental conditions							
Membrane thickness	0.8 mm						
pH	6						
ΔP	100 kPa						
Results							
Volume solution (mL)	C_e ($mg.L^{-1}$)			Bed volume	C_e/C_{in}		
	50	100	500		50	100	500
0	0.0	0.0	0.0	0	0.00	0.00	0.00
5	0.0	0.0	10.0	4			0.02
10	0.0	1.0	400.0	7	0.00	0.01	0.80
15	0.0	0.0	490.0	11			0.98
20	1.0	2.0	500.0	14	0.02	0.02	1.00
30	1.0	9.0		22	0.02	0.09	
40	2.0	20.0		29	0.04	0.20	
50	2.0	45.0		36	0.04	0.45	
60	5.5	65.0		43	0.11	0.65	
70	10.0	85.0		50	0.20	0.85	
80	20.0	90.0		58	0.40	0.90	
90	30.0	95.0		65	0.60	0.95	
100	40.0	99.0		72	0.80	0.99	
150	47.5	100.0		108	0.95	1.00	
200	50.0			144	1.00		

F-4. Other factors influencing adsorption

Table F-4.1: The effect of cations and anions on membrane adsorption.

Experimental conditions	
Membrane thickness	0.8 mm
pH	6
ΔP	100 kPa
T	298 K

Results

Contaminant	C_e ($mg.L^{-1}$)	q_e ($mg.g^{-1}$)	Concentration ($mg.L^{-1}$)							
			Zn	SO_4	NO_3	Cl	K	Mg	Na	Ca
$ZnSO_4.7H_2O$	463.8	119.2	500	735	-	-	-	-	-	-
$ZnSO_4.7H_2O$	462.6	123.0	50	73.5	-	-	-	-	-	-
$Zn(NO_3)_2.6H_2O$	469.6	99.9	50	-	95	-	-	-	-	-
$ZnCl_2$	467.0	108.4	50	-	-	54	-	-	-	-
KCl	465.1	114.9	-	-	-	50	55	-	-	-
$MgCl_2.2H_2O$	466.7	109.6	-	-	-	50	-	17	-	-
NaCl	466.0	111.9	-	-	-	50	-	-	32	-
$CaCl_2.2H_2O$	467.1	108.2	-	-	-	50	-	-	-	28
$CaCl_2.2H_2O$	469.2	101.2	-	-	-	88	-	-	-	50
$CaSO_4.2H_2O$	465.8	112.6	-	120	-	-	-	-	-	50

Table F-4.2: The effect of pH on membrane adsorption.

Experimental conditions			
Membrane thickness	0.8 mm		
Temperature	298 K		
Results			
pH	C_{in} ($mg.L^{-1}$)	C_e ($mg.L^{-1}$)	q_e ($mg.g^{-1}$)
4.5	500	472.6	90.0
5.4	500	466.6	110.0
6	500	465.0	115.0
6.43	500	465.6	113.0

F-5. Desorption and recovery

Table F-5.1: Adsorption and desorption using different acids.

Desorption medium	pH	C_{in} ($mg.L^{-1}$)	C_e ($mg.L^{-1}$)	V (L)	Membrane mass (g)	q_e ($mg.g^{-1}$)
Water	7.4	498.0	335.5	1	1.45	112.1
HCl	2	499.0	334.6	1	1.50	113.4
HCl	4	500.0	341.0	1	1.48	102.6
H_2SO_4	2	499.9	329.0	1	1.45	113.9
H_2SO_4	4	498.2	340.4	1	1.55	107.0

Table F-5.1 (continued): Adsorption and desorption using different acids.

Desorption medium	C_{in}- C_e ($mg.L^{-1}$)	Desorption (mg)	Desorption (%)	Membrane mass (g)	Mass loss (g)	Mass loss (%)
Water	162.5	3	2	1.45	0.000	0
HCl	164.4	140	85	1.43	0.075	5
HCl	159.0	112	70	1.44	0.035	2
H_2SO_4	170.9	153	90	1.40	0.050	3
H_2SO_4	157.8	128	81	1.54	0.015	1

Table F-5.2: Cycles of adsorption and desorption using H_2SO_4 solution at pH 2.

Cycle	C_{in} ($mg.L^{-1}$)	C_e ($mg.L^{-1}$)	V (L)	Membrane mass (g)	q_e ($mg.g^{-1}$)	Sorption (%)
1	499	491	1	0.075	114	100
2	500	494	1	0.072	86	75

Table F-5.2 (continued): Cycles of adsorption and desorption using H_2SO_4 solution at pH 2.

Cycle	C_{in}- C_e ($mg.L^{-1}$)	Desorption (mg)	Desorption (%)	Membrane mass (g)	Mass loss (g)	Mass loss (%)
1	9	8	90	0.072	0.0026	3
2	6	4	70	0.067	0.0080	11